Science with ALMA

Contents

1 Introduction

1.1 Millimeter Astronomy

The millimeter and submillimeter wavebands are unique in astronomy in containing more than 1000 radio spectral lines of interstellar and circumstellar molecules as well as the thermal continuum spectrum of cold dust in space. They are the only bands in the electromagnetic spectrum in which we can detect cold dust and molecules far away in young, high-redshift galaxies in the early Universe, and nearby in low-temperature cocoons of protostars in our own Galaxy. They are the only bands that can give us the fine-scale kinematic details in young stellar disks that can potentially form planets, and in old ejected stellar envelopes that are forming dust grains and enriching the interstellar medium with carbon, oxygen and nitrogen. They lie at the crossroads between the radio and infrared/optical wavebands, containing both the synchrotron emission extending from the radio and the thermal emission extending from the optical/infrared. They contain the peak of the microwave background. And technically, they have the huge advantage that the heterodyne techniques of the radio can be used throughout.

Millimeter/submillimeter astronomy is entering a period of great discovery. Over the last decade, three dramatic events have spectacularly opened up this spectral region to the distant Universe: the discovery of CO emission in a $z = 2.3$ ultraluminous IRAS galaxy, the discovery of the far-infrared background radiation, and the discovery of a large population of star-forming galaxies that probably dominate the luminosity of the Universe at high redshift. Both dust continuum emission and CO line emission have been detected in some of the most distant known objects, at redshifts near 5. And all of these pioneering developments have been made with telescopes of modest size. They have just touched the tip of the iceberg, and they point the way to a wealth of discovery to come with the development of a major new telescope operating at millimeter and submillimeter wavelengths.

1.2 A Major New Telescope for Millimeter Astronomy

A large millimeter/submillimeter telescope would be a major step for astronomy, and would bring a revolution in millimeter astronomy. It would provide a millimeter/submillimeter equivalent to the world's major facilities operating at other wavebands - a counterpart to the HST and VLT, with similar angular resolution and sensitivity but unhindered by dust opacity. It should be capable of seeing star-forming galaxies throughout the entire Universe, star-forming regions across our Galaxy, and planet forming regions in our solar neighborhood. It should have the capability to open up new fields of science.

In order to resolve both distant galaxies and nearby protoplanetary systems, as well as for compatibility with facilities at other wavelengths, the new telescope should provide angular resolutions in the range 0.01-0.1 arcsec. This implies baselines of order 10 km, hence an array of antennas. However, one can only exploit the high angular resolution if there is a corresponding increase in sensitivity. The array must have a large number of antennas of substantial size. Such an array should cover the atmospheric windows in the millimeter and submillimeter wavebands up to the atmospheric cutoff near 1 THz. Thus,
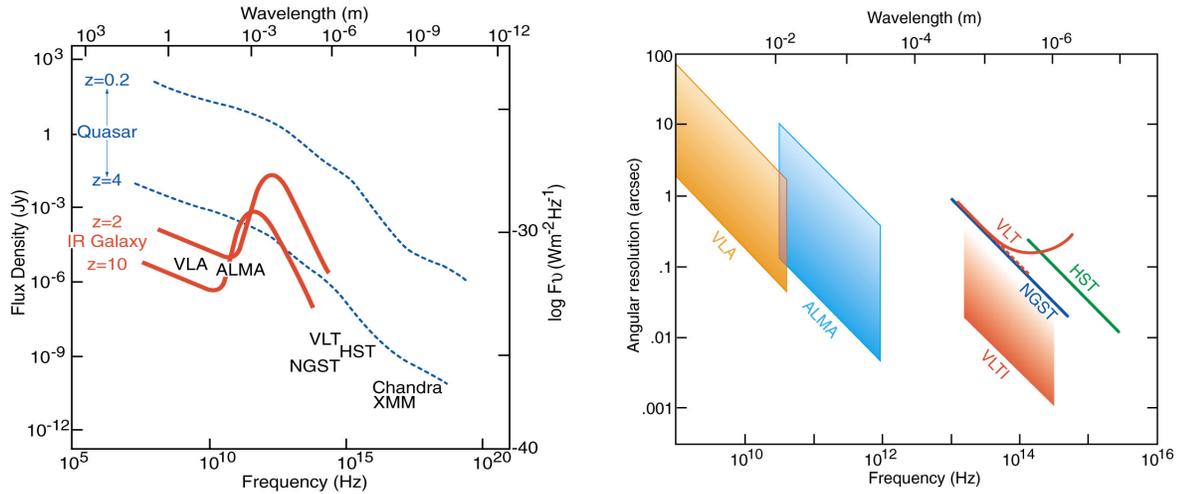
Figure 1: **Left** Sensitivity of ALMA, compared with some of the world's other major astronomical facilities, for typical integration times of several hours. **Right** Angular resolution of ALMA, compared with other major telescopes. The top of the band shown for ALMA corresponds to the compact 150 m configuration, and the bottom corresponds to the large array with 12 km baselines. For the VLT, the solid line corresponds to the seeing limited case, and the dashed line to the diffraction limited case with adaptive optics.

a site that is high, dry, large and flat is required, and a plateau at high elevation (5000 m) in the Atacama region of northern Chile is ideal - hence the Atacama Large Millimeter Array (ALMA).

Figure 1 show the sensitivities and resolving powers of some of the world's major astronomical facilities. These define the "front line" of astronomical research, and any new large telescope opening up a new part of the electromagnetic spectrum should have comparable performance. ALMA will be far more sensitive than either existing millimeter arrays or single telescopes with bolometer arrays. Furthermore, single-dish telescopes can only survey as deep as the confusion limit imposed by the finite beamsize. ALMA represents a giant step for millimeter/submillimeter astronomy, placing it in a unique position at the front line of astronomical research.

1.3   The Atacama Large Millimeter Array

The scientific objectives presented in the sections below lead to the high-level science requirements and technical specifications of the array. It is clear from HST observations of high-redshift galaxies that an angular resolution of at least 0.1 arcsec is required to image the features of star-forming regions in the early Universe, and an angular resolution of order 10 milli-arcsec is required to study the details of nearby protoplanetary systems. At the same time, high surface brightness sensitivity is required in order to image faint extended star-formation regions in our Galaxy and the total emission over nearby galaxies. Thus, a "zoom-lens" capability is called for, with movable antennas and the longest baselines extending to 10 km or more.

The sensitivity requirement is given by the need to detect the most distant star-forming
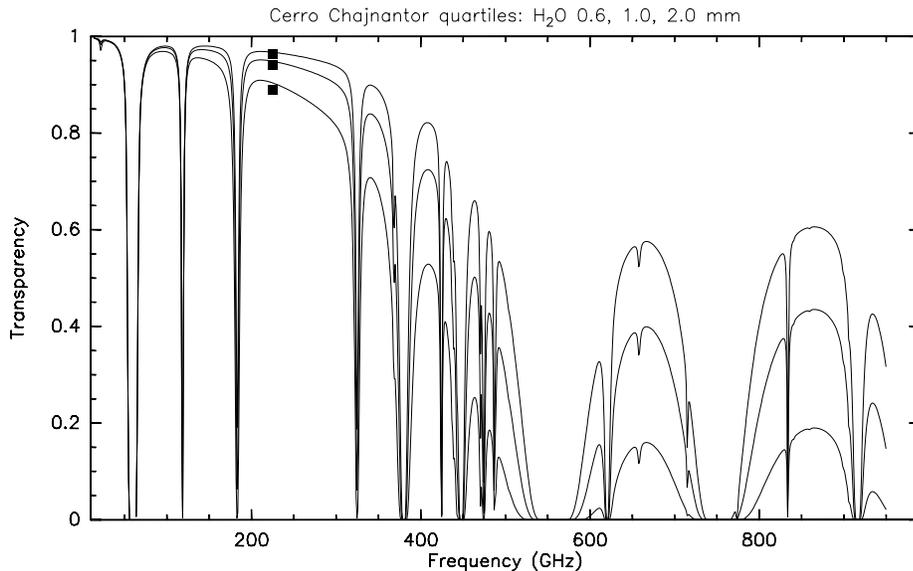
Figure 2: Zenith transmission as a function of frequency under typical atmospheric conditions at the ALMA site. The three curves correspond to the 25%, 50% and 75% percentiles.

galaxies, and to achieve adequate surface brightness sensitivity at high angular resolution. For constant system temperature, the noise in brightness temperature increases as the baseline length squared, and can rapidly dominate the signal, which is limited to a few tens of degrees by the emission physics. In the case of spectroscopic observations, the bandwidths are governed by the linewidths, not the receivers. Furthermore, in some of the millimeter/submillimeter windows, receiver performance is close to the atmospheric noise limits. Thus, for much of the spectral line research, the only way to increase sensitivity is to increase the collecting area. In particular, an angular resolution of $< 0.1''$ can only be reached for thermal lines if the collecting area is increased by an order of magnitude over current values. The high sensitivity is also required for calibration purposes, and for image quality.

The collecting area of an array can be enhanced by increasing the number of antennas, their size, or both. There are clearly several trade-offs to be considered. Small antennas have higher precision, larger field of view, and their large number gives better image quality. The use of large antennas maximizes the collecting area, and reduces the number (and therefore cost) of receivers and the demands on the correlator. For ALMA, 64 antennas of 12-meter diameter gives a good solution.

Excellent imaging capabilities are important to achieve many of the scientific objectives. ALMA should provide instantaneous imaging capability, with the large number of antenna pairs allowing complete uv coverage in snapshot mode. It should provide high fidelity imaging, and wide field imaging capability through the use of mosaicing techniques.

The receiver bands should ultimately cover all the millimeter and submillimeter atmospheric windows. The atmospheric transparency at the high altitude of 5000m considered for ALMA is shown in Fig.2. In total, ten bands would cover the available spectral range, and the ALMA dewars will be built to accommodate all of them. Initially the four highest-priority bands will be provided. The system must be capable of high spectral resolution

Table 1: Flow-down of scientific goals to technical requirements

Science Requirement	Implied Technical Requirements
1. High Fidelity Imaging • Imaging spatial structure within galactic disks; • Imaging chemical structure within molecular clouds; • Imaging protostars in star formation regions	⋄ Reconfigurable Array ⋄ Robust Instantaneous uv-coverage, $N_{ant} > 60$ ⋄ Precision Pointing, 6% of the HPBW ⋄ Antenna Surface Accuracy RMS = 20μm ⋄ Primary Beam Deviations < 7% ⋄ Total Power and Interferometric Capability ⋄ Precise (1%) Amplitude Calibration ⋄ Precise Instrumental Phase Calibration (<10 degrees rms) ⋄ Precise atmospheric phase calibration ($<$ 15 degrees rms) ⋄ Fast switching and water vapor radiometry
2. Precise Imaging at 0.1″ Resolution • Ability to discriminate galaxies in deep images; • Imaging tidal gaps created by protoplanets around protostars; • Imaging nuclear kinematics	⋄ Baselines longer than 3 km ⋄ Precise Instrumental Phase Calibration ($<$ 10 degrees rms) ⋄ Precise atmospheric phase calibration ($<$ 15 degrees rms) ⋄ Fast switching and water vapor radiometry
3. Routine Sub-milliJansky Continuum Sensitivity • To enable imaging of the dust continuum emission from cosmologically-distant galaxies • To enable imaging of protostars throughout the Milky Way • To enable astrometric observations of solar system minor planets and Kuiper-belt objects	⋄ Array site with median atmospheric transparency at 225 GHz $<$ 0.05 ⋄ Quantum-limited SIS receivers ⋄ Antennas with warm spillover $<$ 5 K and aperture blockage $<$ 3 % ⋄ Antennas of aperture efficiency $>$ 75 % ⋄ Wide correlated IF bandwidth, 16 GHz ⋄ Dual polarization receivers ⋄ Array collecting area, $N_{ant}D^2 > 7000$ m^2
4. Routine milli-Kelvin Spectral Sensitivity • Spectroscopic probes of protostellar kinematics • Spectroscopic chemical analysis of protostars, protoplanetary systems and galactic nuclei • Spectroscopic studies of galactic disks and spiral structure kinematics • Spectroscopic studies of Solar System objects	⋄ Array site with median atmospheric transparency at 225 GHz $<$ 0.05 ⋄ Quantum-limited SIS receivers ⋄ Antennas with warm spillover $<$ 5 K and aperture blockage $<$ 3 % ⋄ Antennas of aperture efficiency $>$ 75 % ⋄ Wide correlated IF bandwidth, 16 GHz ⋄ Dual polarization receivers ⋄ Array collecting area, $N_{ant}D^2 > 7000$ m^2 ⋄ Array collecting length, $N_{ant}D > 700$ m
5. Wideband Frequency Coverage • Spectroscopic imaging of redshifted lines from cosmologically-distant galaxies • To enable comparative astrochemical studies of protostars, protoplanetary disks and molecular clouds • To enable quantitative astrophysics of gas temperature, density and excitation	⋄ Receiver bandwidths matched to the width of the atmospheric windows ⋄ Tunable local oscillator matched to the bandwidth of the receivers ⋄ Cryogenic capacity $>$ 1 W at 4 K

for molecular line studies.

The flow-down from major scientific requirements to implied technical requirements is

Table 2: Flow-down of scientific goals to technical requirements (cont.)

Science Requirement	Implied Technical Requirements
6. Wide Field Imaging, Mosaicing • Imaging galactic disks • Imaging the astrophysical context of star formation regions • Imaging surveys of large angular regions • Imaging Planetary surfaces • Solar astrophysics	⋄ Compact array configuration, filling factor > 0.5 ⋄ Instantaneous uv-coverage that fills more than half the uv-cells, $N_{ant} > 60$ ⋄ Antenna surface accuracy 20 μm ⋄ Total power and interferometric capability ⋄ Precision pointing, 6% of HPBW ⋄ Precise amplitude calibration, 1% ⋄ Precise Instrumental Phase Calibration (< 10 degrees rms) ⋄ Correlator dump time 10 msec ⋄ Capability to handle data rates > 100 Mbyte/sec
7. Submillimeter Receiving System • Measurement of the spectral energy distribution of high redshift galaxies • Chemical spectroscopy using CI and atomic hydrides • Determination of the CII and NII abundance in galaxies as a function of cosmological epoch • Chemistry of protoplanetary systems	⋄ Array site with median atmospheric transparency at 225 GHz < 0.05 ⋄ Quantum-limited SIS receivers ⋄ Antennas with warm spillover < 5 K, aperture blockage $< 3\%$ ⋄ Antennas with aperture efficiency > 0.75 ⋄ Precise Instrumental Phase Calibration (< 10 degrees rms) ⋄ Precise atmospheric phase calibration (< 15 degrees rms)
8. Full Polarization Capability • Measurement of the magnetic field direction from polarized emission of dust • Measurement of the magnetic field strength from molecular Zeeman effect observations • Measurement of the magnetic field structure in solar active regions	⋄ Measure all Stokes parameters simultaneously ⋄ Cross correlate to determine Stokes V ⋄ Calibration of linear gains to < 1 %
9. System Flexibility • To enable VLBI observations • To enable pulsar observations • For differential astrometry • For solar astronomy	⋄ Ability to phase the array for VLBI ⋄ Sum port on the correlator for external processing ⋄ Sub-arraying, 4 subarrays simultaneously ⋄ Optics designed for solar observations

detailed in Tables 1-2, and a summary of the technical specifications that satisfy these requirements is given in Table 3. These are the top-level requirements and specifications for ALMA. Table 4 shows the resulting angular resolution and sensitivity for a range of typical observations.

The ALMA project as defined in Table 3 represents the best compromise to achieve the science goals within the capabilities of the current ALMA partners. Negotiations are proceeding with Japan to define an "Enhanced ALMA", which may in addition cover all atmospheric windows from 30 GHz to 950 GHz, provide a compact array of smaller antennas for better wide field imaging, particularly at the highest frequencies where the primary beam of the ALMA antenna is quite small, and provide increased sensitivity and flexibility through a new generation correlator system.

The site selected for ALMA is the high altitude (5000m) Llano de Chajnantor, 60 km

Table 3: ALMA Technical Summary

Array

Number of Antennas	64
Total Collecting Area (ND^2)	7238 m^2
Total Collecting Length (ND)	768 m
Angular Resolution	$0.2''\ \frac{\text{lambda (mm)}}{\text{baseline (km)}}$

Array Configurations

Compact: Filled	150 m
Intermediate (2)	400 m, 1100 m
Precision Imaging	3 km
Highest Resolution	12.0 km

Antennas

Diameter	12 m
Surface Accuracy	20 μm
RMS Pointing	$0.6''$ RSS in 9 m/s wind
Path Length Error	< 15 microns during sidereal track
Fast Switch	1.5 degrees in 1.5 seconds
Total Power	Instrumented and gain stabilized
Transportable	By vehicle with rubber tires, on roads

Receivers

86 - 119 GHz HFET or SIS	$T(Rx) < 6\,h\,\nu/k$ K SSB
211 - 275 GHz SIS	$T(Rx) < 6\,h\,\nu/k$ K SSB
275 - 370 GHz SIS	$T(Rx) < 4\,h\,\nu/k$ K DSB
602 - 720 GHz SIS	$T(Rx) < 5\,h\,\nu/k$ K DSB
Dual polarization	All frequency bands

Intermediate Frequency (IF)

Bandwidth	8 GHz, each polarization
Sampling	4 Gbit/sec, 2 or 3 bits
IF Transmission	Digital

Correlator

Correlated baselines	2016
Bandwidth	16 GHz per antenna
Spectral Channels	4096 per IF

east of the village of San Pedro de Atacama in northern Chile. This is an exceptional site for (sub)millimeter astronomy, possibly unique in the world. The median precipitable water-vapour content of the atmosphere is only about 1 mm, and the topography of the site can accommodate the large configurations required for ALMA. Site characterization studies have been underway since 1995, a collaborative effort between Europe, the US and Japan. These will help to optimize the array and its operation.

1.4   Science with the Atacama Large Millimeter Array

Because it represents a jump of two orders of magnitude in sensitivity and angular resolution, ALMA will undoubtedly produce a major step in astrophysics, comparable to that

Table 4: ALMA angular resolution and sensitivity at $230\,\mathrm{GHz}$ in 1^{hr}, with $T_{\mathrm{sys}} = 140\,\mathrm{K}$, dual polarization, and area $= 7200\,\mathrm{m}^2$.

max. baseline	230 GHz beam	—— Galactic ——		— Extragalactic —		Continuum	
		resolution at 10 kpc	$5\,\sigma$ in δv $= 0.5\,\mathrm{km/s}$	resolution at 10 Mpc	$5\,\sigma$ in δv $= 20\,\mathrm{km/s}$	$5\,\sigma$ in $\delta\nu$ $= 8\,\mathrm{GHz}$	
150 m	$2''$	0.1 pc	0.05 K	100 pc	7.5 mK	$60\,\mu\mathrm{Jy}$	0.4 mK
1.0 km	$0.3''$	$1.5\ 10^{-2}$ pc	2 K	15 pc	0.3 K	$60\,\mu\mathrm{Jy}$	0.015 K
12.0 km	$0.025''$	$1.2\ 10^{-3}$ pc	290 K	1.2 pc	45 K	$60\,\mu\mathrm{Jy}$	2.1 K

provided by the Hubble Space Telescope. A comprehensive review of the scientific capabilities of ALMA is therefore a difficult task, especially as ALMA will be an all-purpose telescope, equally capable of observing the most distant galaxies or our sun.

The main scientific objectives will be the origins of galaxies and the origins of stars and planets. ALMA will make absolutely unique contributions in these areas. It will be able to detect dust-enshrouded star-forming galaxies out to the epoch of reionization - galaxies whose light is both obscured by dust extinction and redshifted out of the usual optical/UV bands. It will also be able to explore in detail the physical and chemical processes of star and planet formation hidden away in nearby dusty molecular clouds and protoplanetary disks.

ALMA will, however, go far beyond these major science objectives, and will contribute to virtually every area of astronomy. It may well have a user community as large as that of the VLT itself. To make this possible, ALMA will be operated in pure service mode, and its data products will be images that are readily accessible to astronomers who are not specialists in the techniques of millimeter astronomy. The following chapters give some idea of the wide range of exciting science that will become possible with ALMA.

2 Galaxies and Cosmology

2.1 The High-Redshift Universe

The early Universe is particularly accessible to observations in the millimeter and submillimeter wavebands. Whereas the broadband flux from distant galaxies is diminished in the UV and optical both due to the redshift and obscuration by internal dust, the same dust produces a large peak in the rest-frame far-infrared, which, when redshifted, greatly enhances the millimeter and submillimeter emission from these objects. Thus, ALMA may very well provide one of the best ways to find the first galaxies that formed after the "dark ages". Indeed, some of the highest redshift objects known today are very luminous sources
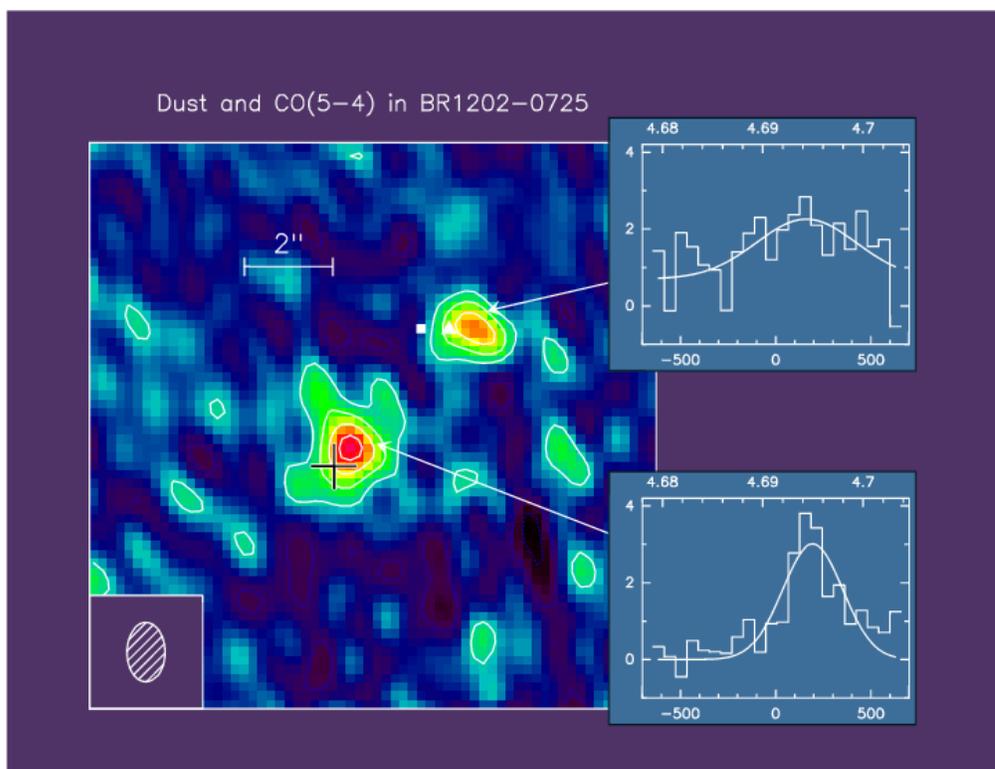

Figure 3: The quasar BR1202-07 at $z = 4.69$, mapped in the dust continuum at $1.3\,\mathrm{mm}$ with the IRAM interferometer. The insets show the CO(5-4) spectra of each component [Omont et al. 1996]

at millimeter wavelengths. The discovery of CO in the $z = 2.3$ galaxy IRAS F10214+4724 dramatically opened up the distant Universe to millimeter and submillimeter astronomy [Brown & vanden Bout 1991]. Since then CO has been detected in several other high redshift objects. The most remarkable discovery is that large amounts of dust and CO molecules are present already at $z = 4.7$, in the object $BR\,1202-0725$ [Omont et al. 1996], the image of which is shown in Fig. 3. This redshift corresponds to a look-back time of 92% of the age of the Universe, showing that enrichment of the interstellar medium occurred at very early epochs.
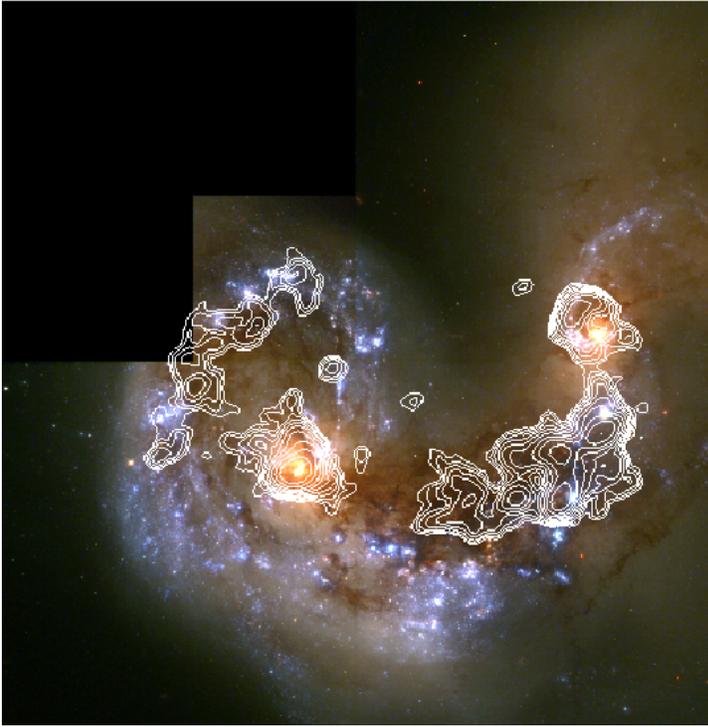
The complementarity of observations made using optical and submillimeter-wave radiation. The Antennae are a well known pair of interacting low-redshift galaxies [Wilson et al. 2000, Mirabel et al. 1998]. Only by comparing their appearance in CO emission (contours) and the *Hubble Space Telescope* image can the starlight absorbed by dust and reradiated at long wavelengths be accurately accounted for.

Figure 4: Optical and submillimeter views of a star forming galaxy

The spectra of luminous star-forming galaxies are dominated by a pronounced feature that peaks at wavelengths close to $100\,\mu$m. This feature arises because the optical and ultraviolet radiation emitted by the hot young stars is absorbed by interstellar dust in the galaxy, which then re-radiates the energy at longer wavelengths. Thus, only a fraction of the total luminosity from a star-forming galaxy may be detectable in the optical/UV, and observations at far-infrared and millimeter wavelengths are essential to provide a complete picture. This is well illustrated by observations of the merging galaxy, the Antennae ([Wilson et al. 2000]; see Fig. 4). The *HST* image is not sensitive to emission from the most dramatic regions of the galaxy where the new stars are being formed; these regions are traced instead by the CO line emission and by the dust continuum emission detected by *ISO* [Mirabel et al. 1998]. The complementarity between the submillimeter and optical wavebands is further illustrated by SCUBA observations of the cluster A1835 ([Ivison et al. 2000]; Fig. 5): while the red cluster members are faint in the submillimeter band, the strongest submillimeter sources are very faint in the optical.

Fig. 6 shows how the far-infrared dust peak becomes redshifted into the submillimeter and millimeter wavebands at high redshifts. The fraction of the energy emitted by a galaxy in the ALMA bands increases with the redshift of the galaxy, due to the large negative K-correction induced as the wavelength of observation is redshifted up the Rayleigh–Jeans slope of the thermal dust spectral energy distribution (SED). This K-correction overcomes the effect of the inverse square law and cosmological surface brightness dimming, so that the flux density measured in the submillimeter waveband is almost independent of redshift from redshifts of about 0.5 to greater than 10. This gives an enormous advantage to
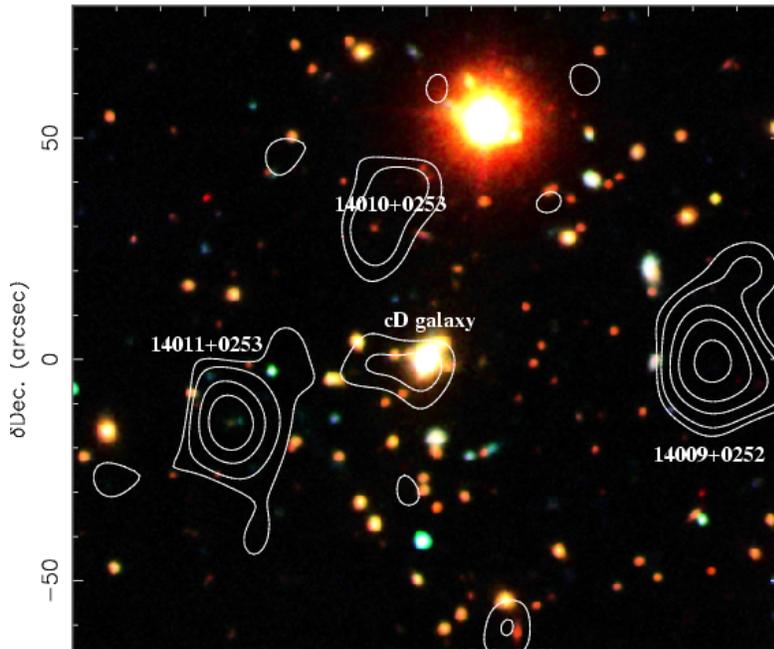
A 850 μm SCUBA image of the core of the cluster A1835 (contours) superimposed on a multi-colour Hale telescope image of the field [Ivison et al. 2000]. Despite the coarser resolution of the SCUBA image, it is clear that the red cluster member galaxies are not typically submillimeter sources, while the counterparts to the labeled submillimeter sources are faint optical objects. The two views of this field hence provide complementary information. ALMA will provide submillimeter images with finer resolution than the optical image.

Figure 5: Optical and submillimeter images of a galaxy cluster

observations at submillimeter wavelengths, where deep surveys are dominated by galaxies at the highest redshifts.

It is now known that there is a very large population of dusty star-forming galaxies at high redshifts. Over the last five years, the intensity of the isotropic background radiation that is generated by all galaxies, both those detected directly and those either too faint or too distant to detect, has been determined. By combining the results of deep optical and ultraviolet observations with measurements made in the far-infrared and submillimeter wavebands using the *COBE* satellite, the amount of energy that has been released by galaxies over the history of the Universe has been assessed (see Fig. 7). This appears to be dominated at high redshifts by energy absorbed and reprocessed by dust, and thus detectable at the wavelengths to which ALMA, rather than near-infrared and optical telescopes, is most sensitive. The intensity of the background radiation at far-infrared wavelengths is only consistent with strong evolution of the population of dusty galaxies with increasing redshift. Evidence for the same strong evolution at redshifts less than about unity is provided by the statistical properties of the galaxies detected in deep surveys using the *ISO* satellite at 15, 90 and 170 μm. This strong evolution greatly enhances the detectability of galaxies over the redshift and wavelength ranges probed by ALMA.

A complete understanding of the star-formation history of the Universe requires a knowledge of the discrete sources that produce this far-infrared/submillimeter background. The pioneering first generation of surveys to explore this distant population has recently been carried out using the SCUBA camera on the JCMT and the MAMBO array on the IRAM 30-m telescope. So far over 100 galaxies have been detected, and the promise of submillimeter-wave surveys of the distant Universe has begun to be realized. The results show that luminous dusty galaxies are both much more numerous and make up a greater

Figure 6: Left: a detailed view of the typical spectral energy distribution of galaxies in the millimeter, submillimeter and far-infrared regime which will be probed by ALMA. The curves show various templates that describe the spectral energy distribution of a typical dusty galaxy. The solid curve also includes the wide range of spectral CO and atomic lines that are detectable in this wavelength range [Blain 2000]. Right: Redshift effect on such spectra, showing the negative K-correction in the submillimeter band, with existing or planned telescope sensitivities mentioned [Guiderdoni et al. 1999].

fraction of all galaxies at high redshifts as compared with the local Universe. However, the angular resolution with these instruments is only 10-15 arcseconds, and the flux limits of existing surveys correspond to the detection of only the most luminous galaxies, with intrinsic luminosities of order $10^{13}\,\mathrm{L_\odot}$. Therefore the properties of less-luminous, more typical high-redshift galaxies cannot be addressed using existing instruments.

As a result of the limited angular resolution, it is difficult to identify the galaxies detected, and to obtain their redshifts. This is clear from Fig. 8, which shows the SCUBA image of the Hubble Deep Field alongside the HST image. The resolution of the HST image is very much greater, but the most luminous SCUBA galaxy is either very faint or absent in the optical and radio [Hughes et al. 1998, Downes et al. 1999], as shown in the right hand panel. Advances in technology for submillimeter wave continuum cameras are making larger fields of view, and thus more rapid deep surveys, possible. However, the fundamental diffraction limit to the resolution that can be obtained using single-antenna telescopes remains. Even the 50-m LMT, the largest millimeter-wave telescope that will be in service in the next few years, will have a resolution limit of about 5 arcsec, and so will still be unable to image high-redshift galaxies. The diffraction limit also prevents the detection of very faint galaxies, as the superposition of the signals from faint sources clustered on the same angular scale as the observing beam adds noise to the images. Beyond a certain depth this confusion noise dominates the images, and sets a limit to the depth of any survey.

Observations   using   the   IRAM   and   OVRO   arrays   [Frayer et al. 1999,
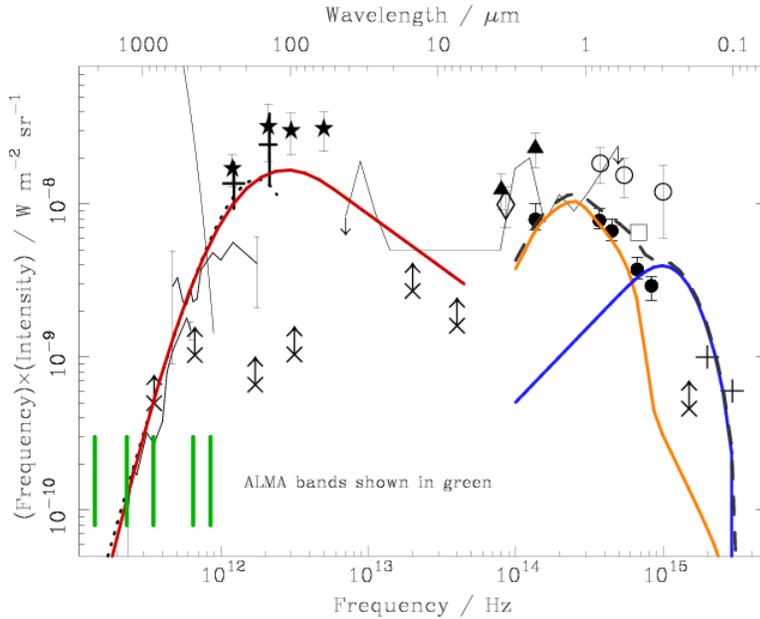
Figure 7: A wide range of measurements of the background radiation from galaxies. The region of the spectrum that will be probed by ALMA is highlighted. The amount of energy emitted from galaxies over the Universe's history in the far-infrared (red line) and optical/ultraviolet (blue line) wavebands are comparable, and so observations of submillimeter and redshifted far-infrared radiation from galaxies using ALMA are important if we are to fully understand the process of galaxy evolution.

Downes et al. 1999, Gear et al. 2001] have been crucial in understanding more about galaxies detected using SCUBA. Detections of CO emission from three SCUBA galaxies, including the bright SCUBA source to the left of Fig. 5, have provided valuable confirmation of their identification with particular optical galaxies, tying together both the submillimeter and optical positions and redshifts accurately. However, these arrays are much smaller than ALMA, with far less sensitivity and angular resolution. It is not practical to use them for carrying out deep galaxy surveys. Observations of submillimeter-wave CO line emission from high-redshift galaxies selected in other wavebands, for example the optical [Omont et al. 1996] and radio [Papadopoulos et al. 2000], and in some cases with several lines [Downes et al. 1999], have provided information about the physical conditions in the interstellar medium of these galaxies. The integrations required are very challenging and time-consuming, however, and the capabilities of ALMA will be required to make such detections rapid and routine.

   The unique sensitivity and resolving power of ALMA will allow submillimeter galaxy surveys to unprecedented depths. MAMBO and SCUBA are limited by confusion to detecting galaxies no fainter than about 1–2 mJy at 240 and 350 GHz, respectively. At any reasonable redshift, this corresponds to the detection of only the most luminous of galaxies, with luminosities of several $10^{12} \, L_\odot$. SCUBA can image about $5 \, \mathrm{arcmin}^2$ of the sky to this depth in several tens of hours of observing time. ALMA will be able to make a high-resolution image of the same field to a similar depth in minutes. Free of limitations due to source confusion, ALMA will be able to image much deeper. Potentially, ALMA
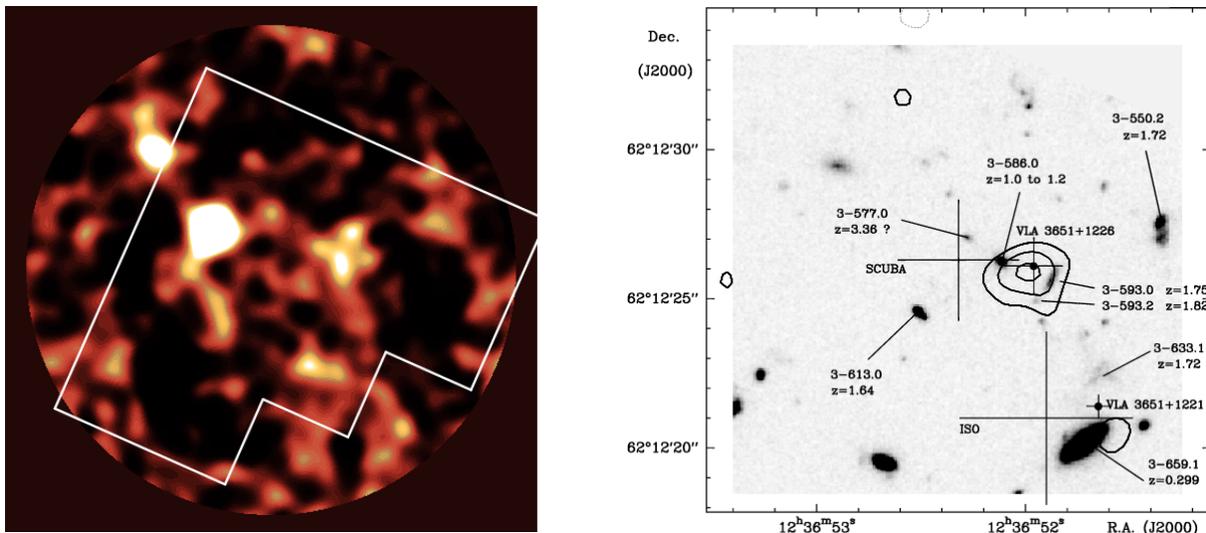
Figure 8: Left: SCUBA 850-μm image of the Hubble Deep Field, with the outline of the optical frame superimposed [Hughes et al. 1998]. The field size is approximately 2.5 arcmin across. Right: an image of the region around the brightest SCUBA source (HDF 850.1) made using the IRAM interferometer at Plateau de Bure at awavelength of 1.3 mm, superimposed on a greyscale version of the *BVI* image from the Hubble Deep Field [Downes et al. 1999]. The cross marked SCUBA indicates the position and 3σ uncertainty of HDF 850.1. Small crosses with black dots indicate radio sources, and the large cross marked *ISO* indicates a 15-μm source. The SCUBA beam is the size of this entire image. ALMA will have higher resolution than the *optical* image at submillimeter wavelengths.

could detect normal galaxies similar to the Milky Way, if they still exist at high redshifts. After staring at a single field for about 2 hours at 350 GHz, ALMA would reach a 5-σ depth of 0.09 mJy. The luminosity of a high-redshift galaxy with a dust temperature of 40 K detected at this flux density is likely to be about $10^{11}\,\mathrm{L_\odot}$, similar to that of the Milky Way, even with this warmer dust temperature (the Milky Way is about 20 K), and so many of these ALMA pointings would thus provide a fair probe of the high-redshift luminosity function. In a shallower two-month survey at 350 GHz, ALMA could detect about 15,000 galaxies in a $1\,\mathrm{deg}^2$ area to a 5-σ depth of 0.7 mJy. Some more detailed discussions of deep ALMA surveys can be found elsewhere[Blain 2000]. The expected populations of faint galaxies that ALMA will probe are shown in Fig. 9, along with the current data available from SCUBA surveys.

Finding high redshift galaxies through their submillimeter continuum emission is only the first step. The useful information comes from the redshift distribution. Some of the submillimeter sources will be identified with optical counterparts, is which redshifts could be measured by large telescopes like the VLT. Others will be too weak, or too obscured. But ALMA will not only be able to locate the continuum sources, but also to measure their redshifts. An estimate of redshift can be obtained photometrically, based on the shape of the Spectral Energy Distribution of the galaxies. The typical spectrum of an active galaxy
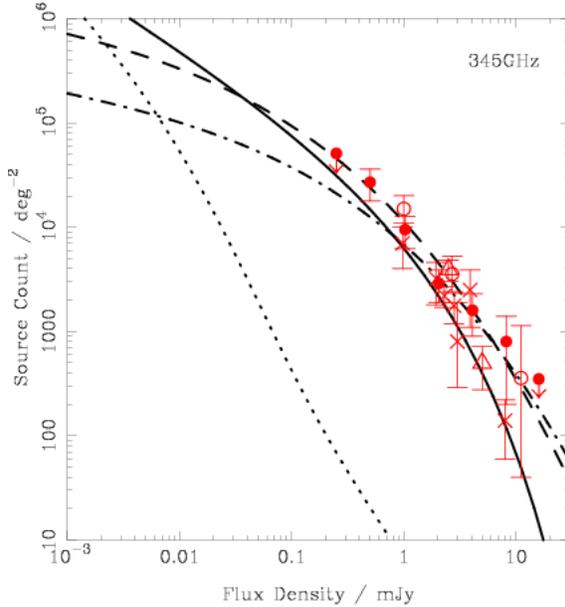
Count data from the array of published SCUBA surveys (red data points), and models of the underlying source population (lines). The data and lines represent the number of galaxies per square degree on the sky that are brighter than the flux density that is plotted on the x axis. The dashed and solid lines represent different models of the numbers of very luminous high-redshift galaxies that both currently fit the data. By probing much deeper in flux density, far beyond the confusion limit of SCUBA, ALMA will be able to discriminate between these cases. The dot-dashed line shows the number of line-emitting galaxies that ALMA will also be able to detect. The dotted line shows the much less numerous population of low-luminosity galaxies like the Milky Way. By probing to extremely faint flux densities, ALMA may start to detect these ordinary galaxies out to high redshifts.

Figure 9: Galaxy counts

produces different millimeter to submillimeter flux ratios, or radio to millimeter flux ratios, for different redshifts (see Fig.6). At low redshifts (≤ 1), the 1.4 GHz radio to 350 GHz submillimeter flux ratio can provide an estimate of the source redshift [Carilli & Yun 1999]. For higher redshifts, this flux ratio saturates, but the peak of the Planck curve at the typical 50–80 K expected for hot dust becomes redshifted into the ALMA frequency bands. Hence, obtaining a broad band SED will constrain the source redshift. Such methods are not very accurate, since individual source properties will produce scatter in these redshift/flux ratio correlation, but should still be useful for determining the global redshift distribution of the sources.

The most exciting prospect, however, is that redshifts will be measured directly and precisely in the millimeter and submillimeter wavebands themselves, using the many spectral lines available, and it will not be necessary to resort to the optical. In some cases the redshift could be determined from a unique spectral line, for which identification is not an issue. This may be possible for the strong [CII] line, which is redshifted into the ALMA bands for $z > 1.5$. This line could be particularly useful for the highest redshift sources at $z > 4$ (Fig.10). Continuous frequency coverage is important for these studies. The detectability of the powerful [CII] line by ALMA is shown in detail in Fig. 10; other lines are similarly easy to detect out to high redshifts. In the case of individual CO lines, information about the redshift could be obtained from the ratio of the intensity of the line and the underlying continuum radiation – a submillimeter equivalent width. This ratio is likely to be greater for lower-excitation lines, thus allowing a preliminary identification of the CO transition most likely to be identified with the line.

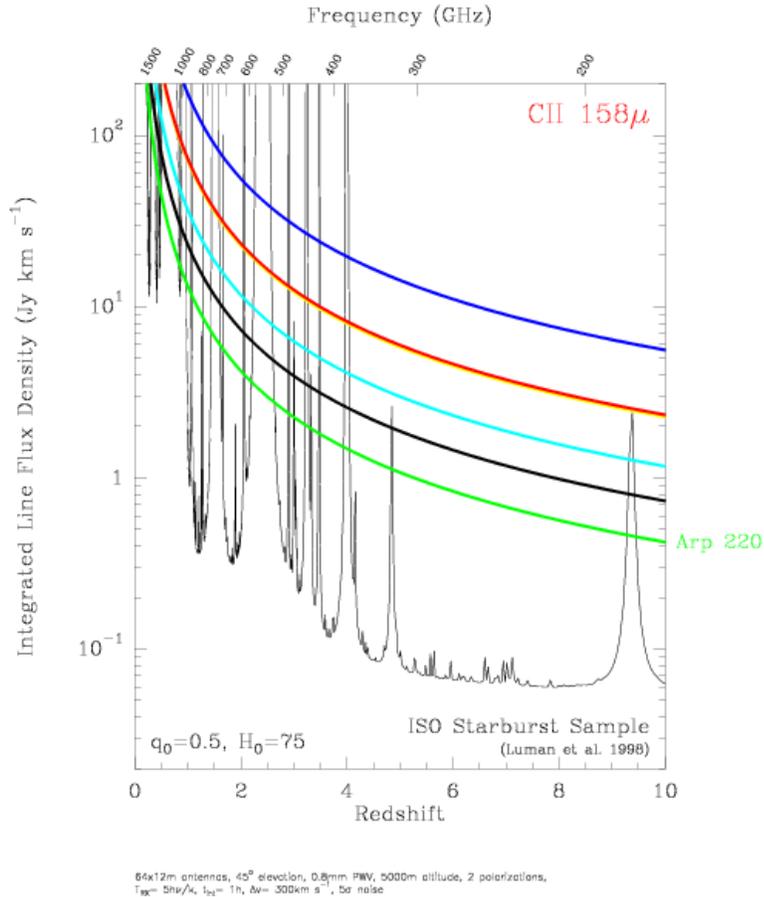The most unambiguous, approach, of course, is to measure two lines from the CO

Figure 10: The detectability of the powerful [CII] line by ALMA.

The colored lines represent the integrated line flux densities one would observe for the 158 μm CII fine structure line from the sample of ultraluminous infrared galaxies observed by [Luhman et al. 1998] using the ISO satellite if those galaxies were at the redshifts indicated by the abscissa. The thin line indicates the typical 5σ noise level of ALMA in two hours of integration, for a velocity resolution of 300 km s^{-1}, and assuming the precipitable water vapor content of the atmosphere is 0.8 mm.

rotational ladder. That ladder is compressed in frequency by a ratio $1 + z$ for redshifted sources, so that, for example at redshifts larger than 3, CO lines are never separated by more than 28 GHz. This property should be related to the frequency layout of ALMA. In a single tuning, ALMA receivers may provide one or two 8 GHz bands. In the latter case, 3 adjacent tunings would cover 48 GHz, and guarantee the detection of two CO lines in sources at redshifts higher than 3.8, and one line for sources at redshifts greater than 1.4. The rate of detection of line-emitting galaxies in a deep survey using ALMA is currently less certain than that of continuum sources, as it depends on details of the line emission properties and the redshift distribution of the dusty galaxies, both of which are relatively poorly known. In the current, limited, sample of detected sources, the typical CO line flux (measured in the 3 mm band) is of order 1–3 Jy.km/s, for 1 mm flux densities of order 3–15 mJy [Guilloteau 2000]. With such numbers, the signal-to-noise ratio on the CO line and 3 mm continuum is nearly identical when a blind search is made by retuning the receivers to cover a 32 GHz bandwidth.

Table 5 gives an example of a redshift survey which would discover ~ 300 sources and determine their redshift distribution. There are of course other possible strategies, but it is clear from the example shown that redshift surveys can be made completely in the millimeter/submillimeter bands, without need for recourse to other (eg optical/IR)

wavebands.

Table 5: An ALMA redshift survey in a $4' \times 4'$ field (about twice the area of the Hubble Deep field)

- **Step 1**
  A continuum survey at 300 GHz, down to 0.1 mJy (5σ). This requires 140 pointings, each with 30 minutes of observation, for a total of 3 days. Fig.9 suggests that such a survey should find about 100–300 sources, of which 30–100 sources will be brighter than 0.4 mJy.

- **Step 2**
  A continuum and line survey in the 3 mm band down to a sensitivity of 7.5 μJy (at 5 sigma). This requires 16 pointings, each with 12 hours of observation, so a total of 8 days. The survey is done with 4 tuning covering the 84–116 GHz frequency range.

    - The 300 to 100 GHz flux density ratio gives the photometric redshift distribution for redshifts $z > 3 - 4$.
    - For expected line widths of 300 km/s, the line sensitivity of this survey is 0.02 Jy.km/s at 5σ. Using the typical SED presented in Fig.6, this should detect CO lines in **all** sources detected in Step 1.
    - At least one CO line would be detected for all sources above $z = 2$, and two for all sources above $z = 6$. The only "blind" redshift regions are 0.4-1.0 and 1.7-2.0.

- **Step 3**
  A continuum and line survey in the 210-274 GHz band down to a sensitivity of 50 μJy (at 5 sigma). 8 adjacent frequency tunings would be required. On average, 90 pointings would be required, each with 1.5 hours, giving a total of 6 days. Together with Step 2, this would allow detection of at least one CO line for all redshifts, and two lines for redshifts greater than 2.

ALMA will deliver exquisite sensitivity and angular resolving power within a relatively narrow field of view. High-redshift galaxy surveys using ALMA will be most efficient if they probe the deepest sensitivity levels that are out of reach of other instruments. Untroubled by confusion, ALMA has unique access to these depths. Wider, shallower surveys will be conducted by single-antenna telescopes to their respective confusion limits; these include SIRTF, ASTRO-F, FIRST and Planck Surveyor in space, and the 50-m LMT and the 15-m JCMT fitted with the SCUBA-2 camera on the ground. However, while these facilities will produce very large catalogues of high-redshift dusty galaxies, none will be able to resolve them, and so detailed studies of the astrophysics of even these bright galaxies will also demand follow-up observations using ALMA to rapidly provide detailed images of both continuum dust emission and spectral line radiation. For example, a 10-mJy source

detected by FIRST at $500\,\mathrm{GHz}$ could be imaged at $10\text{-}\sigma$ significance using ALMA at $650\,\mathrm{GHz}$ in just seconds. These ALMA images will be crucial for enabling the maximum amount of scientific information to be extracted from complementary wide-field surveys.

The long baselines and short operating wavelengths of ALMA will provide the resolving power to image substructure in high-redshift galaxies in detail, revealing their internal structure and the physical processes occurring within. A high-redshift merging galaxy with properties similar to those of the Antennae could be imaged directly by ALMA in as much detail as the image shown in Fig. 4. Furthermore, the kinematics of high-redshift galaxies can be mapped using the many spectral lines available. It will be possible to measure rotation curvces, and hence estimate masses – of great importance for theories of structure formation. Thus, in many ways, ALMA will make a great contribution to the study of distant galaxies and the high-redshift Universe.

2.2   Gravitational lenses

Because of its capability to make extremely deep, high-resolution images of high-redshift galaxies, ALMA will be an excellent and unique instrument for studying gravitational lensing.

The gravitational fields of foreground galaxies, clusters and large-scale structure in the Universe deflect light rays, and so distort the appearance of the background sky. Close to massive objects, the deflection can generate highly magnified multiple images of background galaxies – strong lensing. At greater impact parameters, the effects of gravitational lensing are less dramatic; the shapes of background galaxies are subtly and systematically sheared with negligible magnification – weak lensing. ALMA is ideally suited to studying all aspects of strong lensing in detail. In additional, the faithful determination of the shapes of distant galaxies at high resolution in its interferometric images should allow the systematic effect of weak lensing to be studied from large numbers of archival images. ALMA will further contribute to the study of weak lensing by detecting the spatial distribution of dust emission from high-redshift galaxies, and so determine whether extinction effects are likely to modify significantly the shapes of the optically selected galaxies used in conventional weak-lensing surveys.

By observing the relative positions and magnifications of images produced by a lens it is possible both to study background galaxies that would be too faint to detect without the gravitational magnification, and to impose tight constraints on the gravitational potential of the foreground lens.

In order to study lensing by galaxies, which generates multiple images separated on arcsecond scales, a telescope must have sub-arcsecond angular resolution. The performance of ALMA greatly exceeds this requirement, and so ALMA will be capable of generating very detailed images of lensed objects. There is a double advantage of using ALMA to study distant lensed galaxies. Because luminous dusty galaxies are rare as compared with optically selected galaxies in the local Universe, it is unlikely that the submillimeter-wave emission from a foreground lensing galaxy will be very bright in most cases. ALMA will thus typically obtain a view of distant lensed images without any confusing emission from the lensing galaxy. In addition, while absorption by dust and gas in the lensing galaxy modifies the relative brightness of multiple images observed in the optical waveband,

reducing the amount of information we can obtain about the potential of the lens, ALMA images are immune to this effect. As an example, the Cloverleaf quasar H1413+117, which has already been observed by the IRAM Plateau de Bure interferometer (Fig. 11) could be imaged at much greater resolution in just seconds by ALMA. Both continuum dust emission and submillimeter-wave spectral lines could be detected. High-resolution CO spectral-line observations with ALMA will allow the velocity structure within each image to be resolved, and thus the internal structure and dynamics in the lensed galaxy to be imaged in detail.

a) Total line flux, b) Difference between the blueshifted and redshifted part of the line, c) emission from the blueshifted (with respect to the systemic velocity) part of the line d) emission from the redshifted part of the line. The difference visible in panel b) indicates velocity gradient which, using an appropriate lens model, can be attributed to a circumnuclear disk of about 100 pc around the quasar. In all panels, the greyscale background is an HST optical image.

Figure 11: The Cloverleaf quasar, H1413+117, at $z = 2.56$, mapped in the CO(7-6) line at 0.6″ with the IRAM array [Kneib et al. 1998]

Massive clusters of galaxies generate multiple images with separations on arcminute scales. Bright lensed images of background galaxies have already been detected in such fields using SCUBA, as for example in the case of Abell 1835 shown in Fig. 5. The simulated appearance of a similar rich cluster both in the optical waveband and in the submillimeter is shown in Fig. 12. ALMA's greater sensitivity and resolution ensures that very many more magnified background galaxies will be detected than in existing SCUBA images.

There are well-defined regions in the field of a cluster where images of background galaxies experience very large magnifications, by factors of several tens. ALMA has the capability of making extremely deep images of the regions along these critical lines, to search for extremely faint high-redshift galaxies. This type of critical line mapping is just becoming possible using sensitive spectrographs on 8-m class optical telescopes. About 20 pointings of the ALMA beam would be required to map a 2-arcmin-long critical line at 350 GHz around a rich cluster of galaxies. If 1 hour was spent at each position, then the ALMA image would be able to detect a 120 μJy source at a significance of 5-σ anywhere
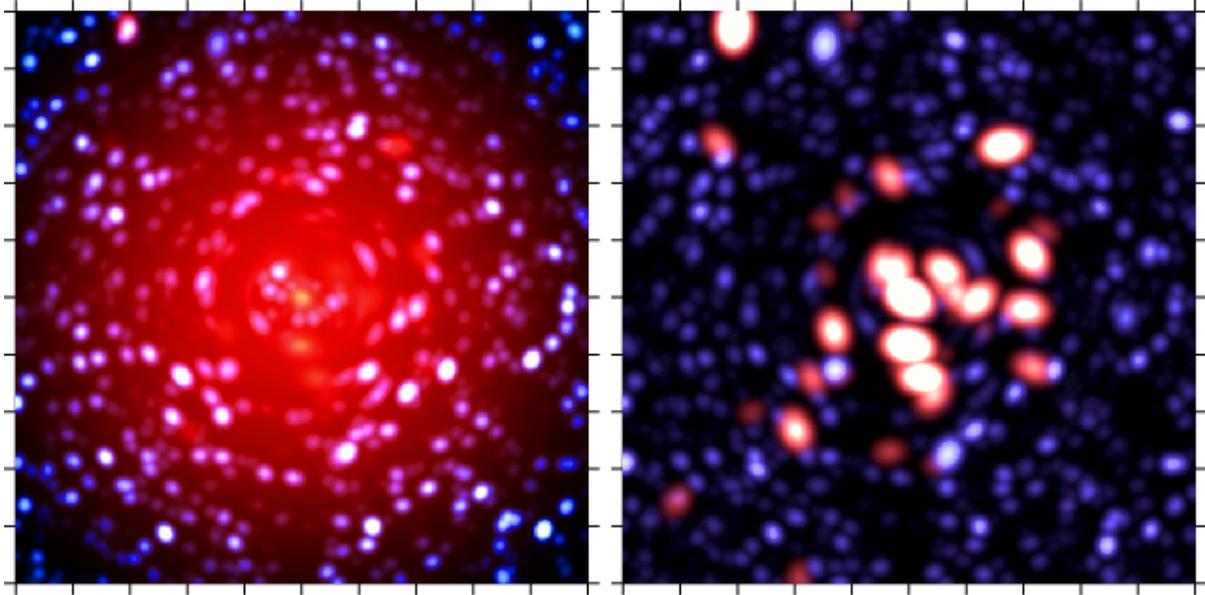
Figure 12: The simulated appearance of a cluster of galaxies at a redshift $z = 0.2$ observed using ALMA at a frequency of 350 GHz at a relatively low resolution of 3 arcsec (left). Red is used to denote galaxies that are members of the cluster and the diffuse emission from the Sunyaev–Zel'dovich effect. Blue is used to represent background galaxies magnified by the cluster. A simulation of the same field in the optical R-band is also shown (right). The submillimeter image is much more sensitive to the high-redshift background galaxies. The images are 100 arcsec on a side. A survey of the whole field with ALMA (about 30 ALMA pointings) would reveal the brightest sources, while the faintest sources (with fluxes of 0.01 mJy) in the 350-GHz image could be detected in about 70 hours of integration per field.

along the critical line. This is the flux density expected from a normal high-redshift galaxy, even in the absence of a lensing magnification. When the magnification of at least a factor of 10 on the critical line is taken into account, galaxies considerably less luminous than the Milky Way could be detected. Hence, ALMA will offer the unique ability to determine the form of the faint end of the luminosity function of high-redshift dusty galaxies.

The source counts of bright submillimeter-wave galaxies that will be detected using future wide-field survey instruments, like the FIRST and Planck Surveyor satellites, are expected to be steeper than those in other wavebands. The steepness of the counts controls the fraction of lensed galaxies expected to be discovered in a survey, with steeper counts corresponding to a greater fraction of lenses. As a result, ALMA will be a unique and powerful tool to rapidly sift through catalogues of potential lenses, and identify those with characteristic multiple image geometries for further detailed investigation [Blain 1998].

2.3   Quasar absorption lines

In order to gain an understanding of star formation processes at high redshift, it is necessary to have a detailed knowledge about the physical and chemical properties of the molecular gas in distant galaxies. This requires observation of rare but diagnostically important

molecules. These lines are weak, but can be accessible when seen in absorption against a continuum background source. In contrast to the strengths of emission lines, which decrease with distance, the depths of absorption lines are, to first order, independent of distance. This has previously enabled optical astronomers to gain detailed information about the atomic gas in galactic halos of high redshift galaxies and to study the intergalactic medium, using high redshift quasars (QSOs) as background continuum sources. The same principle holds true for molecular absorption lines, but the number of studied systems is still very small. This is mainly due to the low continuum sensitivity of present day instruments.

The utility of molecular absorption lines for obtaining detailed information about molecular gas in distant galaxies has been demonstrated through the detection of four such absorption systems at redshifts ranging between z= $0.25 - 0.89$ [Wiklind & Combes 1998, Combes & Wiklind 1997]. In these systems more than 30 different transitions, from 18 different molecules have been detected. Examples are shown in Fig. 13. Most of the molecules have been observed in two or more transitions, allowing a direct derivation of physical properties. In addition 5 different isotopic variants have been detected: ^{13}CO, $C^{18}O$, $H^{13}CO^+$, $HC^{18}O^+$ and $H^{13}CN$.
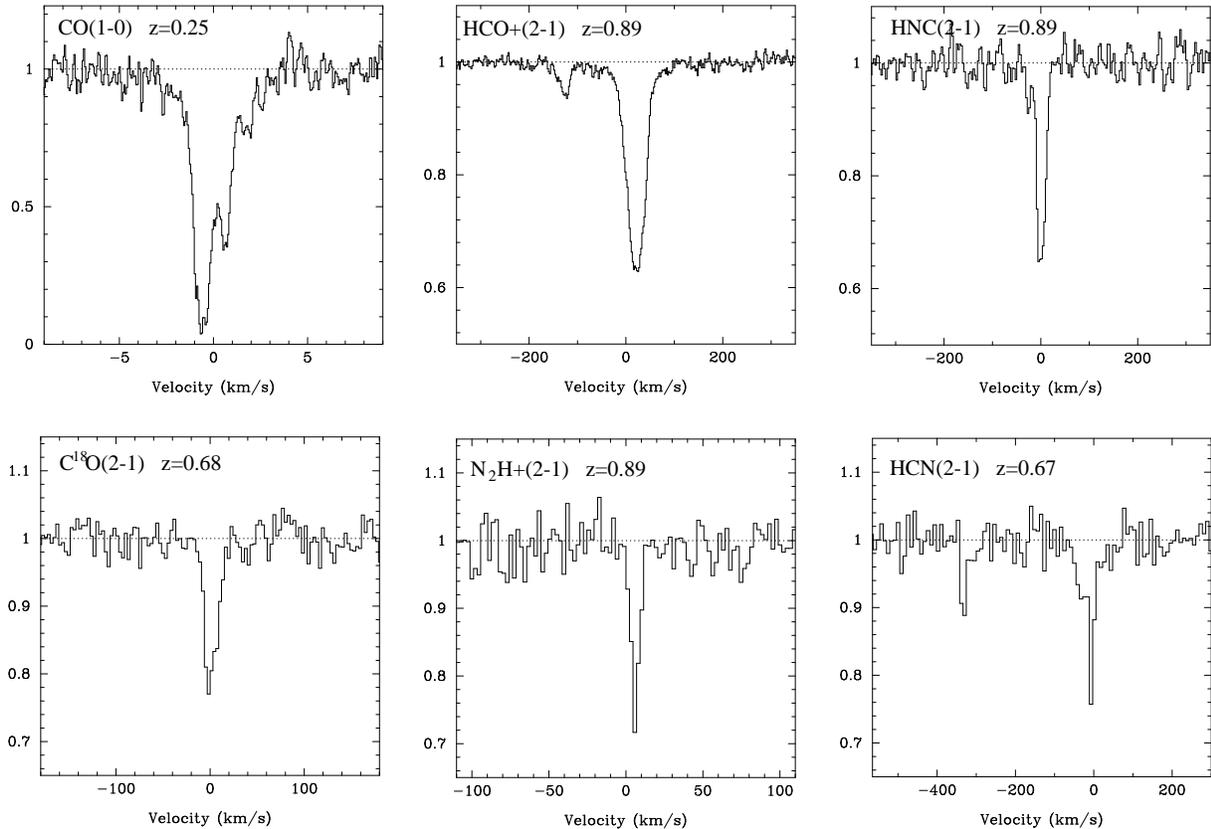

Figure 13: A set of millimeter absorption lines observed along the line of sight towards the quasar PKS 1830-211. The molecular absorption occur at various intermediate redshifts which are given in each panel with the line identification [Wiklind & Combes 1998]

The main reason for studying the detailed properties of molecular gas at high redshifts is that the composition of the molecular gas and its physical conditions are important for

understanding the star formation processes. The assumption of a universal initial mass function, for instance, can only be tested by a detailed comparison of the properties of molecular gas in distant galaxies with that of our own Galaxy. The chemical evolution as a function of redshift is important for understanding the evolution of galaxies as a whole and the star formation activity during different epochs of the Universe. Another important reason is that molecular absorption lines allow a measure of the temperature of the cosmic microwave background (CMB) as a function of redshift. The energy levels of the lower transitions of many common molecules is in the range 4-10 K. At redshifts $z > 0.5$, these transitions will be radiatively coupled to the CMB radiation field. At $z \geq 2$ the CMB is likely to dominate the excitation. Molecular absorption lines are therefore excellent thermometers of the temperature of the CMB.

Molecular absorption lines can also be used to probe the molecular tori surrounding Active Galactic Nuclei (AGN). This has so far had limited success, possibly owing to a coupling between the excitation of the molecules and the radiation field of the AGN itself. By going to much higher transitions and by having a much improved sensitivity, ALMA may make it possible to use molecular absorption lines as a probe of the obscuring regions close to AGNs. This will, among other things, allow a test of the Unified Scheme for Type 1 and 2 AGNs.

The observational strategy for using ALMA to observe molecular absorption line systems consists of two parts. The first is to search for new absorption line systems towards radio loud QSOs, and the second is to study the detected absorption line systems in great detail. Since the detectability of molecular absorption lines depends mostly on the strength of the background continuum, the great advantage of ALMA will be its enormous point source continuum sensitivity compared to present day telescopes. Molecular absorption lines are very narrow compared to emission lines, a few $\mathrm{km\,s^{-1}}$, requiring high spectral resolution $\sim$0.5-5 $\mathrm{km\,s^{-1}}$. In addition, the redshifts of potential absorption line candidates are often poorly known (if at all), requiring a wide frequency coverage. These constraints limit the possibility of detecting more molecular absorption line systems with present day instruments. ALMA will overcome these limitations by offering a high sensitivity and a large instantaneous frequency coverage. With a spectral resolution of 100 kHz, 8 hours of observing time with ALMA gives a 3σ detection limit of 4 mJy (($\nu < 370$ GHz).

The number of radio continuum sources that can be used to search for molecular absorption lines can be estimated from existing number counts at lower frequencies. AGN can have a 'flat' spectrum, i.e. $\alpha \geq -0.5$ ($S_\nu \propto \nu^\alpha$), or a 'steep' spectrum, i.e. $\alpha \approx -0.85$. A 4 mJy detection limit at 100 GHz thus corresponds to a continuum flux of $\sim$25 mJy at 2.7 GHz for a flat-spectrum AGN and $\sim$85 mJy for a steep-spectrum AGN. Radio continuum sources at these flux limits are dominated by AGN, as opposed to milli-Jy sources, where star forming galaxies start to dominate the population. From number-counts of low frequency radio sources we can now estimate the number of sources accessible to ALMA. For a 2.7 GHz flux cut-off at 25 mJy, the number of sources is in excess of 50 000, while the number of sources with a flux cut-off at 85 mJy amounts to 15 000. Hence, even assuming that all radio continuum sources are steep-spectrum, the number of point-like continuum sources available for ALMA will be in excess of 15 000. The number of continuum sources available with present day instruments are just a few hundred.

Another possible source of continuum emission which can be used for molecular absorption line observations is the newly detected class of submillimeter sources at high redshift. These sources emit most of their luminosity through thermal dust emission. At redshifts $z \geq 2$, the modified black-body emission gives a detectable continuum at millimeter and submillimeter wavelengths. From tentative results obtained with SCUBA, the number of sources giving a flux $\geq 4\,\mathrm{mJy}$ at an observed frequency of $350\,\mathrm{GHz}$ is ~ 1000 per square degree. For the hemisphere visible to ALMA, the total number of sources amounts to 2×10^7. Their usefulness to molecular absorption lines, however, depends on how concentrated the dust emission is. If it is caused by galaxy wide star formation activity, an intervening gas cloud will only obscure a small part of the continuum emission and the depth of the line will be strongly diluted. If, on the other hand, the SCUBA sources are powered by AGN, the dust emission is likely to be present on scales of at most a few hundred parsec. This would allow molecular absorption to be used as a probe of the physics and chemistry of the gas itself. In fact, the huge number of such sources means that even if the AGN fraction is low, say 1%, these sources will outnumber the AGNs by a factor >10.

For strong continuum sources, ALMA will be sensitive to extremely small amounts of molecular material. For instance, with a background continuum source of 1 Jy, the 3σ detection level for several CO transitions will be around $3 \times 10^{13}\ \mathrm{cm}^{-2}$ and for HCO^+ (which in absorption gives an opacity similar to that of CO) the detection level will be 6×10^{12} cm^{-2}. These column densities correspond to very small optical extinctions. ALMA will thus be able to detect molecular gas at a level where we do not expect to see any evidence of intervening gas from broad band colours of QSOs.

2.4   Sunyaev-Zel'dovich observations with ALMA

ALMA's very high brightness sensitivity will provide a unique tracer of CMB anisotropies on small angular scales. Operating in the 35 GHz band (Band 1) in close-packed configuration, ALMA will achieve a brightness sensitivity of a few micro Kelvin on angular scales of a few to tens of arcseconds in only a few transits of a source. No other planned instrument is capable of making these observations, and when ALMA begins observing it will provide the natural complement to the dedicated Sunyaev-Zel'dovich (SZ) telescopes currently being planned in Europe and the US. These latter instruments are optimized to achieve micro-Kelvin sensitivity on scales of 2-10 arcmin, to allow surveys for clusters and proto-clusters through detection of the SZ effect, which peaks on these angular scales for virialized cluster gas. ALMA will provide the same brightness sensitivity as the planned SZ survey telescopes, but on angular scales an order of magnitude smaller. The key range of angular scales for ALMA is roughly 15 arcsec (multipole l = 25,000) to 2.5 arcmin (multipole l = 2,500).

The first unique application for ALMA will be high-resolution imaging of the SZ effect in clusters. Fig. 14 shows a simulation of a 2.5×10^{14} solar mass cluster at redshift 1, imaged by ALMA at 35 GHz in the compact array in 4 hours of integration time. Although many hundred such clusters should have been detected by the end of the decade, by both satellite missions such as Planck and ground-based interferometers, only ALMA will be able to make the well-resolved images of these clusters which are necessary to understand the dynamical processes within the cluster gas. This is an essential requirement if accurate

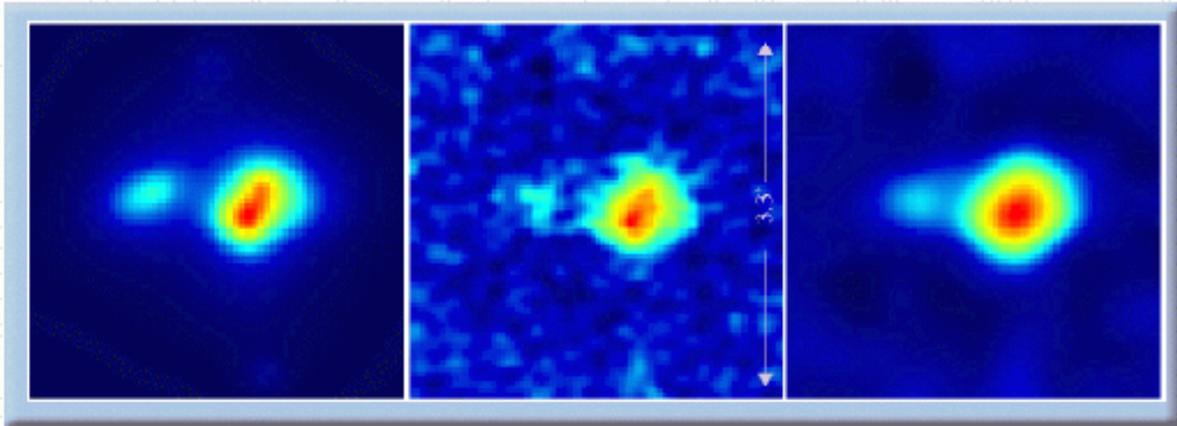Hubble constant values are to derived from SZ observations.

Figure 14: The left panel shows a hydrodynamical model of a 2.5×10^{14} solar mass cluster at redshift 1. The center panel is a 4-hour ALMA image of the cluster at 35 GHz in compact configuration. The rightmost panel shows the same image, smoothed to a resolution of 22 arcsec. (Figure courtesy of John Carlstrom).

The second unique application for ALMA will be imaging of small scale CMB anisotropies caused by early-universe physics. Existing limits from current millimeter interferometers such as BIMA are already coming very close to interesting levels [Holzapfel et al. 2000]. For example, reionisation of the intergalactic medium at high redshift due to early bursts of star formation and massive black hole formation will both leave small-scale SZ imprints on the CMB which are only detectable with ALMA. [Benson et al. 2000] have recently studied the anisotropies caused by star-formation-induced reionisation, and predict a power spectrum with 10^{-6} anisotropies which peak on scales of multipole $l = 10,000$. The effects of massive black-hole formation have been studied by [Aghanim et al. 2000] who predict that the CMB power spectrum should show a strong peak due to these at multipole numbers of 10^5 to 10^6 (i.e. angular scales of 0.6-6 arcsec). The Vishniac-Ostriker effect also peaks around $l = 10^4$ to 10^5. Although the detailed physics which goes into these predictions is somewhat poorly constrained, it is clear that ALMA is the only instrument planned capable of probing the CMB power spectrum on these angular scales with sufficient brightness sensitivity.

2.5   Gas in Galactic Nuclei

The centers of galaxies are often invisible or at least partially obscured at optical wavelengths because of the presence of large amounts of dust. With its high spatial resolution, sensitivity and wide frequency coverage, ALMA will offer a unique means to study both the dust and the gas, which is predominantly molecular in the nuclei of galaxies incuding the center of our own Galaxy. It will be possible to map at an unmatched level of detail the structure of the nuclei, trace the kinematics of the molecular gas and probe the

physical and chemical conditions pertaining deep in the central regions of galaxies from starbursts to AGN. Such detailed studies, which will be done for a large number of sources, will address one of the most fundamental problems of modern astronomy - the nature and evolution of the nuclei of galaxies.

The power of galactic nuclei spans a continuous range covering quasars, AGN, radio galaxy nuclei, ultraluminous and starburst galaxies, and the more modest activity in nearby galaxies and the center of the Milky Way. While discs around massive black-holes are suspected to be the source of power for AGNs and quasars, it is clear that huge luminosities can be generated by starbursts triggered by galaxy-galaxy interactions and mergers that drive large quantities of gas towards the central regions. ALMA will throw much more light on these problems. It will allow us to determine the masses and kinematics of optically obscured galactic nuclei with a resolution of a few parsecs and image the distributions of a variety of molecules. In nearby galaxies, the current resolutions of $1 - 2''$ reveal details on scales of $\approx 15 - 30 \, \mathrm{pc}$. This is sufficient to resolve hitherto unseen clumps in the central molecular concentrations - already IRAM interferometer observations of, e.g. NGC 1068, are revealing the structure around the nuclei of nearby Seyfert galaxies [Schinnerer et al. 2000]. An array with ten-times the sensitivity would allow such studies to be extended to all currently known Seyferts and give high resolution maps of their circumnuclear discs.

The potential of this kind of research is shown in the case of Arp 220. Arp 220 with an infrared luminosity of $1.5 \times 10^{12} \mathrm{L}_\odot$ is one of the nearest ultraluminous infrared galaxies (ULIRGs). In optical images, two faint tails are seen indicating a recent tidal interaction. High-resolution radio and near-infrared imaging show a double nucleus separated by $0.98''$ (see Fig. 15). Pratically all of Arp 220's prodigious luminosity originates in a small disk-like region (of 250 pc radius) which contains most of the gas and dust mass ($\mathrm{M_{H_2}} \sim 9 \times 10^9 \, \mathrm{M_\odot}$). This central core is hidden from direct observation at all wavelengths shortward of the far-infrared range and the opacity is so high that the dust is optically thick even at far-infrared wavelengths. Analysis of ISO observations of fine-structure lines from various atoms and ions, in particular the absence of high-ionization lines, leads to the conclusion that the energy output of Arp 220 is produced by a massive starburst with a star formation rate of $100 \, \mathrm{M_\odot} \, \mathrm{yr}^{-1}$ and not by an active galactic nucleus.

This conclusion has been reinforced by recent milliarcsecond resolution radio imaging, which did not reveal a high brightness continuum that could be identified with an AGN. These observations, which resolve out most of the radio continuum emission, show the presence of a dozen unresolved sources, identified as luminous radio supernovae, providing direct evidence for Arp 220's violent star formation [Menten 2000].

Given the high dust opacities and the fact that sub-arcsecond resolution observations at far-infrared wavelengths have to await future space interferometer missions, radio and (sub)millimeter interferometry provides the only means for detailed studies of the excitation and dynamics of the interstellar medium in the cores of ULIRGs in the local universe. The limited spatial resolution achieved today with current millimeter interferometers precludes detailed studies of the molecular clouds in Arp 220 and the interactions of newly formed and exploding stars with their environment. ALMA will allow us to probe the warm molecular gas and the dust continuum emission with a resolution of $\approx 0.02''$, which corresponds to $\sim 7 \, \mathrm{pc}$ at Arp 220's distance of 75 Mpc. It will thus be possible to resolve
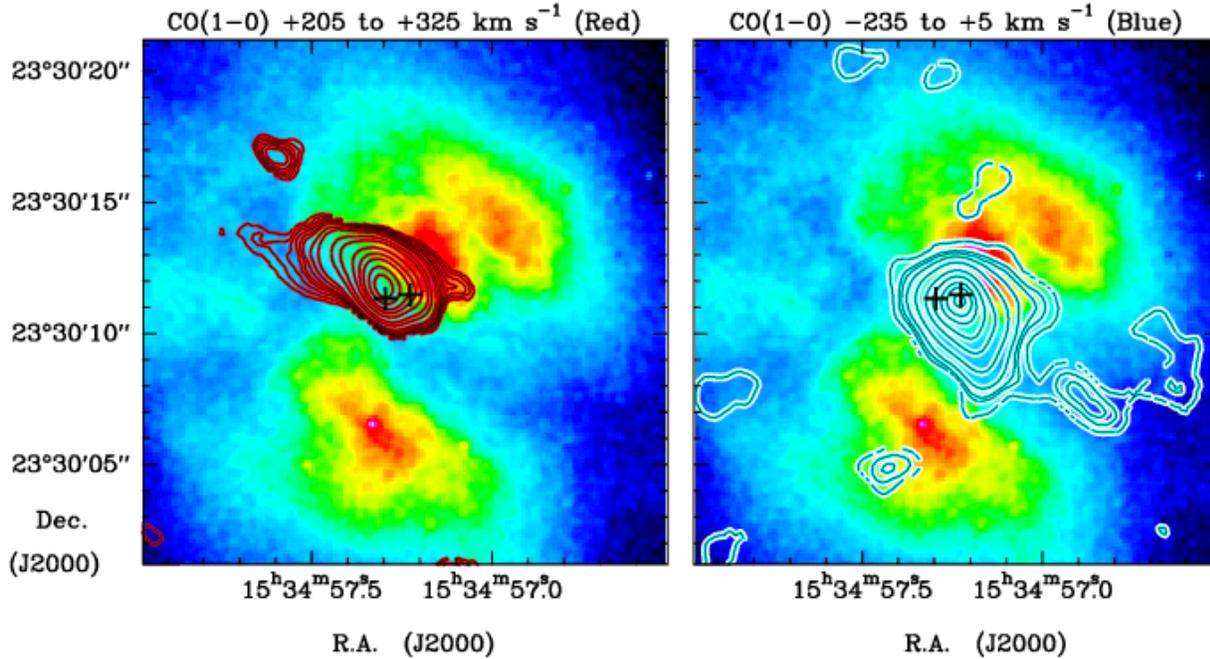
Figure 15: Arp 220 in the CO $J = 1 - 0$ emission (contours) superposed on a false-color presentation of the HST V-band image. The CO emission (mapped with a beam of $1.6'' \times 1.1''$) is shown in two different velocity ranges corresponding to the red- and blue-shifted gas (left and right panels, respectively). The crosses indicate the radio nuclei at centimeter wavelengths. Adapted from [Downes & Solomon 1998].

single molecular clouds in Arp 220 and study their physics and chemistry using tracers including the higher rotational lines of CO, HCN and the [C I] fine structure lines.

A key aspect of ALMA's capabilities is its combination of mapping speed and high sensitivity on the longest baselines. This will enable to observe a statistical sample of galactic nuclei and to resolve scale structures of a few parsecs in nearby nuclei and of $\approx 100\,\mathrm{pc}$ in luminous galaxies at redshifts of 0.1-0.2. The existing millimeter arrays have already provided details of gas streaming along central bars, central 100 pc scale disks or torii in nearby AGN (< 15 Mpc), and the dynamics of the merging process at scales of a few 100 pc in nearby ULIRGs. VLBA observations at centimeter wavelengths are able to probe into the sub-parsec scale structures through observations of, e.g. H_2O masers and radio continuum emission, revealing a thin disk-like structure surrounding the AGN as in the spectacular case of NGC 4258 [Greenhill & Gwinn 1997]. A critical missing size scale is from ~ 50 pc to 1 pc. There is no information about the molecular gas distribution and dynamics in this region, and it is exactly these size scales that are important to view directly how the gas loses sufficient angular momentum to bring it down to the scales where it can feed and/or obscure the AGN. ALMA will be able to resolve a structure like the circumnuclear disk of the Galaxy [Guesten et al. 1987] at distances out to 20 Mpc. Molecular imaging with ALMA will enable us to image directly a parsec-scale molecular torus in a large number of galaxies, and determine accurately the column densities and optical depths through the torus. These measurements will unambiguously test and refine the unified models for AGN. For these nearest cases, ALMA will enable to study the violent
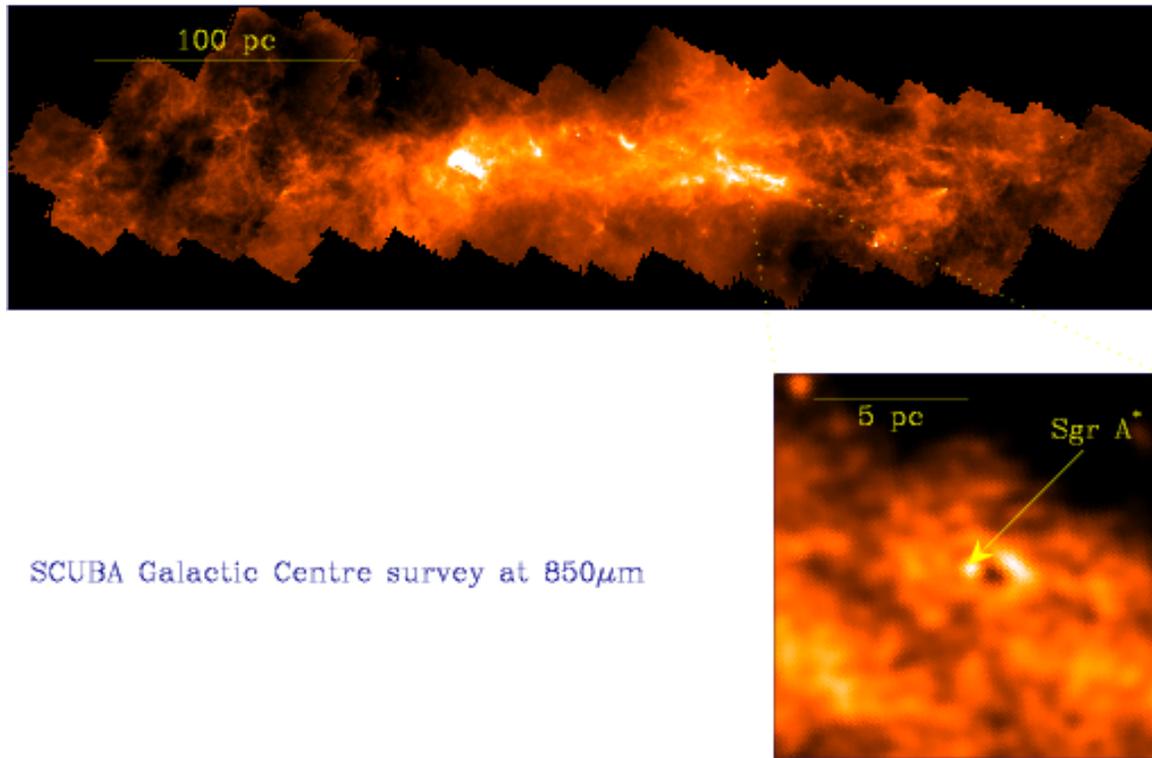
Figure 16: SCUBA survey of the Galactic Centre central molecular zone at 850 μm ([Pierce-Price et al. 2000]). The resolution is $14''$ (corresponding to 0.6 pc at the distance of 8 kpc to the Galactic Centre). The map covers a region 350 pc in extent, showing the incredible complexity of the gas in galactic nuclei. Around 10 per cent of the Galaxy's ISM is visible in this image. Inset is an image of the dynamical center of the galaxy, the black-hole candidate Sgr A* and its circumnuclear disk. ALMA will be capable of imaging individual star forming cores in this region, and probing the gaseous environment of Sgr A* on scales of tens of AU.

merger process on scales of tens of parsec, such that we might actually be able to witness the birth of a new massive black hole as a result of the galaxy collision. Studies similar to those of Arp 220 will be carried out in hundreds of more distant mergers, enabling us to identify which conditions present in the progenitor galaxies govern the presence of an intense starburst, the formation of a quasar nucleus, and the (possible) ultimate evolution into an elliptical galaxy.

Finally, our own Galactic center provides a unique opportunity to study at very high spatial resolution the physical processes occurring in a galactic nucleus, in particular the nature of the molecular cloud population and the physical phenomena occuring in the vicinity of a massive black hole. Roughly one tenth of the Galaxy's ISM resides within a region 400 pc in extent, in a crowded environment with strong shear, magnetic fields and frequent cloud-cloud collisions. At the dynamical center lies Sgr A*, a strong radio continuum source and the best black hole candidate in the known Universe - proper motion studies indicate it has a mass of approximately 2.5 million solar masses. ALMA's southern hemisphere location makes the Galactic center a key science target.

An indication of the complexity of the ISM in galactic nuclei is shown in Fig. 16, which shows a SCUBA image at 850 μm of the central 300 pc of our own Galactic plane. This

map is dominated by optically-thin dust emission, tracing about 5×10^7 solar masses of molecular clouds with a mean temperature of 20 K. Its structure is extremely complex, showing numerous filaments, wind-blown bubbles and supernova remnants. ALMA will be capable of studying the details of star formation and molecular cloud structure within this region at a resolution of better than 1000 AU in both dust and molecular emission, probing a wide range of densities and temperatures. Such observations are essential if we are to understand the nature of the ISM in the Galactic center and its star forming properties. Polarisation measurements will also be extremely important in establishing the magnetic field geometry within the molecular gas – strong fields are thought to permeate much of the nuclear region.

2.6   The Active Galactic Nucleus engine

In the field of continuum studies of powerful AGN, ALMA will open up many new possibilities. Amongst these are the following: (1) Studies to understand the jet physical properties and production mechanisms. Observations would include flux density and polarisation monitoring with ALMA itself and using ALMA as the largest element of a global mm-VLBI array. Such a millimeter VLBI array would have the highest angular resolution of any instrument in astronomy i.e. $\approx$10μas. (2) ALMA can also be used as a millimeter survey instrument to discover new classes of AGN. Very little is known about the AGN population selected at frequencies > 20GHz, and there are reasons to believe such new classes of very young or intermittently emitting AGN exist. (3) ALMA can be used to image individual resolved classical double sources in detail, at frequencies above the spectral ageing break in hotspots and jet shocks. (4) ALMA can be used to study the properties of the host galaxy via its thermal and molecular emission.

In the nuclei of radio-loud AGN millimeter and submillimeter observations are special in being able to probe closer to the base of the jet than at any other waveband except X-ray [Königl 1981, Hutter and Mufson 1986]. Millimeter observations can probe much closer than centimeter because opacities due to synchrotron self-absorption are lower. The short variability timescales observed in millimeter/submillimeter wavebands [Türler et al. 1999] supports the expectation that the millimeter and submillimeter emission arises on very small scales. ALMA will be able to monitor the total flux and polarisation variability of thousands of blazars. Such monitoring can statistically constrain jet properties such as Doppler boosting factor. In addition there is increasing evidence of a strong correlation between millimeter and the gamma-ray flares which dominate the total radiation budget of jets [Krichbaum et al. 2000]. ALMA combined with future gamma-ray satellites will be able to confirm this correlation, derive time lags between the two phenomena and see whether the gamma ray flux is linearly or quadratically related to the millimeter flare intensity. Such observations will constrain the gamma-ray production mechanism (internal Synchrotron Self Compton, or Inverse Compton scattering of external seed photons).

ALMA will also be used to study active nuclei as a single phased-up element of the global mm-VLBI network. In this role ALMA, because of the large increase in sensitivity it provides, will revolutionise the range of AGN targets accessible to the mm-VLBI technique. In combination with other large telescopes detection thresholds at 90 GHz will approach 20 mJy compared to about 1 Jy today. Such an array will have 20 μas

resolution at 215 GHz. There are in addition plans for a 30 m class space based VLBI antenna operating up to 90 GHz (ARISE) which would further increase both resolution and sensitivity. Whereas present day mm-VLBI is restricted to studying the cores of bright blazars, a future ALMA-centered mm-VLBI array would have enough sensitivity to be able to observe new classes of objects such as cores of lobe-dominated radio loud sources. Furthermore in many nearby sources the resolution will approach the scales on which jets are thought to form (10–100 gravitational radii). As an example of what might routinely be possible in the ALMA era consider the recent 90 GHz and 43 GHz VLBI results on M87 [Junor et al. 1999]. In this AGN HST observations show that there is a central black hole of mass 10^9 solar masses. The 3 mm VLBI observations with a resolution of 100 Schwarzschild radii show an increasing opening angle as the base of the jet is approached. This observation suggests that we are resolving the region in which the jet is being collimated. Similar studies could be done on Centaurus A and other southern AGN using a future ALMA-centered mm-VLBI array.

An exciting class of objects to study with future mm-VLBI are the sources showing intra-day variability (IDV) at centimeter wavelengths. These objects are most likely explained via interstellar scintillation of < 5 μas sized emission components [Kedziora-Chudzer et al. 1997]. The very high brightness temperature emission ($\approx 10^{15}$ K) and significant circular polarisation inferred in these IDV sources [Maquart et al. 2000] have been argued as being due to a coherent continuum emission mechanism. Confirmation of such a mechanism will require high resolution mm-VLBI observations with 10 - 20 μas resolution. Confirmation would strongly constrain the physical conditions in the jet. There is the possibility that such high brightness temperature emission could also illuminate the relatively cold ionised gas in the accretion disk, via the induced Compton scattering mechanism [Simcell & Coppi 1996]. This would make it possible to study the structure of the accretion disk directly with VLBI observations.

Finally for mm-VLBI studies, there is the exciting possibility of directly imaging the gravitational shadow of the supermassive black hole in our galactic center [Falcke et al. 2000]. Based on fits to the spectrum of Sgr A* a very compact sub-millimeter emission component has been identified with size comparable to the Schwarzschild radius. General relativistic bending of the radiation by the central black hole is then expected to cause an apparent hole in this emission of size 10 gravitational radii (30 μas), see Fig. 17. Such an observation would be a direct confirmation of a black hole, would give a independent estimate of its mass and would be a confirmation of general relativity in the strong limit. Existing 3 mm and short baseline 1 mm wavelength VLBI observations have already shown compact, sub-AU, emission from our galactic center [Krichbaum et al. 1998]. Given these detections the proposed VLBI experiment to detect the black hole shadow should be feasible using global VLBI involving ALMA at 215 GHz or 350 GHz.

ALMA will also be able to contribute to AGN studies via survey observations. There are as yet no large area blind surveys of the sky above 30 GHz, but 100-beam single dish surveys are planned [Browne 2000] which should be followed up by ALMA observations to determine accurate positions and spectra. Deep ALMA-only integrations over limited areas of sky are another strategy for detecting new source populations [Cooray 1998]. It is probable that such surveys will reveal whole new classes of AGN. As well as blazar sources they might
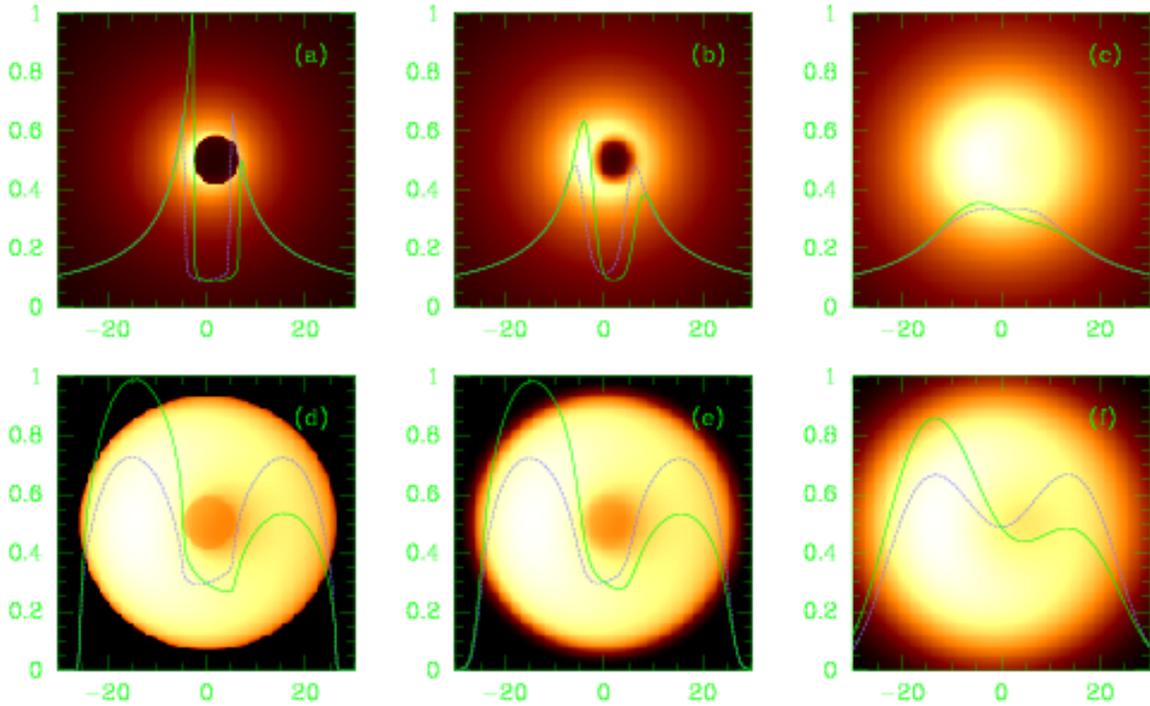
Figure 17: An image of an optically thin emission region surrounding a black hole with the characteristics of Sgr A* at the Galactic Center [Falcke et al. 2000]. The black hole is here either maximally rotating ($a_* = 0.998$, Figs. a-c) or non-rotating ($a_* = 0$, Figs. d-f). The emitting gas is assumed to be in free fall with an emissivity $\propto r^{-2}$ (top) or on Keplerian shells (bottom) with a uniform emissivity (viewing angle $i = 45°$). Figs. a&d show the GR ray-tracing calculations, Figs. b&e are the images seen by an idealised VLBI array at 0.6 mm wavelength taking interstellar scattering into account, and Figs. c&f are those for a wavelength of 1.3 mm. The intensity variations along the x-axis (solid green curve) and the y-axis (dashed purple curve) are overlayed. The vertical axes show the intensity of the curves in arbitrary units and the horizontal axes shows the distance from the black hole in units of R_g which for Sgr A* is 3.9×10^{11} cm ~ 3 μarcseconds.

also confirm a significant population of "high frequency peak" (HFP) sources, with spectra peaking at 40 GHz or higher that have recently been identified [Dallacasa et al. 2001]. These are interesting objects because analogous sources which peak in the GHz range have been shown via VLBI monitoring to be very young AGN with sizes 100 pc–1000 pc and ages 1000 to 10000 years [Owisanik & Conway 1998]

Observations suggest a very strong correlation between peak turnover frequency and source size and age so that even younger sources (age < 100 years) are expected to peak at millimeter wavelengths. If the HFP population are indeed very young sources then by studying the properties of the host galaxies it should be possible to constrain proposed mechanisms by which AGN activity is triggered. Detected objects can also be followed up by mm-VLBI or via total flux monitoring with ALMA to constrain rates of expansion and ages.

ALMA can also be used to image synchrotron emission in resolved "classical double" sources like Cygnus A or kiloparsec jet sources like M87. In comparison with radio observations ALMA observations will image relatively young electrons which have not yet lost energy to synchrotron losses even at millimeter wavelengths. ALMA images will therefore trace sites of electron acceleration in hotspots or jet shocks. Detailed inter-comparison with radio images will constrain the age since the electrons were accelerated. Another advantage of millimeter observations is that they will be unaffected by Faraday depolarisation or Faraday rotation allowing for the unambiguous determination of the intrinsic magnetic field directions and strength in the radio source lobes.

2.7   Galaxies in the Local Universe

ALMA will have both the high-resolution ($< 0.1''$) and the sensitivity required to map in detail the main dynamical components of spiral galaxies: spiral arms, bars, and also the nuclear embedded bars and resonant rings that will constrain theoretical scenarios of galaxy evolution. In nearby galaxies, the identification of gravitationally bound individual molecular clouds will give insight into the H_2/CO conversion ratio through virial analysis.

ALMA will make large-scale, fully-sampled images of the molecular gas in galaxies, with the resolution of the HST ($0.1'' = 14$ pc at 30 Mpc) and better. These maps will give the information on both parsec and kiloparsec scales needed to explore the relationship between star formation, gas density and gas kinematics, in comparison with other tracers, like the atomic gas, Hα or radio-continuum. The role of density waves and spiral structure will be addressed in detail. The small scale structure of the molecular component revealed by these high-resolution maps will clarify the mechanisms of starbursts in galaxies, and the associated feedback processes, such as outflows of molecular gas, bubbles and winds. In starbursts and mergers, young stellar clusters that are thought to be the progenitors of globular clusters have been discovered [Whitmore et al. 1999].

ALMA will improve our knowledge on the formation of globular clusters by resolving the giant molecular clouds (20 pc in size) in which they are born. The high-resolution images from ALMA will allow us to study individual molecular clouds in nearby galaxies of all types up to 100 Mpc distance. This will not only improve our knowledge in the star-formation processes at small and large scales, but also determine the H_2/CO conversion ratio in all environments (starbursting or quiescent galaxies, with various metallicities), through virial mass analysis. This is of prime inportance, since at the present day there are still large uncertainties (order of magnitude) concerning in the true molecular content of galaxies.

It has been known now for more than a decade that elliptical galaxies also possess small amounts of cold interstellar gas and dust [Knapp et al. 1989, Wiklind et al. 1995] that is thought to have been acquired in galaxy interactions and mass exchange, or come from the vestiges of the merger of two gas-rich spiral galaxies. The goal in mapping the molecular gas component in these galaxies is to determine from the dynamics and morphology of the medium the origin of this gas, and the formation scenarios of ellipticals.

Already maps at high spatial resolution with HST have revealed nuclear disks of a few arcseconds in scale in many ellipticals, through the absorption of dust lanes. The high spatial resolution and sensitivity of ALMA will allow us to trace these disks in the CO

lines to determine their dynamical state. In some circumstances, counter-rotating disks have been observed, pointing to the external or merger origin of the gas (cf the prototype of major mergers between spirals, NGC 7252, [Wang et al. 1992]).

The gas can be used also to trace the triaxial potential and the possible dark matter contribution in elliptical galaxies. These systems are much less well known than spiral galaxies in this aspect, since there is usually no gaseous rotating disk, where a low-dissipation component traces the potential without ambiguity. With high sensitivity it will be possible to tackle the problem of the existence of cooling flows, and the fate of the cooled gas. At present, it is still a puzzle to know the fate of the cooling gas: present millimeter instruments are not sufficiently sensitive, and the gas might form very low mass stars that are not bright enough.

If elliptical galaxies are formed essentially by accumulated minor mergers, there should exist shells of stars and gas surrounding most of them, as the remains of the accreted small companions. Recently CO lines have been detected in stellar shells around Centaurus A [Charmandaris et al. 2000]. Detecting such vestiges of the formation mechanisms in most elliptical galaxies requires the sensitivity of ALMA.

Finally, the higher excited CO lines (e.g. CO(6-5)) will be useful to quantify the starbursts that occur sometimes in elliptical galaxies, as the result of external accretion. High spatial resolution is necessary to distinguish the extent of the molecular component, and the origin of the excitation. The radio-galaxies, mostly ellipticals, are suspected to have a dense molecular torus surrounding the AGN, and this particular component could be traced by high-dipole molecules such as HCN or CS.

2.8   ALMA and the Magellanic Clouds

Observations of the Magellanic Clouds also require a high sensitivity, high resolution instrument like ALMA. These low metallicity systems provide unique opportunities to study molecular clouds in an interstellar environment which is very different from that in the Milky Way. This is important in the study of star formation since, although it is accepted that molecular clouds are the birth-places of stars, the details of cloud formation and evolution into stars are poorly understood. The investigation of the process under different conditions is essential and the Magellanic Clouds provide us with just that possibility.

The Magellanic Clouds differ from our Galaxy in having a lower metallicity (about 1/4 for the LMC and 1/10 for the SMC), a lower dust content (by a similar amount), and a star formation rate per unit area about 10 times larger than in the solar region. These factors are expected to cause important differences in the properties of the interstellar medium and of stars, some of them already well established. For example, the molecular clouds have different properties and the winds of the young, massive stars are less intense, causing strong differences in their evolution. The CO emission is weak, partly because of metallicity, partly because of poorer dust shielding (and greater photodissociation) but partly because the angular resolution of present observations is insufficient to investigate the compact molecular sources within these clouds. ALMA, with a resolution better than 0.1 arcsec, will facilitate high sensitivity observations of molecular clouds with a linear resolution equivalent to studies of clouds in the Milky Way with several arcsec. ALMA will bring decisive new observations to bear on a number of specific areas of study, and

some examples are given below.

Molecules in the diffuse interstellar medium. Plateau de Bure observations of various galactic molecular lines in absorption in front of strong extragalactic radiosources have revealed relatively high abundances of molecules like HCO^+, H_2CO, HCN or HNC. Their chemistry is not understood. Similar observations will become possible with ALMA in front of weaker radiosources behind the Magellanic Clouds. It is already known from HI emission/absorption measurements that the diffuse interstellar medium is colder in the Magellanic Clouds, probably due to more efficient cooling by C^+. Differences with our Galaxy are also expected in molecular line absorptions. Their observation with ALMA should bring a better understanding of the diffuse medium in general when combined with the current observations of atomic, ionic and molecular absorption with FUSE and with future observations of the [CI] lines with ALMA.

Structure of molecular clouds. The weakness of the CO lines in molecular clouds of the LMC and SMC in spite of their higher temperatures suggests that the line emission comes only from clumps, while CO and probably H_2 are entirely photodissociated in the interclump medium. This should be observable directly with the high angular resolution of ALMA, which will also observe higher lines of CO and lines of molecules sensitive to density, bringing a better understanding of physics and chemistry within the clouds.

Star formation. ALMA will be able to discover and to resolve molecular dense cores, young stellar objects with their jets and envelopes, and ultracompact and compact HII regions ionized by very young massive stars. This has not been possible until now in the Magellanic Clouds, and as a consequence we know essentially nothing on the first steps of star formation in an astrophysical context different from the galactic one.

Stellar mass loss. The best way to obtain quantitative information on mass loss is by observing the envelopes in the millimeter/submillimeter continuum for hot massive stars and in the CO lines for cold (AGB) stars. This is not currently feasible in the Magellanic Clouds, but will be within reach of ALMA at least for the brightest cold objects. Combined with near- and mid-infrared observations already available or to be performed soon, this will allow a significant advance in our understanding of the final phases of stellar evolution.

Planetary nebulae and supernova remnants. ALMA will be able to observe the brightest of these objects in the millimeter continuum and for some of them in molecular lines, with unprecedented sensitivity and angular resolution. This may reveal differences with their galactic counterparts. An important advantage of observing them in the Magellanic Clouds is that their distance is well known, contrary to the situation in our Galaxy.

3 Star and Planet Formation

Stars form from the gravitational collapse of dense cores within the innermost regions of interstellar molecular clouds. The new stars and protostars are often hidden by hundreds of magnitudes of visual extinction, so the details of the star formation process are far from being well understood, and the formation of stars and planets continues to be a central problem in modern astrophysics. Protostars and proto-planetary systems can only be studied at millimeter and sub-millimeter wavelengths. ALMA will be the first telescope capable of resolving the key physical processes taking place during the collapse of molecular clouds, the structure of protostars and that of the proto-planetary disk systems, and determine the chemical composition of the material from which future solar systems are made. Morevover, ALMA will also be capable of studying the detailed structure and kinematics of the molecular clouds where stars are born with unprecedented detail. There is no doubt that a detailed understanding of star and planet formation and molecular cloud structure will be one of ALMA's great scientific legacies.

3.1 The initial conditions of star formation

3.1.1 Structure of interstellar clouds

The galactic molecular clouds where stars are born present a remarkable self-similar structure, characterized by fractal dimensions and power laws relating their mass, size and internal velocity dispersion [Falgarone et al. 1991, Stutzki et al. 1998]. The origin of these scale-free properties may be linked to the turbulent nature of the gas motions. Self-gravity could also be the driver [Pfenniger & Combes 1994]. Small scale structure is observed in all molecular clouds, even far from star-forming regions. Sizes as small as ≈ 200 AU are inferred (from arguments related to radiative transfer) [Falgarone et al. 1998] but no threshold has been found yet to the hierarchy, outside of star forming regions [Heithausen et al. 1998]. In starless dense cores, the sites of future star formation, turbulence is still present, likely fed by magnetic waves.

If turbulence is at the origin of the fractal structure of molecular clouds, the hierarchy stops at the dissipative scale. Dissipation may occur in MHD shocks, since interstellar turbulence is supersonic and magnetized. The thickness of a C-shock in a molecular cloud is linked to the strength of the ion-neutral coupling and ranges between 100 and 1000 AU depending on the ion density. Instabilities are expected to develop in these shocks producing still smaller structures [Mac Low & Smith 1997]. Dissipation may also occur at the edge of intense coherent vortices thought to contribute to the intermittent nature of turbulence dissipation. The viscous dissipation scale depends only on the energy transfer rate in the cascade and on the molecular viscosity. We expect the size of such dissipation regions to be ≈ 10 AU in molecular gas which can be reached with ALMA in nearby clouds. The local heating of the gas in these dissipative structures is as large (and probably as rare) as the burst is intense. The signatures are therefore kinematic (large velocity shear or divergence), thermal (temperatures much larger than average) and chemical (formation of species characteristic of hot chemistry) [Joulain et al. 1998, Flower et al. 1998]. These size scales are close to the smallest scales observed in the cold neutral medium [Heiles 1997],

suggesting a common origin in the small scale structure of the cold medium, whether atomic or molecular.

With ALMA, for the first time, the threshold of the hierarchy of non-star-forming clouds may be reached and characterized. It is probably the only way to identify the agents producing the observed structure (turbulence, self-gravity,...). This will open new, unique perspectives in the understanding of star formation for the following reasons. First, spectroscopic information is essential because the dissipation scales (whether shocks or vortices) have specific kinematic signatures. Mid-infrared spectroscopy presently does not have sufficient spectral resolution. In dense cores, confusion may be alleviated by the velocity information. Second, high spatial resolution is essential since 10 AU at 100 pc corresponds to 0.1″. Third, access to high excitation transitions is a tool of major importance due to the large anticipated temperature of the regions of dissipation (several hundreds Kelvin or more) buried in much colder material. Fourth, access to several molecular species is also important because of the specific chemical signatures and for a comparison at small scales of ion and neutral kinematics, probing their coupling. Fifth, mosaicing capabilities are needed because *(i)* not all the regions will show up as active in terms of dissipation, although the surface filling factor of such regions is predicted to be close to unity and because *(ii)* the texture of shocks and regions of large vorticity in turbulence is closer to long filaments or convoluted sheets than to point sources [Pety & Falgarone 2000]. Last but not least, the enormous sensitivity of ALMA will have a crucial impact because the tiny regions of dissipation are not bright in any molecular line. The same is true for precursors of protostellar cores which will have little contrast above the background.

3.1.2   Millimeter absorption spectroscopy

Exploring the physical and chemical properties of the diffuse interstellar gas is essential to understand the initial conditions of the gas which will be incorporated into the denser clouds from which stars might ultimately form. Comparing the chemical characteristics of the diffuse gas with those of dense molecular clouds is also important to follow the chemical evolution of matter as it cycles through the various phases of the interstellar medium. ALMA will bring a entirely new dimension to this type of studies.

Traditionally, physical and chemical studies of diffuse interstellar clouds have been carried out at optical wavelengths. Besides a handful of simple diatomic molecules, these studies have revealed the presence of hundreds of diffuse interstellar bands (DIBs), a spectroscopic mystery for more than 50 years which has not yet been unravelled. Recent suggested identifications include (ionized) Polycyclic Aromatic Hydrocarbons (PAHs), fullerenes, and long carbon chains [Ehrenfreund 1999]. The inferred abundances are $10^{-6} - 10^{-7}$. How can these complex molecules survive under the intense ultraviolet radiation? Attempts to observe other related molecules at visible and ultraviolet wavelengths have failed. Recently, however, it has proven possible to observe this diffuse gas in absorption at millimeter wavelengths against background continuum sources, leading to the first detection of tri-atomic molecules in diffuse clouds [Lucas & Liszt 1997, Hogerheijde et al. 1995]. Relative abundances of the molecules are grossly similar to those of dark clouds, but with several notable differences.

With present instruments only a few sources are strong enough to obtain detailed

absorption spectra. With ALMA this number will be increased by a factor of ~ 100, and consequently the field of low density cloud studies should be rejuvenated. Simple statistics currently limit the studies to diffuse clouds in absorption. The large number of sources that can be observed with ALMA will greatly increase the chance that the line of sight passes through a translucent cloud and even a few dark clouds. It will be possible to measure abundances in these clouds without the bias of selective collisional excitation. The relative abundances of many species will then be measured by a straightforward, non-ambiguous method. The study of line shapes will be used to obtain clues to the physical structure of the gas. Monitoring of time variations of absorption profiles (at ~ 1 yr time scales) will allow the sampling of extremely small scale (a few AU) structures within molecular clouds. Comparison of the spectra of several sources behind the same cloud will allow determination of the geometrical influence of the surrounding radiation on the cloud chemistry. In contrast to optical and UV absorption studies, millimeter absorption will allow comparison of diffuse cloud properties in different regions of the Galaxy beyond the solar neighborhood.

Observations may include a systematic frequency survey of a few selected sources (for a 2 Jy source, 4 hours of integration are needed to cover the whole 3 mm band at a level of $\tau = 0.005$ rms). Such surveys of the chemistry may also reveal the building blocks of the DIB carriers. Systematic observations of many sources close to the galactic plane at the HCO^+ frequency could be extremely rewarding for galactic structure and dynamics, as the population of sampled clouds is complementary to that of previous HI studies, and not biased against molecular clouds.

Another aspect is that it will be possible to use measurements of this type to compare our galaxy with nearby external galaxies wherever background continuum sources of ~ 0.1 Jy can be found. It will also be possible to refine present limits on putative cold molecular gas in outer galactic regions by at least one order of magnitude.

3.1.3 Dense pre-stellar cores

The starless cloud cores from which low-mass stars form have been the subject of much recent study, since they provide clues to the initial conditions of gravitational collapse. ALMA's high sensitivity, high angular resolution, and full uv-coverage will allow us to measure the properties of both the large and the smallest dense cores in star-forming regions; hence the distribution of clump masses will be studied with very high detail down to limiting masses well below a Jupiter mass, in different complexes of star formation.

Recent studies of some nearby star-forming regions have allowed detailed studies of the structure of clouds just prior to and during the process of star formation. A highly "clumpy" structure is observed, and it is natural to guess that the mass distribution of the high density clumps within the region of star formation is related to the mass distribution of stars which eventually are formed in the clumps. In other words, the fragmentation of the cloud may determine the initial mass function (IMF) of the young stars. This is of importance for many reasons, including the fact that the IMF is a crucial parameter in the study of the evolution of galaxies. As an example, Figure 18 shows the region in the ρ Oph molecular cloud at 160 parsec from the sun imaged by [Motte et al. 1998] with the IRAM 30-m telescope. The figure also shows the mass distribution of 59 pre-stellar cores
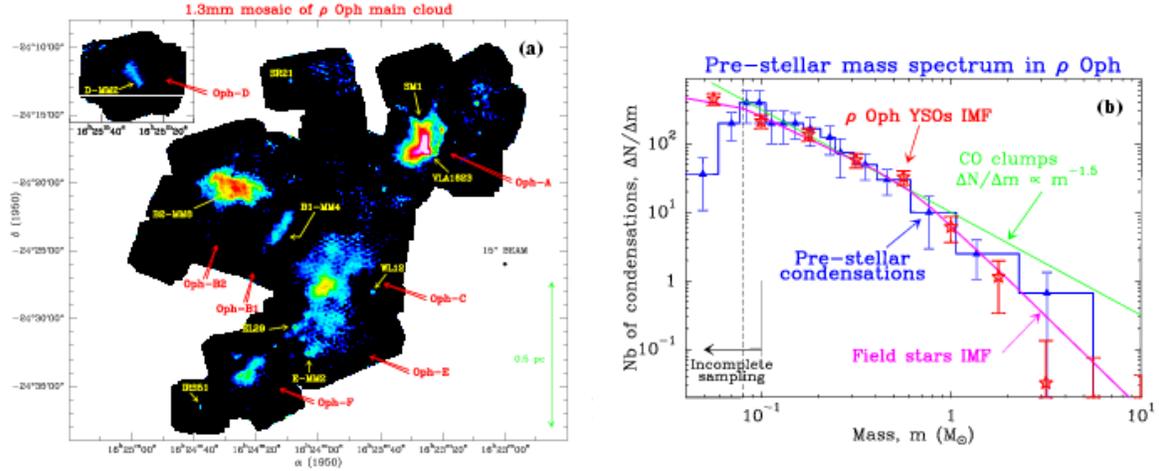
Figure 18: Left: Millimeter continuum mosaic of the ρ Oph main cloud obtained with the MAMBO 19-channel bolometer array at the IRAM 30-m telescope [Motte et al. 1998]. The dense cores (e.g. Oph-A) show small scale ($< 5\,000$ AU) fragments which are either circumstellar structures around infrared YSOs (e.g. EL 29) or pre-stellar condensations (e.g. E-MM2). The pre-stellar condensations may be the direct progenitors of protostars. Right: Mass spectrum of the 59 pre-stellar condensations identified in the map (blue histogram; adapted from [Motte et al. 1998]). Above the Jeans mass of dense cores (i.e. for $> 0.5\ M_\odot$), it is significantly steeper than the power-law observed for CO clumps (green line, e.g. [Williams et al. 2000]). In contrast, the mass spectrum of pre-stellar condensations looks remarkably similar to the field star IMF (pink curve, e.g. [Kroupa et al. 1993]) and to the ρ Oph YSOs IMF (red star markers, [Bontemps et al. 2000]). This result suggests that the stellar IMF is determined at pre-stellar stages by the fragmentation. ALMA will allow to probe the clump mass distribution well below $0.1\ M_\odot$, and down to planetary masses at the distance of ρ Oph.

identified within the cloud. The mass distribution follows a law $\Delta N/\Delta M \propto M^{-1.5}$ below $0.5\ M_\odot$, and $\propto M^{-2.5}$ above $0.5\ M_\odot$. Such a mass spectrum is thus similar to the stellar IMF, which follows a law $\propto M^{-1.2}$ for stellar masses in the range 0.1 to 1 $M_\odot$, and $\propto M^{-2.5}$ for stellar masses in the range 1 to 10 $M_\odot$. This similarity suggests that the IMF of embedded clusters might be established at the prestellar stage of the star formation process. But higher sensitivity observations are clearly needed. For instance, the mass spectrum remains unknown for clump masses below 0.1 $M_\odot$ due to the sensitivity limitations of current telescopes. ALMA will permit study of the clump mass distribution down to planetary masses in complexes at the distance of ρ Oph, and this will give important clues about the low-mass end of the IMF. In addition, it is unclear how many of the clumps so far detected will form multiple rather than single stars; only very high angular resolution observations with ALMA can answer this question. ALMA will also make possible an estimate of the clump mass distributions in many more molecular complexes. This will give important information about the variations of the IMF throughout the Galaxy.

Recently, slow gravitational infall has been detected in several starless cores. Figure 19 shows L1544, one of the best cases for the study of infall. Infall motions are well detected as a deep red-shifted absorption in the J=2–1 line of CS. Such cores are just resolved by
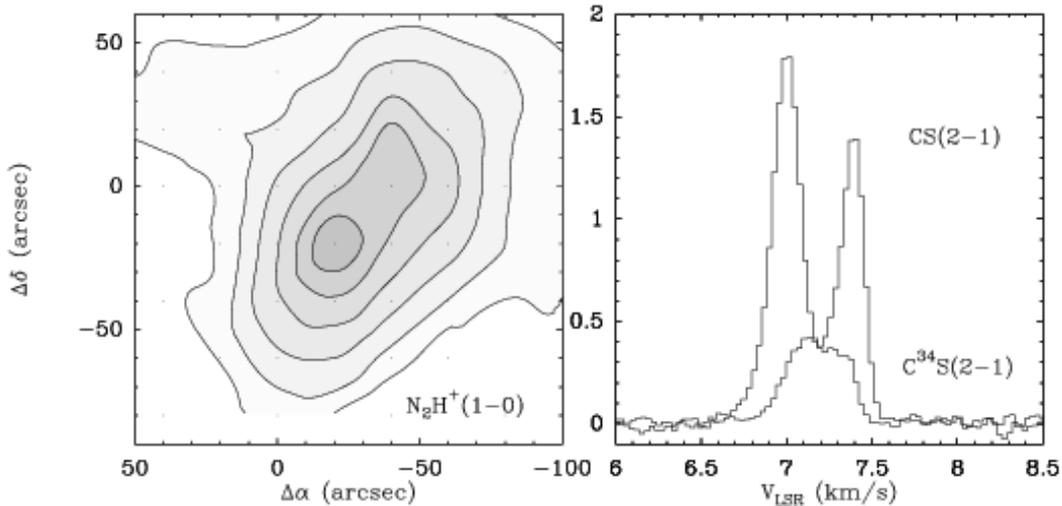
Figure 19: Anatomy of the low-mass starless core L1544. Left: N_2H^+ emission observed with the IRAM 30-m telescope, showing a flattened dense core of $\simeq 10\,000$ AU. Right: spectra of CS and $C^{34}S$ towards the core, showing the strong self-reversal with redshifted self-absorption and blueshift asymmetry which are thought to be characteristic of the signature of infall motion. Infall velocities of only 0.01 km.s^{-1} are inferred from the line profile.

single-dish telescopes, but current interferometers lack the brightness sensitivity to image them in anything but the brightest molecular lines. ALMA will be capable of imaging these systems in both dust and molecular line emission, producing images with hundreds of thousands of spatial pixels, with many tens of spectral measurements at each point. Such data cubes, with many millions of independent data points, will provide unprecedented views of the initial conditions of star formation, and allow us to create detailed models of the physical and dynamical state of these cores.

There is also the very exciting prospect of mapping the magnetic field configuration in star-forming cores through polarized dust emission: current theories suggest that low-mass star formation is controlled by the magnetic field, and ALMA will be the first telescope capable of high-resolution imaging of these magnetic field structures (see Figure 20).

3.2   Young Stellar Objects

A comprehensive theory of both high and low-mass star formation is an essential requirement if we are to understand galaxy formation and evolution, and the formation of sun-like stars and planets. The increased sensitivity and angular resolution of ALMA, which exceeds by far those of present instrumentation, will revolutionize our understanding of the star formation processes. One way of seeing this is to remember that the length scale on which gravitational instability occurs, the Jeans length, is of order 0.1 pc, and is only just resolved even in the nearest star forming regions by current millimeter-wave telescopes. But most of the important physical processes during collapse occur on much smaller scales. The collapsing envelopes of protostars have sizes of 10,000 AU; protostellar disks have radii of order 100 AU (see Tables 6 and 7); the processes which generate stellar multiplicity must operate on scales of 1-1000 AU; protostellar outflows are generated on scales < 10 AU; and
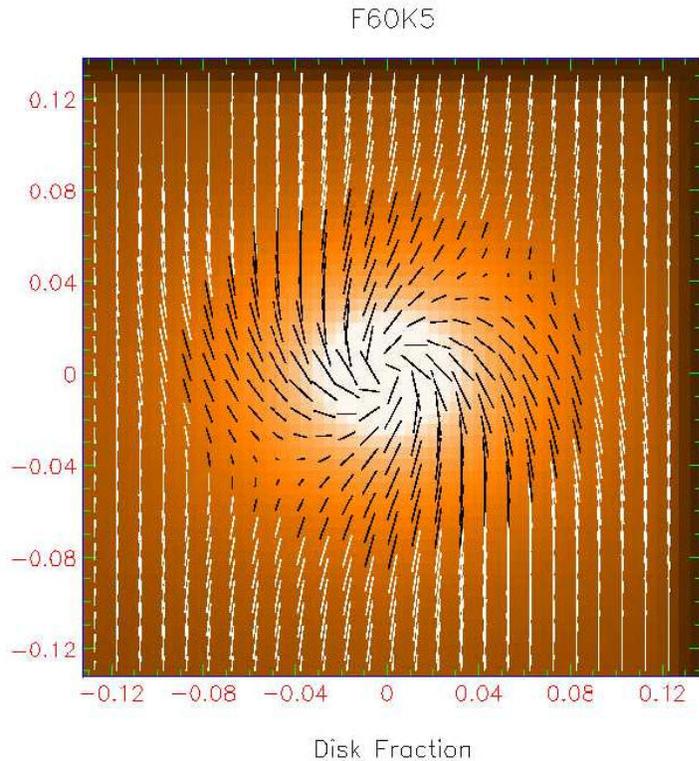
Simulation of an 850-micron polarised continuum image made by ALMA. The object is a model of a high-mass protostar at a distance of 1kpc, containing a mainly poloidal magnetic field, which is twisted and pinched by the protostellar accretion disk. The image shows the continuum brightness, and the lines show the magnetic field traced by the continuum polarisation. The polarisation vectors are typically 2 per cent in size. ALMA is the only telescope capable of making such detailed images of magnetic field structure in star-forming regions, and these are vital if we are to understand the role of magnetic fields in cloud collapse. Figure courtesy of Antonio Chrysostomou.

Figure 20: Simulation of polarisation pattern

finally planet formation must occur on scales of 1-100 AU. The nearest T Tauri stars are 50 pc distant; sites of embedded low-mas star formation can be found at 150 pc; sites of high-mass star formation are 500 pc distant. ALMA is capable of achieving good brightness sensitivity at angular resolutions of 25–100 mas, and so is capable of resolving length scales as small as 4 AU. ALMA will thus provide the first direct probes of these vital length scales. In addition, ALMA will allow the first detailed studies of star-forming regions beyond the solar vicinity: ALMA is capable of resolving the typical Jeans length out to distances of 200 kpc, probing the details of star formation throughout the Galaxy, and as far away as the Magellanic clouds.

3.2.1   The structure of protostellar envelopes and disks

The line and continuum images at ∼4–10 AU resolution provided by ALMA will allow us to trace the structure of the thick envelopes around the youngest and most embedded protostars (the so-called "Class 0" objects, see Figure 21). By studying the detailed spatial distribution of the dust and gas (either intensity distribution or spatial visibility functions) it will be possible to identify compact structures, such as the newly forming disks. There is no doubt that the study of disk formation, and the understanding of disk evolution as planets form, will be a central scientific goal of ALMA.

Motions due to infall, outflow, and rotation are all important in the envelopes of Class 0 protostars resulting in a very complex kinematical behaviour. Images in molecular lines at very high spatial and spectral resolution are thus needed to disentangle the detailed
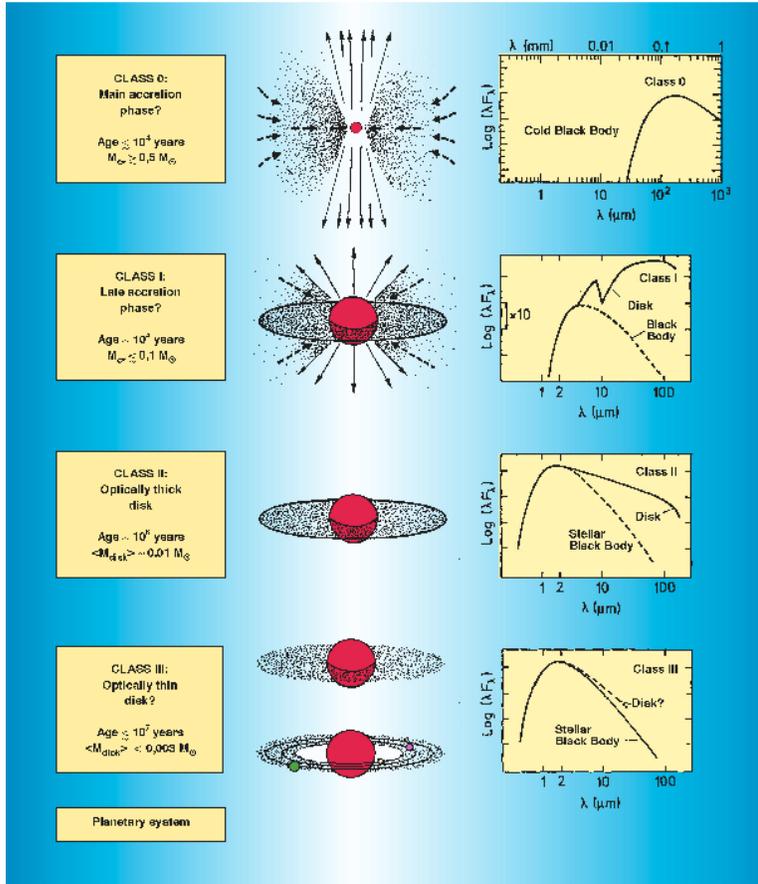
Figure 21: Four stages in the formation of low-mass stars. Adapted from [André 2000]. a) A dense core collapses forming a "Class 0" protostar which is characterized by a violent bipolar outflow. Most of the protostellar energy is emitted at sub-millimeter wavelengths, and ALMA will reveal the precise structure of these complex infall-outflow structures. b) A disk is formed at the late accretion "Class I" stage. c) The envelope is cleared of material and the slowly rotating disk becomes a proto-planetary system. d) The newly formed star surrounded by a planetary system is finally revealed.

velocity field within the envelopes.

In fact infall motions have already been detected around several Class 0 protostars [Mardones et al. 1997], mainly using the lowest (optically thick) rotational transitions of some abundant molecules. The profile shapes of such lines exhibit asymmetric self-absorption features which are skewed to the blue. On the other hand, violent outflows are particularly energetic in this type of object [Bachiller 1996]. Thus when interpreting line profiles in Class 0 protostars, one always has to contend with the simultaneous presence of bipolar outflows and disk rotation together with inward gravitational motions. This complicates the study of the different contributions to the protostellar kinetic energy. One

of the most exciting experiments for ALMA in this field will be direct detection of infalling envelopes by looking for redshifted absorption against the disk/star continuum; current interferometers lack the sensitivity to do this at present in all but a few cases.

Studies currently available have been carried out in low excitation transitions tracing layers of relatively low density and temperature. Clearly the study of the infalling region close to the protostar will require observing higher rotational lines that are only excited in the densest innermost regions of the envelopes. Such high excitation lines, which are not observable with current interferometers, will be easily accessible to ALMA. Observations of different molecules which chemically trace the various components are needed (see Table 6)

The combination of high angular and spectral resolution, together with high sensitivity, will allow us to separate (both spatially and spectroscopically) the different kinematic components of protostars (infall, outflow, and rotation). This will finally allow us to establish the different kinematic contributions to the energy, which is a basic parameter in any model of protostars.

3.2.2   Outflows

Violent outflows of matter are a key characteristic of star formation ([Richer et al. 2000] and references therein). Bipolar outflows limit the mass of the forming star and provide an efficient mechanism to carry away the excess angular momentum of the infalling cloud. In spite of the crucial role played by outflows in star formation, the mechanism of outflow formation remains very poorly understood. The highest resolution images available show that outflows are generated in a circum-protostellar region of size less than a few tens of AU. Figure 22 is an example of a high velocity outflow imaged in the CO J=2–1 line. The jet-like outflow emerges from the embedded Class 0 protostar which is surrounded by a disk of cold dust well detected in the λ 1.3 mm continuum. ALMA will provide detailed images of the outflow origin and of the disk/outflow interface where the outflow is accelerated, and where most of the interesting interactions between the outflow and its surroundings take place (see Fig.23).

Class 0 protostars are known to drive extraordinary jet-like molecular outflows [Bachiller 1996]. The mechanical power of such outflows is often comparable to the bolometric luminosities of the central protostars. Moreover, there is observational evidence that the mechanical power and collimation of the protostellar outflows decline as the protostar evolves from Class 0 to Class I [Bontemps et al. 1996]. The reasons for such a decline are unknown. However, the correlation of outflow momentum with the mass of the protostellar envelope seems to suggest that the decline in outflow momentum is related to a decline in the accretion rate, and this seems to be accounted for by magnetohydrodynamical models (see [André 2000], and references therein). ALMA will permit the study of the envelopes of different kinds of young stellar objects, in particular of Class 0 and Class I protostars. The comparative study of the properties of protostars at different evolutionary stages will reveal the detailed causes for the outflow power decline.

The magnetic field has long been believed to play a fundamental role in the generation of bipolar outflows, but this cannot be demonstrated with current instrumentation. The study of the magnetic field structure, based on polarisation measurements with ALMA,
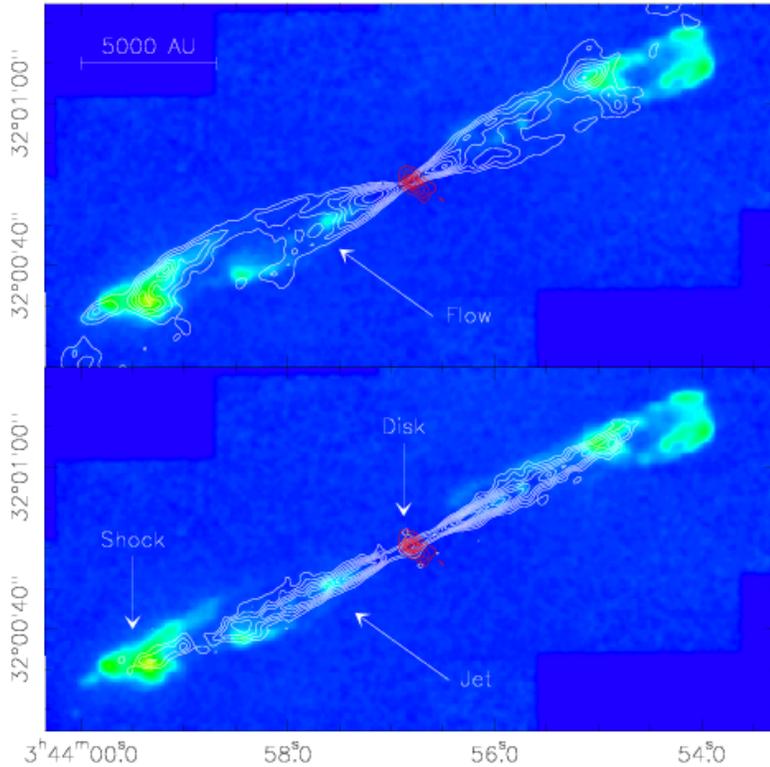
Overlay of the H_2 2.12 μm emission in the HH 211 molecular outflow (color-coded intensities; [Mc Caughrean et al. 1994]) and CO and dust emission (contours, [Gueth & Guilloteau 1999]). The angular resolution is 1.5″. The white contours represent the CO emission: low velocity ($<$ 10 km/s) in the upper panel, high-velocity ($>$10 km/s) in the lower panel. The 1.3 mm continuum emission is shown with the red contours; contour step is 10 mJy/beam.

Figure 22: The HH 211 molecular outflow

will finally provide hard evidence of the role played by the magnetic field in the generation of bipolar outflows.

The violent protostellar outflows are strongly supersonic, so they drive shock waves into the surrounding medium. Shocks heat and compress the molecular gas, and hence trigger a peculiar chemistry. Dust grains can be processed by the shocks and some components can be ejected from the grains into the gas phase. Strong gradients in the physical conditions (density and temperature) and in the chemical composition happen on scales of 10–100 AU. Very high angular resolution is thus mandatory to study the complex structure of interstellar shocks. The detailed physical conditions, as well as the chemical structure, of shocks and outflows will certainly be elucidated by the means of multiline observations with the unprecedented angular resolution and sensitivity provided by ALMA.

Clustering is very important for stars with spectral type earlier than B5-B7 [Testi et al. 1999]. The overlap of outflows from different stars result in a very complex kinematical structure within the gas associated with clusters, and identifying the sources driving the different outflows is not an easy task. For instance, many energetic outflows which were initially associated with Herbig Be stars, were found to be driven by more deeply embedded infrared companions when studied with the higher resolution provided by millimeter-wave interferometers. With high-resolution observations provided by ALMA we will be able to identify the distinct outflows from different stars and protostars at scales of a few tens of AU in most known young clusters.
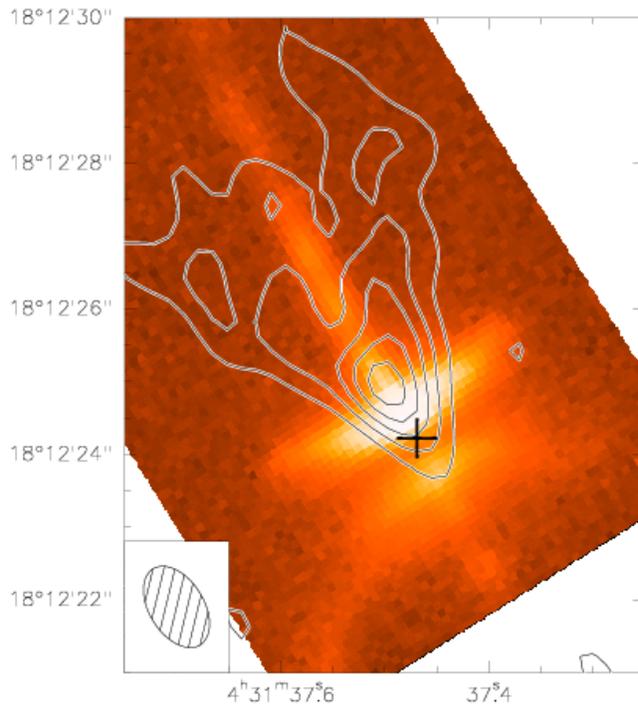
CO(2-1) contours superimposed on an HST image of HH 30. The HST observations in false colors (from Burrows et al. 1996) show the optical continuum emission tracing the reflected light in the flared circumstellar disk, together with the emission of bright atomic lines ([SII], Hα, [OI]), tracing a highly collimated jet, perpendicular to the disk. The contours represent the CO(2–1) emission, as observed with the IRAM Plateau de Bure interferometer with an angular resolution of $1.2'' \times 0.7''$ by [Gueth et al. 2001]. Only the channel map at a velocity of 11 km/s is plotted (contours are 80 mJy/beam). It shows the conical molecular outflow emanating out of the disk and surrrounding the jet. The cross indicates the position of the peak of the λ 1.3 mm continuum emission.

Figure 23: An outflow around a T Tauri star

3.2.3   Fragmentation and multiplicity

Most stars are members of binary of multiple systems, yet to date most theoretical work has concentrated on the formation of single, isolated protostars. In part this is due to the simplifications this introduces to theory, and because of the importance of single stars such as our Sun. However, a complete theory of star formation must explain the origin of binary, triple and quadruple systems in which most stars on the main sequence occur [Bodenheimer et al. 2000]. Many theories of multiple protostar formation have been studied in detail, notably envelope fragmentation during collapse, disk fragmentation, and capture. In addition to the intrinsic importance of establishing which of these mechanisms dominate, it is also interesting to establish what effect multiple star formation has on the individual (and circum-binary) disks, and on subsequent planet formation.

To date, there are very few observational constraints on multiple star formation, because high angular resolution ($< 0.5''$) is needed to probe the detailed structures of collapsing envelopes and disks. Only a very small number of protostellar binary systems have so far been detected [Looney et al. 2000]. For example, the image in Fig. 24 shows the multiple protostellar system IRAS 16293-2422, imaged with 6 to $0.5''$ angular resolution by the BIMA array. Observations with ALMA, with $0.1''$ resolution and better, will for the first time reveal the incidence of binarity in protostellar systems, and the details of the envelope and/or disk fragmentation processes. Comparison of the binary population in protostellar and main sequence systems will yield important constraints on theories of the formation and evolution of multiple systems.
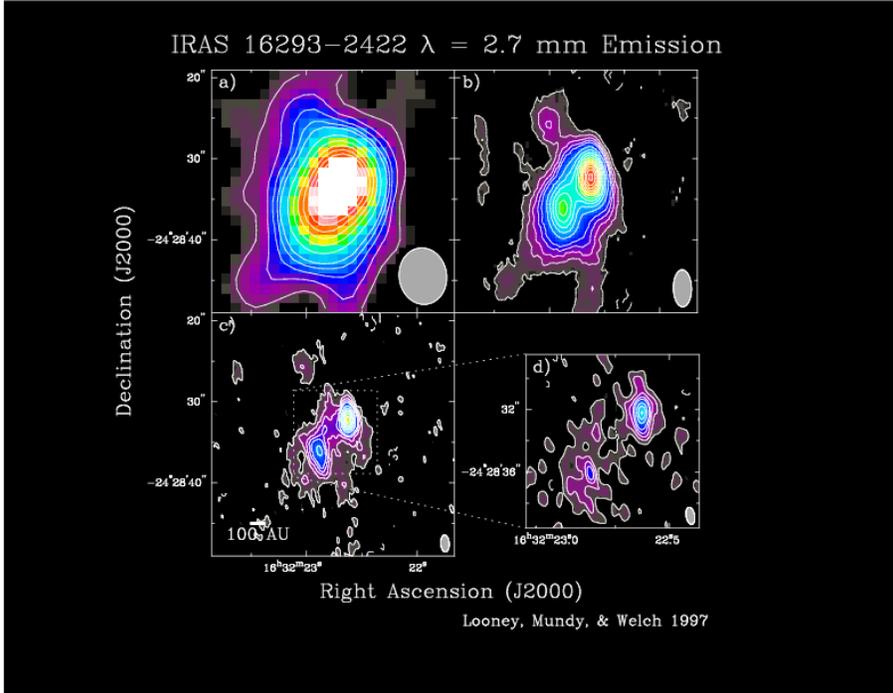
Figure 24: The binary protostar IRAS 16293-2422 imaged in 2.7 mm continuum emission with the BIMA array. The angular resolution increases from $6''$ (panel a) to $0.5''$ (panel d). [Looney et al. 2000]

3.2.4 Dispersal of circumstellar material

In their evolution towards the main-sequence, young stars progessively disperse their circumstellar envelopes. In about one million years the envelopes of low mass stars have been completely dispersed and the star becomes visible as a "Class II" object (see Fig. 21). At this stage, the star is still surrounded by an optically thick disk. From 1 to 10 Myrs the mass of the gas and dust of the circumstellar disk decreases to ~ 0.01 M$_\odot$ ("Class III" objects and main-sequence stars). During the pre-main-sequence stages, the ratio of disk mass to stellar mass (M$_{disk}$/M$_*$) remains roughly constant with an average value of ~ 0.04 for stars with spectral types in the range A0-M7 (T Tauri and Herbig Ae stars; M$_* < 5$ M$_\odot$, [Natta et al. 2000]).

The dispersal of circumstellar disks seems to be much more rapid and efficient in more massive stars. This is suggested by the very low rate of disk detections in Herbig Be stars (M$_* \approx 5$ - 10 M$_\odot$). For instance, the upper limit to the mass of a possible disk around Be star HD 200775 indicates that the value of M$_{disk}$/M$_*$ is at least two orders of magnitude lower than the mean value for Herbig Ae and T Tauri stars [Fuente et al. 2000]. Such observations are thus indicating a mechanism for the cirmcumstellar disk dispersal that depends drastically on the stellar spectral type or, alternatively, a mechanism for the

formation of intermediate-mass stars that does not require the existence of circumstellar disks. Theories for massive star formation based on the coalescence of low-mass stars or even pre-stellar clumps have been developed by [Bonnell et al. 1998] and [Palla et al. 2000], but await observational confirmation. ALMA is the unique instrument which is able to solve this kind of question. With the high angular resolution and sensitivity of ALMA, circumstellar disks with masses of $\sim 10^{-3}$ M$_\odot$ will be detected at a distance of 1 kpc, and this will improve by more than two orders of magnitude the best upper limits on disk masses around Be stars available nowadays.

3.2.5 High-mass star formation

O-B stars are our most fundamental tracers of star formation both throughout the Galaxy and, in particular, in extragalactic systems. The mechanisms responsible for their formation are however very different from those which were at the origin of the appearance of the solar system. In contrast to what we imagine happened to the Sun, it is likely that most stars including most low mass stars form in clusters and associations accompanied by one or more massive (> 10 M$_\odot$) objects. Understanding how this happens is a challenge which has not really been answered but to which ALMA may furnish a response.

The case of Orion   The best known region of high mass star formation is that associated with the Orion nebula (Fig. 25) where one sees a dense cluster of young pre-main sequence stars, the Orion Nebula Cluster (ONC), surrounding the Trapezium O6 star Θ^1C Ori which is the source of the Lyman continuum photons which ionize the nebula. Immediately to the rear of this complex of optically visible stars lies the dense molecular cloud OMC1 which enshrouds the cluster of (presumably) still younger stars associated with the Kleinmann-Low nebula. The connection between the optically visible ONC and the Kleinmann-Low cluster is a puzzle which ALMA, and probably only ALMA, can solve. Did the optically visible and the optically invisible clusters form together or separately? Did the formation of one trigger the formation of the other? These are important issues for star formation. They relate to high mass star formation because a variety of theoretical studies suggest that the formation of high mass stars depends in a sensitive fashion on the distribution of both the surrounding gas and the surrounding low mass stars (e.g. [Clarke et al. 2000]).

Towards Orion for example, ALMA will detect essentially all the circumstellar disks surrounding young low mass stars in either the optically revealed or the optically invisible population. As far as the visible population is concerned, one knows that these stars have disks because the "Proplyds" surrounding them have been directly imaged with HST. The Proplyd emission is due to gas ionized by the radiation from Θ^1C Ori and streaming off the disk surfaces. ALMA will however detect the dust emission and hence allow imaging of the underlying disks of the observed Proplyds as well as the detection of the disks surrounding the pre-main-sequence stars embedded in the molecular cloud.

ALMA will be able to detect sources of 50 μJy with comparative ease at wavelengths of around 1 mm and this corresponds at a distance of 500 pc to a disk mass of roughly $2\,10^{-4}$ M$_\odot$. Typical disk masses are of the order of 1 percent of the mass of the central star and thus this suggests that disks around young brown dwarfs will be readily detected in Orion with ALMA. Thus we will be able with ALMA to study the distribution of the
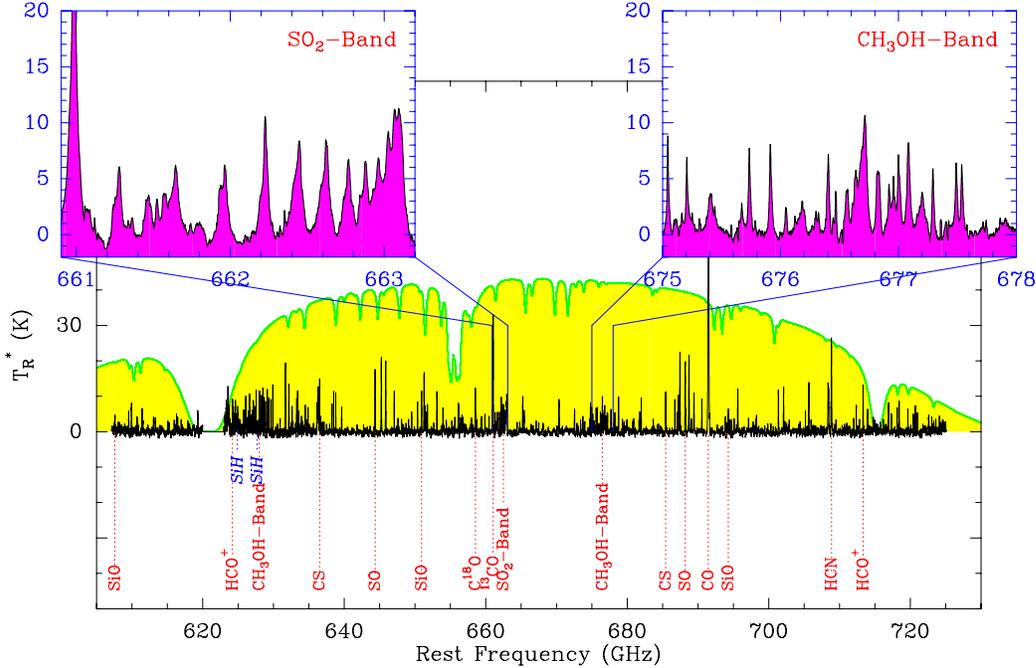
Figure 25: 610-725 GHz spectra obtained with the CSO telescope taken towards the Orion Irc2 hot core [Schilke et al. 2000]. The bottom spectrum shows the whole spectral range covered with the atmospheric transmission (yellow) for comparison. Two excerpts showing (mainly) series of methanol (right) and sulfur dioxide (left) transitions give a better idea of the quality of the data. One expects with ALMA to obtain imaging data for regions similar to Orion throughout the Galaxy.

hitherto invisible population of newly formed low mass stars embedded in the molecular cloud and compare with that of the known visible cluster. ALMA proper motion studies will separate cluster members from background sources and the molecular line emission from the disks will also allow the dynamics to be probed. Moreover, the (interstellar) gas component will also be detected and the relative distribution of the gas and stars will be compared. This will allow for the first time estimates of the true gravitational potential in regions of high mass star formation.

ALMA will also allow us to understand the gas dynamics. For the moment, we see a blur apparently caused by the superposition of the outflows from both high and low mass stars as well as the interaction of these flows with the environment. That a lot is going on is clear even from single-dish spectra (see Fig. 25) where one sees a plethora of molecular species whose origin lies in both shocks and chemistry on the surface of dust grains. The interferometer maps which are available have shown that different molecules have differing spatial distributions and as a result can serve as tracers of different aspects

of the dynamics. With ALMA, we will be able to trace the diverse outflows back to their origin with a spatial resolution corresponding to 15 AU ($0.03''$).

Orion is however only our nearest region of high mass star formation and may be atypical. It is certainly puny by comparison with giant clusters such as NGC3603 in Carina where 20 O and W-R stars have formed within the last few million years [Brandner et al. 2000]. These are an order of magnitude further away and consequently the linear resolution with ALMA will be of order a few hundred AU. Such clusters are already being studied with ISAAC on the VLT and we can expect enormous progress once the infrared and radio data are combined. This will in particular be the case once mid IR imaging with instruments such as VISIR becomes available. However, the most embedded clusters may only be visible with ALMA.

High-mass star formation in W3(OH) A crude idea of the type of science one can hope to do with ALMA by considering recent IRAM interferometer observations of W3(OH), a molecular complex located at a distance of 2 kpc from the sun. As in the case of Orion, there appear in W3(OH) to be two "centers of star formation". On the one hand, one observes a compact HII region of about 1000 AU in diameter ionised by an O8 star. On the other side, at a projected distance of about 0.05 pc lies a second star formation center marked both by water masers and an extremely dense clump (few hundred solar masses) of molecular gas. The presence of the water masers almost certainly indicates the existence of outflows emanating from young stars embedded in the molecular gas, but what is the nature of these young obscured objects ?

Figure 26 shows maps of this region in various molecular species. One sees first that different molecules tell different stories. The spatial distributions differ considerably with N-containing species like ethyl cyanide for example being solely detected towards the water maser clump whereas methanol is seen towards both centers. The high excitation vibrationally excited HC_3N line is only detected towards the western of the continuum peaks associated with the water vapor clump. One manner in which the molecular line data can be exploited is to search for temperature peaks in the hot gas surrounding the embedded stars. A temperature peak as a rule indicates the presence of a source of radiant energy or, in this case, of massive embedded stars. In the case of the data shown in Fig. 26, there is evidence in fact for two temperature peaks in the molecular clump suggesting the presence of two embedded early B-type protostars.

However, the resolutions used in the maps of Fig. 26 were of order $1''$ corresponding to 0.01 pc. This barely separates the two putative temperature peaks. The advantage of an order of magnitude increase in angular resolution will be that one will really be able to judge what the temperature structure is and to look for the sources of the outflows. Since the process of high mass star formation clearly depends on a balance between the opposing forces of accretion, radiative pressure, and outflows, such information will be invaluable. Even more important is the fact that with ALMA many such studies will become possible allowing proper statistical samples to be studied. This in turn will allow objective estimates of the ages of UCHII regions and their associated phenomena to be made.
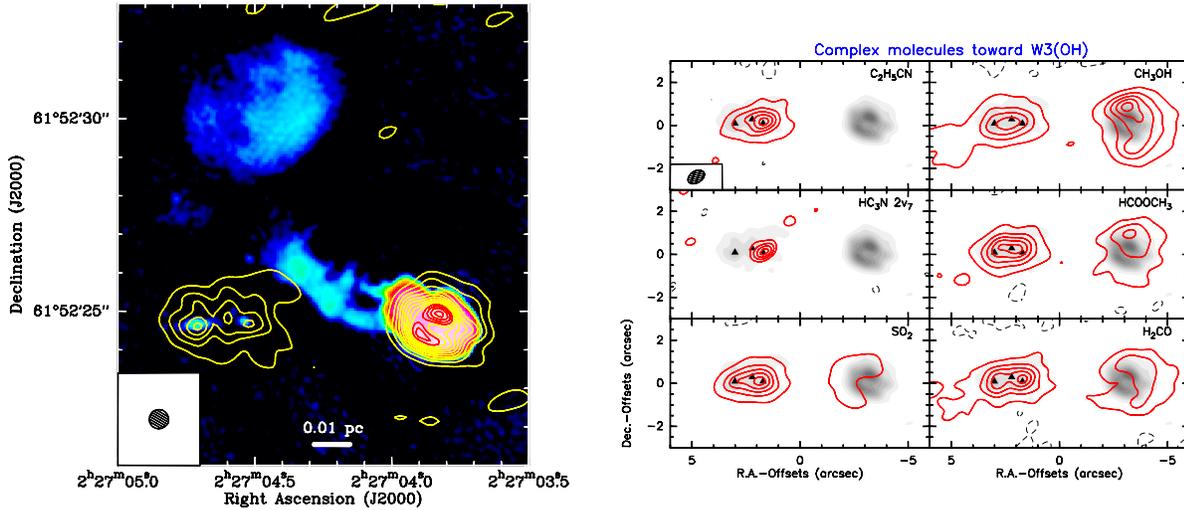
Figure 26: Maps of the well known compact HII region W3(OH). a region of massive star formation at a distance of 2 kpc. Left: false-color image of the continuum at 3.6 cm taken with the VLA (tracing the free-free radiation from ionized gas [Wilner et al. 2000]), and in contours, 1.3 mm continuum emission measured with the IRAM interferometer. The HII region is still detected at 1.3 mm, but dust emission from a second source is seen to the east which is associated with strong water vapor emission and some non-thermal (synchrotron) emission seen at 3.6 cm. Both sources are again seen in the maps of various molecular transitions (Right panel) shown as red contours overlaid on the 1.3 mm continuum. The three triangles show the positions of three (barely resolved) minor continuum peaks. Different molecules behave in radically different ways due to a mixture of excitation and abundance effects. Clearly, study of such objects at 2 kpc distance requires maps of resolution much better than that available in the IRAM interferometer data (roughly 0.7″).

3.3   Chemistry of star-forming regions

From the collapse of a dense cloud core to the formation of a young star and its circumstellar disk, molecules undergo a series of complex chemical changes. Processes such as depletion of molecules onto the cold icy grains during the collapse phase, evaporation of newly-formed species when the protostar starts to heat its surroundings, and high temperature reactions in shocked zones created by the impact of the outflow cycle molecules from one compound into another (see [van Dishoeck & Blake 1998, Langer et al. 2000] for overviews). These changes are not only of chemical interest, but can also be used as diagnostics of the physical state of evolution of the object. Moreover, knowledge of the chemistry is needed to choose the proper molecular line to trace the physical structure of a particular component. In single-dish observations with 15–30″ beams, all of these different chemical processes are "blurred" together (see Table 6 and Figure 27), whereas current interferometers with a few arcsec resolution suffer from poor spatial sampling. ALMA, with its unprecedented sensitivity, resolution and uv coverage will be necessary to zoom in and image these different chemical regimes and quantitatively address the chemical evolution in the initial stages of star formation.
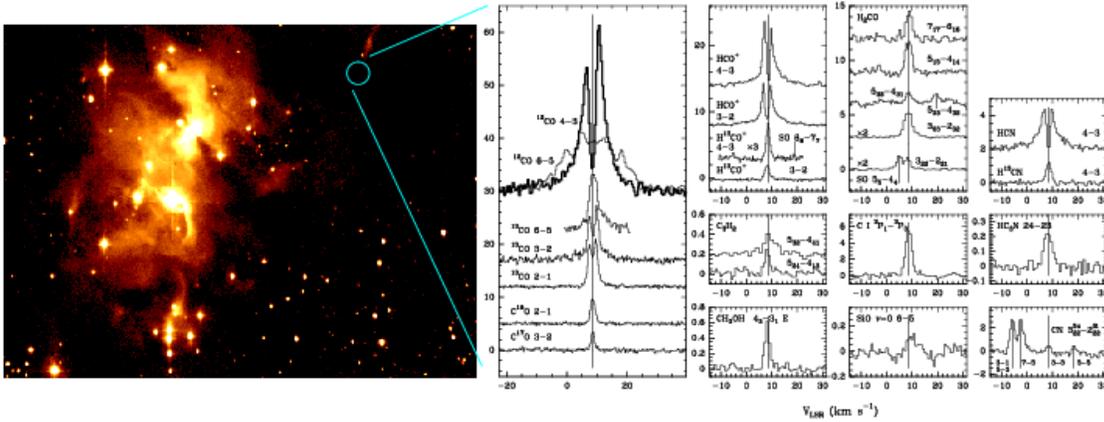
Figure 27: Left: Image of the Serpens molecular cloud (distance 300 pc) at 2 μm by [Hodapp 1994], showing a dense cluster of young stars emerging from the molecular cloud. Right: JCMT spectra of low- and high-excitation molecular lines toward the deeply embedded proto-star SMM1, emphasizing the chemical richness of the protostellar environment. Only ALMA will be able to image the spatial distribution of molecules on scales of less than 50 AU. From [Hogerheijde et al. 1999]

3.3.1   Cold collapse envelopes

In the cold, (pre-)collapse dense cores gas-phase molecules collide with the cold ($T_{\mathrm{dust}} = 10$ K) grains once every $\sim$10,000 yr and stick, forming an icy mantle. Grain-surface chemistry will then lead to new molecules which cannot readily be formed in the gas. In particular, hydrogenation reactions of accreted O, C, N and CO result in H_2O, CH_4, NH_3, H_2CO and CH_3OH, whereas oxidation of accreted CO may lead to CO_2 [Tielens 1989]. Recent mid-infrared absorption observations with ISO have confirmed this picture and produced a complete inventory of ices [Gibb et al. 2000]. Infrared data are limited, how-ever, to bright background sources. ALMA will be able to trace the freeze-out of molecules by high-resolution $< 1''$ maps of both the gas and the dust: in regions of significant de-pletion the dust emission is strong, but the line emission is weak except in species such as N_2H^+ which do not readily deplete. Such maps may be the best way to reveal the earliest star-formation stages where the core is on the verge of collapse or where the protostar has not yet heated its surroundings.

Some pre-stellar cores such as TMC-1 show exceptionally high abundances of long carbon-chain molecules like C_6H and HC_7N. These cores may still be assembling material from surrounding lower-density atomic C-rich gas, but the precise origin of these complex unsaturated molecules has remained a mystery for nearly 30 years. Single-dish data suggest that even different velocity components separated by <1 km s^{-1} have different relative abundances on scales of less than 10,000 AU [Langer et al. 1997]. ALMA will be able to track down the origin of these variations by high-spatial ($< 1''$) and high-spectral resolution images in different species, including atomic C itself through its 492 GHz and 810 GHz

fine-structure lines. In addition, ALMA can trace the ionization of cold cores through observations of ions like HCO^+ and DCO^+. The ionization fraction is a key parameter in the dynamical evolution of magnetized cores.

3.3.2   Embedded phase and outflows

In the early protostellar phase, the envelope mass exceeds that of the star and the circumstellar disk, and separation of the inner envelope and disk will require ALMA observations at subarcsec resolution. Such data will reveal the chemistry of the gas as it is transported from the envelope to the growing accretion disk.
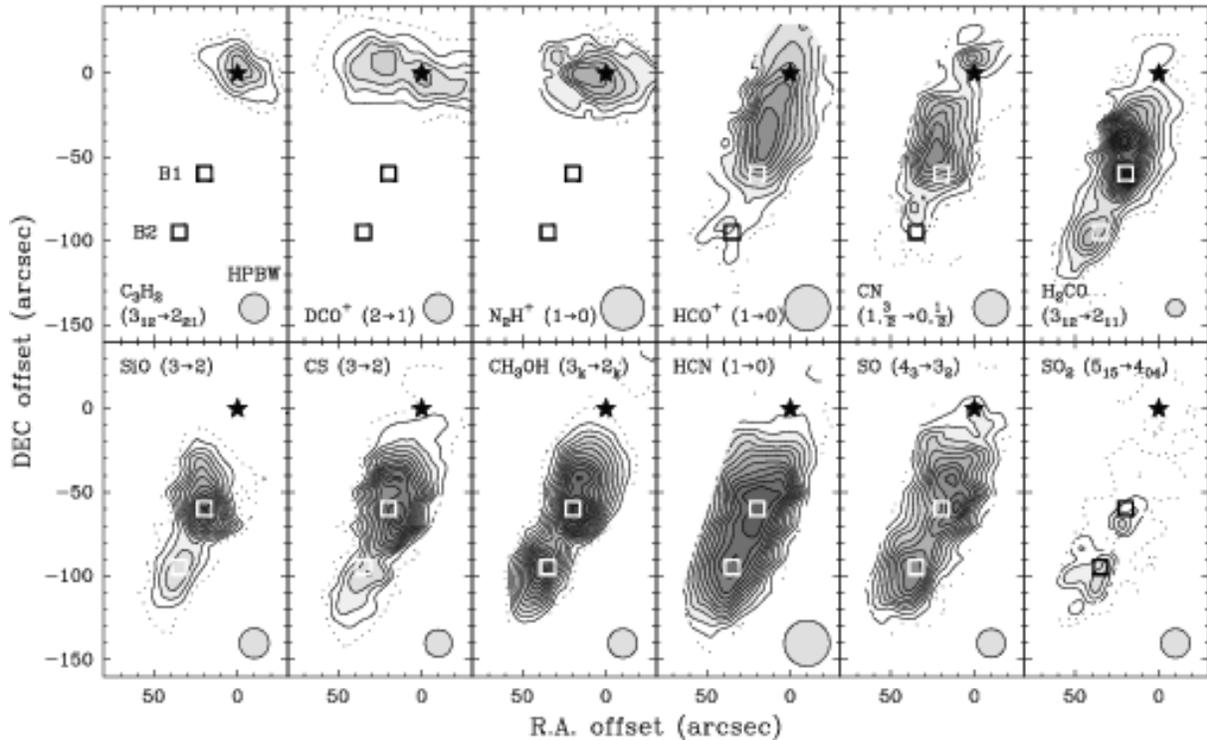

Figure 28: Maps of the molecular emission towards the southern lobe of the bipolar molecular outflow in L1157 [Bachiller et al. 2000]. Note that some molecular species such as C_3H_2 and the ions DCO^+ and N_2H^+ are excellent tracers of the circumstellar envelope around the "Class 0" protostar L1157-mm (marked with a star in all panels). Moreover, a striking chemical stratification is observed along the outflow, with the different molecular species tracing different regions of the shocked gas. ALMA will directly image these chemical changes, which occur on scales of $\sim 10^{15}$ cm in most known chemically-active outflows.

Once the young star starts to heat the envelope, the icy mantles evaporate back into the warm gas, probably in a sequence according to their sublimation temperatures, resulting in strong molecular lines of low- and high-excitation species (see Figures 27 and 28). The heating can either occur through radiation — resulting in thermal evaporation— or through the interaction of the outflow with the envelope — resulting in shocked regions where not only ices are liberated but also grain cores are partially sputtered. In particular, high

velocity (>25 km s^{-1}) shocks can liberate Si and S back into the gas, which subsequently lead to enhanced abundances of molecules such as SiO and SO$_2$ [Schilke et al. 1997] (see Fig.27 and 28 . At the highest temperatures ($>10^4$ K) in fast (>50 km s^{-1}) shocks, any pre-existing molecules in the gas are destroyed, and they reform only slowly in the cooling zones. ALMA can directly image these chemical changes which occur on scales of $\sim 10^{15}$ cm (~ 100 AU). Over the length of the flow, glancing or oblique shocks lead to turbulent layers that mix outflow and ambient cloud material. Some species can be used to trace the walls, or boundaries, of the outflow itself.

3.3.3   Hot cores: how far does chemical complexity go?

Surprisingly large and complex molecules have been found in star-forming regions, especially in so-called "hot core" regions, i.e., small clumps of warm (>200 K) and dense ($n > 10^6$ cm^{-3}) gas associated with massive young stars. Fully saturated species like CH$_3$OCH$_3$ (dimethyl-ether) and CH$_3$CH$_2$CN (ethylcyanide) are found with abundances that are enhanced by many orders of magnitude with respect to quiescent clouds [Blake et al. 1987, Walmsley 1992]. These complex molecules are thought to originate from rapid gas-phase reactions of evaporated molecules (especially CH$_3$OH) in the warm gas [Charnley et al. 1992]. This chemistry only lasts for about $10^4 - 10^5$ yr, after which the normal ion-molecule gas-phase chemistry takes over. The abundance ratios of species like CH$_3$OCH$_3$/CH$_3$OH show strong variations over this period, and may be used as "chemical clocks" to trace the evolution. So far, most data on hot cores comes from single-dish telescopes, which suffer strong beam dilution. Hot cores are prime targets for ALMA at the highest spatial resolution ($<0.03''$, i.e., <100 AU at ~3 kpc) throughout the Galaxy, since the lines are strong with brightness temperatures up to 1000 K.

Some of these complex species may be the precursors of biogenic molecules such as amino acids, bases and sugars. Incorporation of these molecules in disks is relevant for questions related to the origin of life. How far does this complexity go? Searches for the simplest amino acid, glycine, have so far been unsuccessful [Combes et al. 1996], but the possible detection of the first sugar, glycolaldehyde, has just been reported [Hollis et al. 2000]. Could the formation of these species be affected by the observed separation between O-rich and N-rich molecules observed in some hot core regions, as in Figure 26? Current instrumentation prevents deep searches for more complex molecules for several reasons: (a) the regions of high chemical complexity are often very small ($<0.1''$); (b) the crowding of lines is usually so high that the confusion limit is reached; and (c) large molecules have many close-lying energy levels so that the intensity is spread over many different lines, each of them too weak to detect. ALMA will be able to push the searches for prebiotic molecules two orders of magnitude deeper to abundances of $< 10^{-13}$ with respect to hydrogen, because it will resolve the sources, filter out confusing lines from larger scales and have a higher sensitivity owing to its large collecting area.

3.3.4 Photon-Dominated Regions (PDRs)

Intense ultraviolet radiation from massive young stars can dissociate and ionize molecules. The chemistry in such photon-dominated regions (PDRs) leads to high abundances of radicals and ions, which are gradually transformed back into less reactive molecules when the radiation is diminished by dust extinction deeper into the cloud [Hollenbach et al. 1997]. These changes occur on scales of <1000 AU, well accessible to ALMA. Moreover, PDRs are thought to be very "clumpy" on scales down to 100 AU, and ALMA should be able to reveal the chemical stratification in such clumps through imaging in characteristic molecules and [C I]. Since most of the material in galaxies is contained in PDRs, a good understanding of PDR chemistry is also a prerequisite for the interpretation of molecular lines from external galaxies.

Table 6: Physical sizes and chemical characteristics of star-forming regions

Component	Size (AU)	Taurus ($''$)	Orion ($''$)	GMC 3kpc ($''$)	Chemical Characteristics
Pre-stellar core	>10,000	> 70	> 20	> 3	Ions, Long-chains (HC_5N, DCO^+, ...)
Cold envelope	5000	35	10	1.7	Simple species, Heavy depletions (CS, N_2H^+, ...)
Warm inner envelope	500	3	1	0.17	Evaporated species, High-T products (CH_3OH, HCN, ...)
Hot core (high-mass only?)	500	...	2	0.17	Complex organics (CH_3OCH_3, CH_3CN,... vib. excited mol.)
Outflow: direct impact	<100–500	<0.7–4	<0.2–1	<0.03–0.2	Si- and S-species (SiO, SO_2, ...)
Outflow: walls, entrainment	100–1000	0.7–7	0.2–2	0.03–0.3	Evaporated ices (CH_3OH, ...)
Disk	100	0.7	0.2	0.03	Ions, D-rich species, Photoproducts (HCO^+, DCN, CN, ...)
PDR, compact H II regions (high-mass only)	100–3000	...	0.2–7	0.03–1	Ions, Radicals (CN/HCN, CO^+)

3.4 Protoplanetary disks

Protoplanetary disks surrounding young stars which are the progenitors of Solar-type stars are prime targets for ALMA. With typical temperatures of order $\sim 30 - 300$ K at 10 to 100 AU from the star, the disks are cold, making (sub-)millimeter observations a key to their study. Because of their small angular size (see Table 7), current millimeter arrays have only unveiled the largest disks. The orders of magnitude improvement provided by ALMA in both sensitivity and angular resolution will revolutionize the study of protoplanetary disks. Key questions that can be addressed with ALMA are: (i) How do disks evolve from the massive gas-rich disks seen around pre-main sequence T Tauri stars to the tenuous
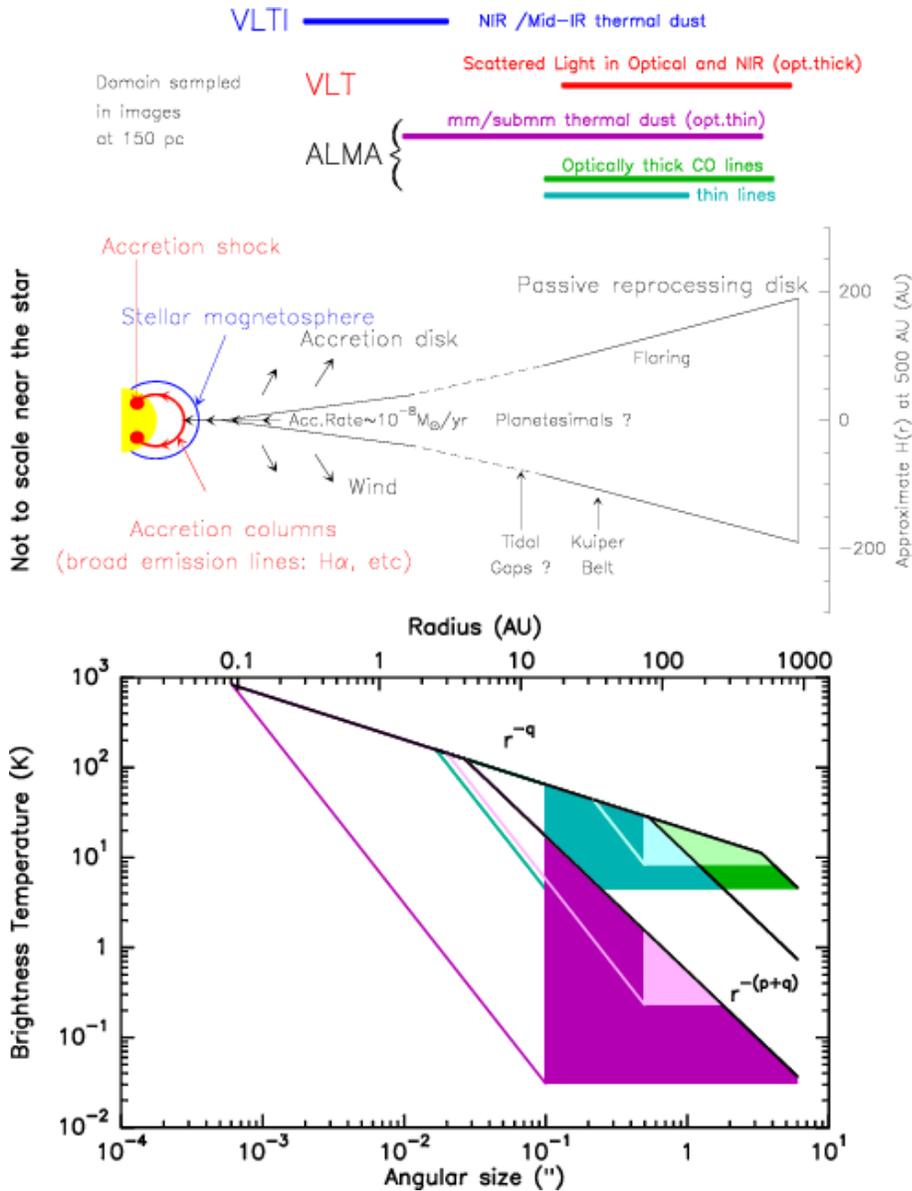
Figure 29: **top** Schematic drawing of a protoplanetary disk, showing the characteristic regions as function of distance from the star. **bottom** Brightness distribution in Kelvin (Rayleigh-Jeans approximation) of dust at 1.3 mm (purple), ^{13}CO J=2-1 (green) and C^{18}O J=2-1 (blue-green) lines in a disk and comparison with the 3σ sensitivity curves of the IRAM interferometer (lighter colors) and ALMA (darker colors) for 6 hours of integration and a spectral resolution of 0.5 km.s^{-1}. The resolution of the array is 0.5″ for IRAM, and 0.1″ for ALMA. The scale is log-log and the angular size (″) is scaled to the Taurus distance (150 pc) with radius in AU. The interferometer is only sensitive to disk emission above the sensitivity curves. Filled areas correspond to the regions of the disk where the emissions are detectable and resolved. Differences between C^{18}O and ^{13}CO emissions come from the fact that C^{18}O is less abundant than ^{13}CO. ALMA can detect and resolve dust and gas emission up to the disk edge. Note also that ALMA is sensitive to the dust contained within the inner AU.

Table 7: Characteristic scales of protoplanetary disks around young stars

Stage	Component	Typical distance of objects (pc)	Radius (AU)	Radius ($''$)
Deeply embedded Class 0	Entire disk	300	100	0.3
Pre-main sequence Class I & II	Entire disk	140	100	0.7
	Solar system/Kuiper Belt		30	0.2
	Planet migration		0.1–15	0.007–0.1
	Gaps by planets		2	0.015
Old pre-main sequence & ZAMS	Entire disk	10–60	100–1000	10–1.7
				100–17

dust debris disks seen around mature stars such as Vega? When are the gas and dust dissipated? (ii) How many disks have formed planets that are revealed by tidal gaps in the disks? What is the associated time-scale for planet-formation? (iii) What is the chemical composition of the gas in disks, providing the building blocks from which future planetary systems are made?

3.4.1 Massive protoplanetary disks around pre-main sequence stars

Large gas disks with masses of $\sim 10^{-2}$ M$_\odot$ have been revealed around classical T Tauri and Herbig Ae stars with ages of a few Myr by millimeter continuum emission and rotational lines of CO [Dutrey et al. 1996, Koerner & Sargent 1995, Mannings & Sargent 1997]. These observations have allowed to study the kinematics, which can only be addressed by spectroscopy. The gas is found to be in Keplerian rotation around the young star, providing unambiguous evidence that it resides in a rotating disk.

Fig.29 compares in log-log scales the brightness distribution of the 1.3 millimeter dust emission and the optically thin ^{13}CO J=2–1 line for a standard disk model with the sensitivity curves of the IRAM and ALMA interferometers (see [Dutrey 2000]). While current millimeter arrays only sample the outer parts of the disks (> 50 AU), with the gas and dust probing different scales, ALMA will dramatically change this picture.

First, ALMA will detect *all* the dust in the disk. ALMA is sensitive enough to detect the dust in the outer part of the disk where the emission is optically thin, and will also resolve the dust emission in the inner disk at the scale of our Solar system (3–10 AU). Second, by using the highest angular resolution and multifrequency observations, ALMA will be able to measure the change of dust properties within protoplanetary disks on scales of a few AU, perhaps showing direct evidence for dust settling and coagulation in the disk midplane. Third, spectral line emission from the outer and inner disk is now detectable. ALMA will be able to map optically thick lines at a few AU resolution, providing information about the gas content and its kinematics. Observations of optically thin lines will also become possible, though more difficult. Fourth, by imaging lines with different excitation conditions, maps of the H$_2$ density distribution will be possible [Dutrey et al. 1997, Zadelhoff et al. 2000]. Finally, the region over which both dust and line emission can be imaged spans almost two orders of magnitude, and allows direct
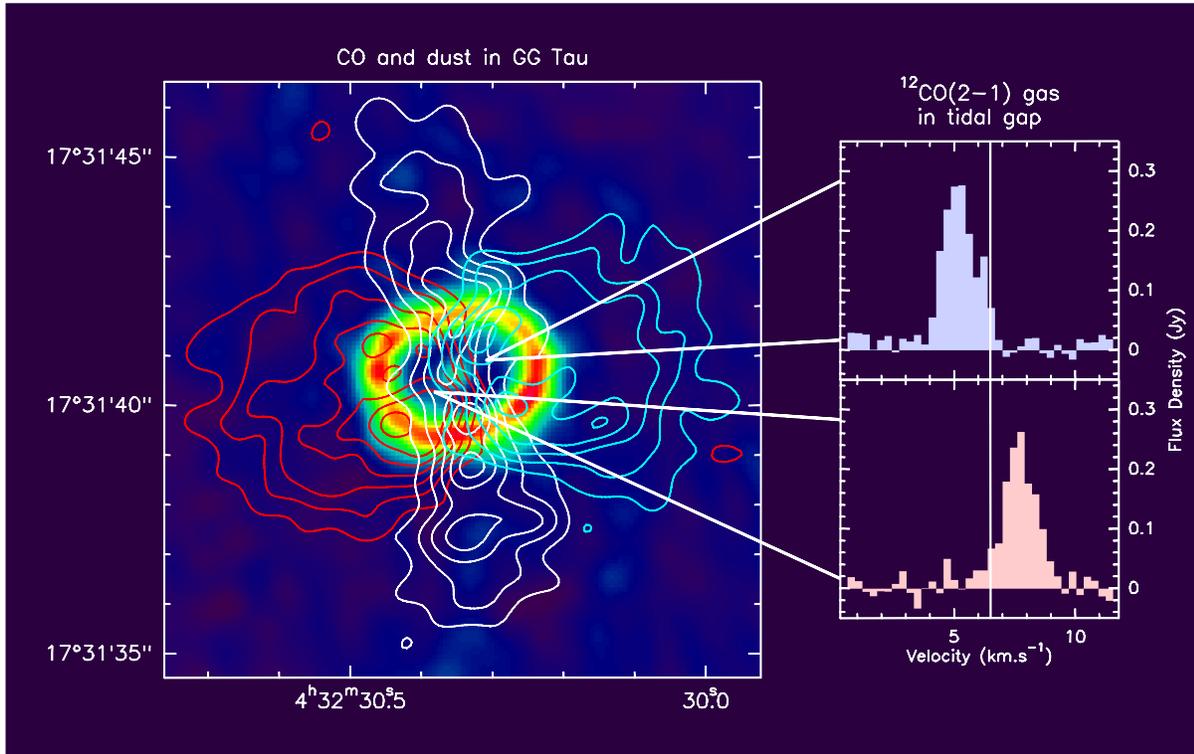
Figure 30: The GG Tau circumbinary disk. This high (0.6″) angular resolution image reveals all the components of the circumbinary material around the binary star GG Tau. The dust emission (in false color) shows the inner circumstellar disk (unresolved central spot) surrounded by a dense, narrow (80 AU), ring at 220 AU. The contours show 3 velocity channels of the ^{12}CO emission which reveal the less dense disk surrounding the ring. Keplerian rotation is clearly indicated by the velocity structure (blue contours are for blueshifted gas, white contours for the systemic velocity, red contours for redshifted gas). On the right, spectra taken towards the tidal gap which exists between the inner disks and the circumbinary ring reveal diffuse gas detected only in ^{12}CO J=2-1, presumably due to accretion streamers which replenish the circumstellar disks. From [Guilloteau et al. 2001]

comparison of the physical properties of the dust and gas over most of the disk.

Millimeter arrays have so far studied only the brightest and largest circumstellar disks, mostly in Taurus. ALMA will be able to provide complete unbiased surveys of several star-forming regions, down to an equivalent sensitivity of a few Earth masses of dust and gas. This will give unprecedented information on the distribution of disk masses and sizes, and how they depend on stellar mass or luminosity. ALMA will also be able to image protoplanetary disks at much larger distances allowing systematic studies of disk properties and lifetimes in widely different environments of star formation, from isolated stars such as in the Taurus cloud up to dense clusters like the Orion region. By using the kinematics from CO images to constrain the stellar mass, as has been done for a few T Tauri stars in Taurus [Simon et al. 2001], direct tests of pre-main-sequence stellar evolution models can be performed.

ALMA should also provide a major step forward in the study of binary systems or
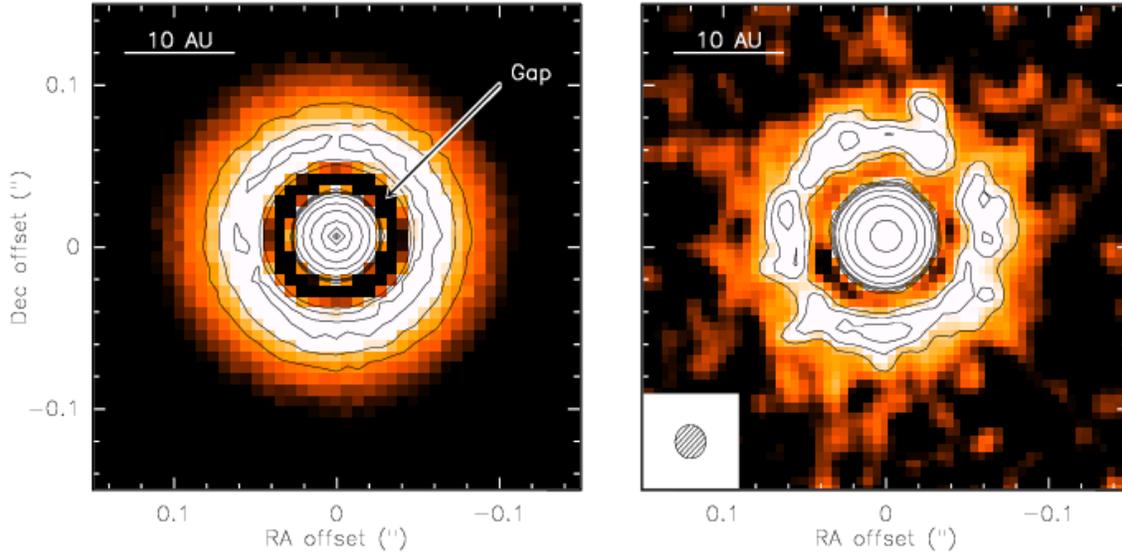
Figure 31: Simulation of a protoplanetary system with a tidal gap created by a Jupiter like planet as observed with ALMA. **left** A model image smoothed to 0.02″ resolution. The model image was obtained using hydrodynamical simulations of a gap created by a Jupiter like planet at 7 AU from its central star, and applying a radiative transfer modeling to the resulting structure. **right** Simulated ALMA observations at 350 GHz in the largest configuration, including noise statistics.

systems with planets. Images of the GG Tau binary [Guilloteau et al. 1999] have demonstrated the importance of tidal effects in shaping circumbinary disks. ALMA should be able to resolve the streamers of gas and dust which are replenishing the inner disks (see Fig.30 [Guilloteau et al. 2001]). The detection of tidal gaps created by low-mass stellar companions should be relatively easy with ALMA.

A particularly exciting prospect is that ALMA can also reveal the tidal gaps created by protoplanets in circumstellar disks, when pushed towards its highest angular resolution (see Fig.29 and 31). Thus, surveys for gaps in disks can provide statistics on the frequency and timescale for planet formation. Protoplanets themselves are in general not detectable except if they are surrounded by an envelope or disk subtending a significant fraction of their Hills radius.

3.4.2   Dispersal of dust and gas in disks

Our current understanding of the evolution of disks beyond the classical T Tauri phase is very limited. Non-accreting, tenuous 'debris disks' have been found around main-sequence stars with ages > 100 Myr by IRAS and ISO (see below), but virtually nothing is known about disks in the transitional period from 5–100 Myr. Near-infrared studies suggest that the dust has disappeared from the disks within ~10 Myr [Strom 1995]. However, such studies are only sensitive to the warm dust in the inner 0.01 AU of the disk. Observations at longer wavelengths are needed to determine how much cold dust remains out to 100 AU. Similarly, single-dish observations of CO have suggested that the gas disappears from the disks in <10 Myr, even more rapidly than the dust [Zuckerman et al. 1995].
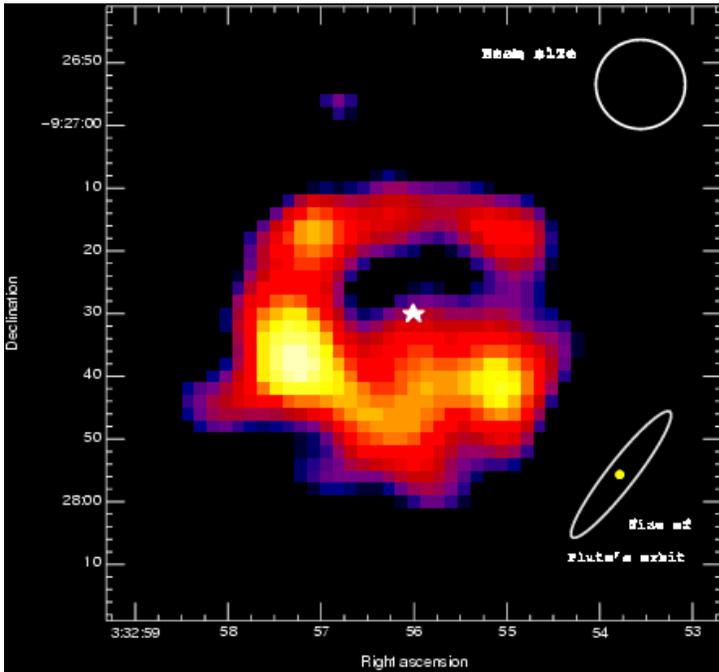
Dusty ring observed around the nearby cool star ϵ Eridani (distance $\sim$3 pc, spectral type K2V). This image at λ 850 μm was obtained with SCUBA at the JCMT 15-m telescope [Greaves et al. 1998]. The 15$''$ JCMT beam is indicated in the top right corner. For comparison, the apparent orbit of Pluto at 3 pc distance is indicated in the bottom right corner. Note that the radius of the clearing gap around ϵ Eridani is about 30 AU. ALMA will be able to study this kind of dusty ring with much more detail, and in a large number of more distant stars.

Figure 32: The dust disk around ϵ Eridani

ALMA will be able probe this critical planet-building phase in the evolution of disks by searching for dust toward a large number of stars with ages of 5 to >100 Myr. Dust masses down to 10^{-2} M_{Earth} can be detected out to $d \approx 100$ pc in $\sim$1 hr. Possible targets include weak-line T Tauri stars associated with star-forming clouds, dispersed post-T Tauri pre-main sequence stars showing X-ray emission, and young stars in nearby open clusters and/or moving groups such as the Pleiades and Hyades. The gas can be probed through observations of CO or other molecules. By observing disks in different environments, proposed disk dispersal mechanisms like photo-evaporation or disruption by tidal encounters in the dense cluster environment can be tested.

3.4.3   Debris disks and zodiacal dust systems

The IRAS and ISO satellites have detected the presence of disks around A-stars near the Zero Age Main Sequence (ZAMS) such as Vega [Backman et al. 1993, Habing et al. 1999]. Contrary to the case for pre-main sequence stars, the gas and dust in these so-called "debris disks" are not the remains of the accreted interstellar material. Instead, they are thought to originate from collisions and evaporation of larger planetary bodies (see review by [Lagrange 1999]). The amount of dust in these disks is very small, less than the mass of the Moon, and most of it is optically thin even at near-infrared and optical wavelengths.

The first images of cold dust in debris disks at submillimeter wavelengths have been obtained by SCUBA [Holland et al. 1997, Greaves et al. 1998] (see Figure 32). Because many of the objects are nearby (<30 pc), the dust can be detected and resolved even with single-dish telescopes, at least for the strongest sources. In a few cases, evidence for cleared inner holes suggests the existence of planetary bodies. ALMA will be able to image the dust in debris disks with an order of magnitude higher spatial resolution in systems which

are more than an order of magnitude weaker. It will also be able to search for analogs of the cold zodiacal dust found in our Solar system in the Kuiper Belt.

Imaging the cold *gas* distribution in such objects clearly requires the sensitivity of ALMA. Since the gas and dust are likely to be extended and resolved, a compact configuration and even mosaicing may be essential. ALMA should be able to detect CO column densities of order $\sim 5 \cdot 10^{12}$ cm^{-2} in one hour at low resolution (2.5″), assuming a typical CO line width of 3 km s^{-1}. This should allow maps of CO to be obtained in systems such as β Pictoris where CO has been detected in the UV by [Vidal-Madjar et al. 1994]. The maps will provide insight as to whether CO is limited to a narrow ring of evaporating comets, or whether it is more widely distributed throughout the disk and produced by another mechanism. Comparison of high-resolution ALMA images of the dust and gas can reveal variations in gas-to-dust ratios.

3.4.4 Chemistry in protoplanetary disks

Chemical studies of circumstellar disks around pre-main sequence stars are only just starting. Since disks provide the raw material from which future planets and outer solar-system objects are made, knowledge of the chemical composition is important. Due to radiation from the central star and the liberation of gravitational energy, there are strong density and temperature gradients in the disks — both radially and vertically. These gradients should be reflected in the chemical composition. In the cold outer regions, much of the gas is expected to be frozen out onto grains in the disk mid-plane. As matter accretes inward, the icy mantles will evaporate in a differential fashion depending on sublimation temperature. The surface of the (flared) disk is suprathermal due to heating by stellar and interstellar radiation [Chiang & Goldreich 1997], and a likely site for photochemistry.

Pioneering single-dish observations have been carried out toward a few T Tauri stars by [Dutrey et al. 1997] and [Kastner et al. 1997], who detected weak emission from species such as HCN, CN, H$_2$CO, HCO$^+$, CS, ... in sources like DM Tau and TW Hya. The data show that both ion-molecule reactions and photochemistry must contribute to the observed abundances, since ratios such as CN/HCN are too high to be accounted for by quiescent models alone. The observed line fluxes also imply strong depletions of most species in the mid-plane of the disks. ALMA will revolutionize this field by directly mapping the chemical gradients in disks with high sensitivity, including the pivotal planet-forming region at 3–30 AU. Comparison of these chemical gradients with the abundances found in comets should yield estimates of the locations in the solar nebula where comets were formed.

4 Stars and their Evolution

Instruments such as the VLA allow very sensitive radio observations of non-thermal emission from many different kinds of stars. With its coverage of the millimeter- and submillimeter ranges, ALMA will greatly expand the field of stellar astronomy. It will provide VLA-like and higher sensitivity and spatial resolution for studies of *thermal* radiation emitted by winds, chromospheres, photospheres, and circumstellar dust from the widest variety of stars of all evolutionary stages from the youngest to the most developed post-AGB objects. Even beyond, ALMA observations will yield crucial input on models of supernovae and gamma ray bursters. Solar studies using ALMA will allow analyses of physical processes on the Sun in a detail unattainable with any other instrument. Even for circumstellar envelopes, for which millimeter observations of dust and a wide variety of molecules have a long history, ALMA's spatial resolution and sensitivity will provide images of the innermost regions near the stellar photosphere, where molecules are converted into dust grains, allowing direct observation of elemental depletion and dust formation processes.
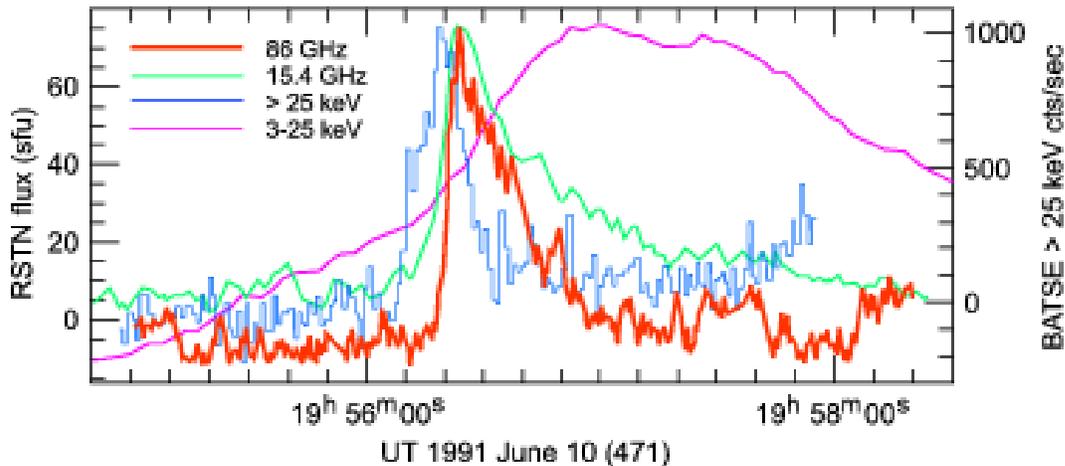

Figure 33: Millimeter (86 GHz, *red line*), radio (15.4 GHz, *green line*), hard X-ray (> 25 kev, *blue line*), and soft X-ray (3–25 keV, *violet line*) data for the solar flare at 19:56 UT on 1991 June 10 (after [Kundu et al. 1994]).

4.1 The Sun

ALMA will be the largest ground-based instrument for solar research built in the new decade. ALMA can address two of the most interesting solar physics problems: the acceleration of the highest energy electrons in flares, and the thermal response of the low chromosphere to waves and shocks from the interior.

4.1.1 Millimeter and submillimeter solar flares

Electrons are accelerated in solar flares to energies beyond 70 MeV and emit synchrotron emission and gamma-ray bremsstrahlung. BIMA observations ([White & Kundu 1992]; review by [Bastian et al. 1998]) suggest that the synchrotron emission continues beyond the millimeter waves into the submillimeter regime (Fig. 33). The MeV electrons appear to form a population of fast particles distinct from those producing centimeter waves and hard X-rays. Moreover, the observations suggest that flares of all sizes, but not every flare, produce MeV electrons on prompt time scales. These results seem to imply that the gamma-ray/millimeter flares may not represent an extreme type of flares and that all flares, possibly even microflares, are to some degree millimeter flares.

The acceleration of energetic electrons in flares is an essential part of flare energy release, but is not understood. The general trigger is presumed to be reconnection of magnetic fields in extremely thin current layers. As the synchrotron emission at millimeter wavelengths is optically thin and has been observed to be very spiky in time, the sources of millimeter wave flares may consist of kernels with a size of a few mas outlining the footpoints of reconnected field lines. At 1 millimeter wavelength, ALMA is more than 4 orders of magnitude more sensitive than gamma-ray observations at 10 MeV by the High Energy Solar Spectroscopic Imager (HESSI), and its spatial resolution is 3 orders of magnitude better. ALMA observations are thus highly relevant for the understanding of the acceleration process of flare particles and of the geometry of flare energy release in general.

4.1.2 Structure and dynamics of the chromosphere

The millimeter and submillimeter emission of the quiet Sun are mainly thermal emissions from the chromosphere, which is a thin layer above the temperature minimum region, where non-radiative heating first becomes manifest. Detailed semi-empirical models of the chromosphere have been constructed [Fontenla et al. 1993]. However, it has become apparent in recent years that these models must be thoroughly revised to reflect the highly inhomogeneous and dynamic nature of the chromosphere [Ayres 1995], reflecting the highly structured photosphere underneath. Moreover, chromospheric models do not yet contain the physics of the heating process, which is believed to be a combination of waves, shocks, thermal conduction, and electromagnetic phenomena (flare-like events).

The two sources of continuum opacity (H and free-free absorption) are well understood, and the continuum emission forms in LTE. Thus millimeter and submillimeter observations provide a convenient, linear thermometer to probe all layers of the chromosphere. ALMA will provide the unique combination of high angular resolution (15 km on the Sun) and short sampling times (< 0.1s) that is necessary to investigate the dynamic processes on scales suggested by photospheric flux tubes (see Fig. 34).

ALMA observations will also be useful for understanding the propagation of seismic oscillations into the solar chromosphere. Such observations will extend the methods of seismology and allow investigations of the structure of the chromosphere; e.g. plage regions associated with sunspots. ALMA will also be used to observe thermal variations due to local chromospheric waves in different frequency bands. Sub-millimeter observations with
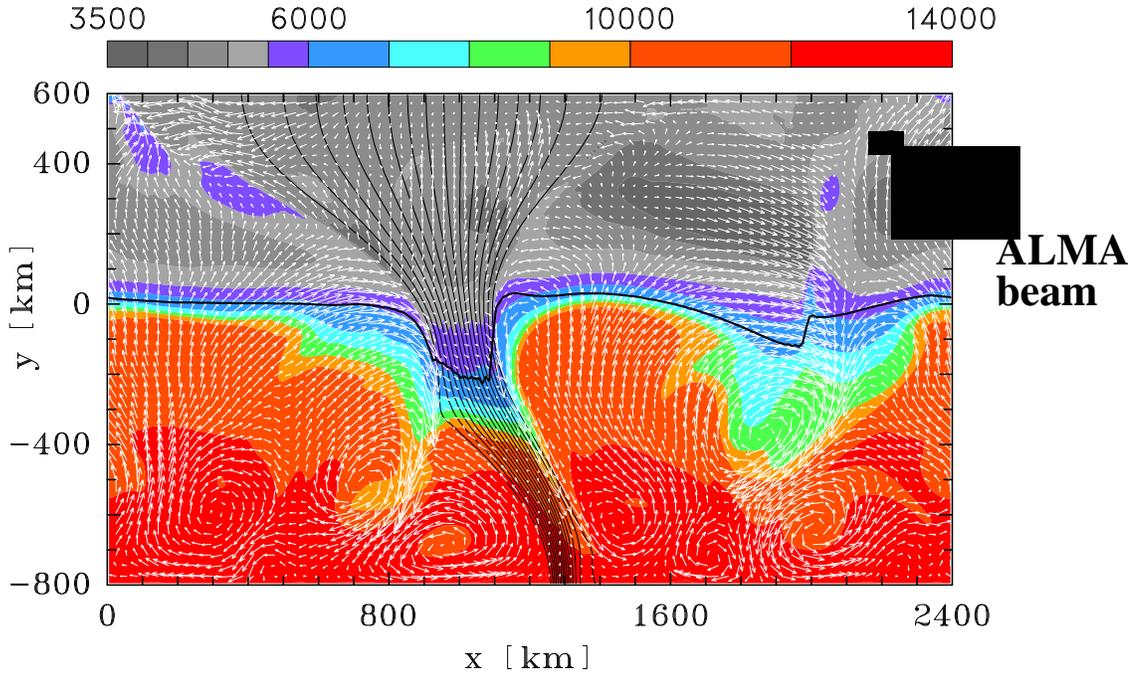
Figure 34: Vertical cross-section through a 2D MHD simulation of the solar surface. The colors indicate temperature in K. The velocity field is given by white arrows, and some magnetic field lines are shown in black, representing a "magnetic flux tube" of enhanced field and flow (after [Steiner et al. 1996]).

1 arcmin resolution show thermal variations of roughly 10 K [Kopp et al. 1992]. Statistics derived from Doppler observations suggest that the temperature amplitude increases in proportion to the inverse root of the spatial resolution. Therefore, thermal variations of order 75 K may be expected with $1''$ resolution. Using ALMA, it will be possible to study the heating effect of non-linear waves and shocks.

ALMA will also provide important new infomation on other structures of great interest, in particular prominences and filaments. The dense filamentary structures at chromospheric temperatures are located in the corona. They are presumed to form via a thermal instability. High spatial resolution ALMA observations can relate the geometry of filaments (optically thick at millimeter waves) to their surrounding coronal cavity, determine the density-temperature structure and study the fine-scale geometry and the formation process. The destabilization and eruption of filaments in eruptive flares is of particular interest.

4.1.3 Solar recombination lines

[Clark et al. 1995] have reported the detection of the H19-α line in the 350μm band. So far, no millimeter-wavelength line has been detected toward the Sun. Nevertheless, recombination lines for ions with Z$>$ 4 have been discussed and may be observable given ALMA's extremely high sensitivity. Their detection would represent direct verification of

dielectronic recombination processes in the low corona and transition region, and would offer the unique possibility of measuring the magnetic field strength in those regions using the Zeeman effect. ALMA will offer unique opportunities to search for solar line emission in the millimeter/submillimeter range.

4.2   Millimeter continuum emission from stars

Over the last two decades, the high sensitivity and spatial resolution of the VLA has revolutionized stellar radio astronomy. Using the VLA, major advances were made in studies of *non-thermal* radiation from a wide variety of stellar types. In contrast, VLA observations of *thermal* emission were restricted to stars with high-mass loss rates producing significant ionized outflows and the radio photospheres of nearby red giant and supergiants.

Because of the Rayleigh-Jeans law, photospheric emission becomes much easier to observe at millimeter wavelengths. ALMA will detect the photospheres of stars across the HR diagram. Its impact on all studies of thermal emission will be as profound as that of the VLA on observations of non-thermal emission. In particular, ALMA will resolve the photospheres and chromospheres of giant and supergiant stars within a few hundred parsecs. Moreover, in addition to free-free emission, ALMA will allow (sub)millimeter imaging of thermal emission from dust in stellar envelopes.

Stellar millimeter astronomy is still in its infancy. Its great promise has been demonstrated by an extensive 250 GHz (1.2 mm) survey using the MPIfR bolometer on the IRAM 30-m single-dish telescope [Altenhoff et al. 1994], during which about half of the 268 observed nearby stars were detected at a limiting sensitivity of $\approx 10 - 30$ mJy. That highly diverse sample consisted of stars covering a wide variety of types and evolutionary stages. An important fraction of the detected sources is due to dust emission from disk around pre-main-sequence stars, which has been discussed in the star formation section. At the limiting sensitivity ALMA can reach within an integration time of 1 hour, hundreds of thousands will be detectable, allowing statistical analyses and multi-wavelength studies of extended samples of objects (see also [Pallavicini & White 1996]). In the following we will illustrate ALMA's potential for stellar astronomy with a few examples.

Wind Acceleration of Hot Stars   The radio emission from hot stars (including both O–B, Wolf-Rayet, symbiotic, and VV Cep stars) is dominated by optically–thick free–free emission from their massive radiatively driven winds. Since the radial distance R_ν from which radiation at a frequency ν originates scales as $\sim \nu^{-3/2}$, the high frequencies of ALMA will sample regions close to the stellar surface where the wind is accelerated, a process that is still poorly understood.

Be stars and other hot stars with shells   Hot stars with shells (of which there is a variety of different types in the survey of [Altenhoff et al. 1994] are usually stronger at millimeter wavelengths than wind sources. The radio spectra show evidence for a turn-over around 5–10 GHz from optically thick to optically thin emission. The spectrum at high frequencies is typically flat indicating optically thin shells. A contribution from warm dust

may be present in some cases. ALMA observations will reveal the physics and possible chemistry of such shells.

Stellar Chromospheres   In cool stars without massive ionized outflows, thermal millimeter radiation originates close to the stellar photosphere. The activity of cool stars has a major impact on their chromopshere. Thus ALMA observations will complement optical, UV and radio observations on all forms of stellar activity, including magnetic cycles, spot sizes and possibly thermal emission of flares and will contribute to the understanding of the physical processes. ALMA thus will make the study of millimeter emission from normal stars a major field of investigation.

Upper photospheres and lower chromospheres of late-type giants and supergiants   In the surveys of [Walmsley et al. 1991] and [Altenhoff et al. 1994], millimeter emission was detected from many late-type giants and supergiants. At 1.2 mm wavelength the emission of all but the highest mass loss objects is dominated by the photospheric contribution [Walmsley et al. 1991]. With ALMA it will be possible to resolve the (sub)millimeter photospheres of many nearby red giants and thus probe the inner boundary of the dust formation zone [Reid & Menten 1997].

Non-thermal Emission of Stars and Accretion-powered Sources   The class of optically variable stars in the survey of [Altenhoff et al. 1994] is very heterogeneous and shows a low detection rate at the present sensitivity levels (only 15 of the 76 surveyed stars were detected, including 5 symbiotics). This class includes RS CVn binaries, flare stars, accretion-powered X-ray sources, β Lyrae binaries, and novae. In many cases, the emission mechanism is likely to be non-thermal. This is the case for flares on RS CVn binaries and active type F to M stars where one expects, by analogy with the Sun, that the impulsive millimeter radiation originates from synchrotron emission of high energy electrons (> 1 MeV). The emission is expected to be highly variable, and so although 3 mm fluxes in excess of 1 Jy may be expected in the millimeter regime at times of outburst, only a few RS CVn's have been detected so far (e.g. HR 1099, UX Ari, UV Psc) and no undisputed detection of flare stars has yet been reported. The higher sensitivity of ALMA should contribute substantially to this area thus allowing the study in other stars of flares similar to, but much more energetic, than solar flares.

In accretion-powered X-ray sources (like SS433, Cyg X-1, Cyg X-3, etc), non-thermal emission is expected to arise from the accreting flow, while in β Lyr variables it is unclear whether non-thermal emission or thermal emission from ionized shells is observed. In novae the radio spectrum is consistent with thermal free-free emission from an expanding shell of ionized gas.

η **Carinae**   The object η Carinae is considered to be an important short-lived unstable phase in the life of the most massive stars in galaxies, shortly before they explode as supernovae. It is one of the most luminous galactic sources and is regarded as an extreme case of a Luminous Blue Variable. This southern source may consist of two very massive (50-80 M$_\odot$) stars in a wide 5.5 year orbit. The binary is surrounded by a highly bipolar,

dusty nebula containing 1-2 $M_\odot$ of material which was ejected by one of the stars in 1843. No other stellar object (apart from supernovae) is known to have such extreme mass loss (i.e., $\approx 2\,10^{-3} M_\odot\,yr^{-1}$). At submillimeter and millimeter wavelengths, η Carinae is also a very strong source showing regular variations with a cycle of 5.5 years (it reaches about 40 Jy at maximum at 230 GHz). The variation in flux density is due to eclipsing events from the binary system. In addition, η Carinae is a strong emitter in the hydrogen and helium recombination lines displaying line widths of about 1000 kms^{-1} and maser activity. It is clear that the high spatial resolution of ALMA will permit to measure in detail the (sub)millimeter emission of this outstanding stellar system and map the variations in the expanding ionized stellar envelope to an unprecedented level of detail.

4.3 Circumstellar envelopes

At the border between stellar and interstellar physics, circumstellar envelopes (CSEs) are key objects in astrophysics. They appear at the end of the Red Giant phase, when the stars eject the bulk of their mass in less than 10^5 years. The episode of high mass loss contributes to the enrichment of the interstellar medium (ISM) in dust and heavy elements. Its timescale and yields control the chemical evolution of galaxies.

In the last stages of their lives, stellar winds rapidly remove the outer layers of the dying stars, resulting in mass loss rates as high as $10^{-6} - 10^{-3}$ $M_\odot$ per year. This material is enriched in heavy elements such as C, N, O, P, S and Si, which have been formed by nucleosynthesis inside stars. When this dense and warm material cools, dust can form. The initial grain nucleation and grain growth are expected to occur at distances of a few stellar radii, and can be observed only by ALMA by imaging the thermal dust continuum and emission from molecules like SiO, SiO_2 and SiS. These programs will require the highest spatial resolution of ALMA, 30 milli-arcsec or better, but the continuum and lines are sufficiently strong that sensitivity is not an issue.

The grains, accelerated by radiation pressure, drag the gas outwards, building a thick, dusty circumstellar envelope. Later, at the end of the high mass loss phase, the star develops a bipolar outflow and evolves toward a planetary nebula. The gas in the envelope is essentially in molecular form; in contact with interstellar UV radiation or with the outflowing matter, it experiences a rich chemistry. To date, over 60 different molecular species have been identified in CSEs. This wealth of molecules, allied to relatively well known physical conditions and timescales, makes of the circumstellar envelopes invaluable probes of photo- and shock-chemistry.

The CSE expansion velocities are of the order of 10 km s^{-1}, and their outer radii $< 10^{18}$ cm. The most interesting regions, the acceleration region, which is also the region of dust formation, and the photochemical region lie respectively at distances of a few 10^{14} cm and a few 10^{16} cm from the star. Since the closest CSEs are 100 pc away, their detailed study requires angular resolutions better than 1–2 arcsec. Because the outer envelopes are cold ($10 < T_K < 100$ K) and opaque up to the mid-IR, these studies are best made with large millimeter and submillimeter interferometers.

The closest CSEs and protoplanetary nebulae (PPNs) have been studied in the emission of a number of molecules with the current millimeter single-dish telescopes and

arrays. The main target of these studies is the closest C-rich CSE, IRC+10216, located between 100 and 200 pc from the Sun. Its spectrum has been almost completely surveyed from 1 cm to 0.8 mm; it is exceptionally rich in radicals and linear C-chain molecules [Cernicharo et al. 2000]. At the level of 10 mJy, the line density is one per 10–20 MHz. The millimeter emission of a score of molecules and radicals has been mapped with interferometers in this CSE. The maps show a clear chemical segregation, the stable species (particularly those with refractory elements) being observed mostly near the star, whereas the reactive species are confined to a thin shell of the outer envelope (Fig.35 and [Guélin et al. 1996]). A few other C-rich or O-rich envelopes have also been studied, but far less in detail, because of their smaller sizes and of the weakness of their emission.

These observations have led to an understanding of the basic processes controlling the chemistry in the outer envelopes [Glassgold 1996]. However, the formation of the grains and the acceleration of the gas remain largely unknown. Yet, they are crucial as they control the mass loss process and the final stages of stellar evolution. Their study, even in the closest stars, requires a high sensitivity, access to submillimeter lines, and angular resolutions of the order of $0.1''$. It is out of the reach of the present mm-wave instruments, but will clearly be a prime research topic for ALMA.
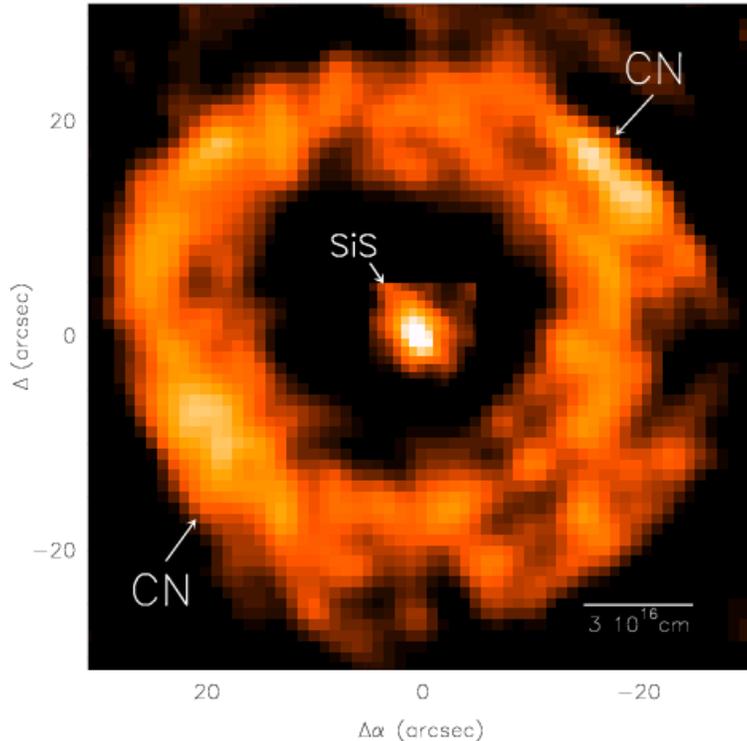

Figure 35: Distributions of the SiS and CN 3-mm emission in the CSE IRC+10216. The colors represent the line intensities integrated in a narrow velocity interval centered on the systemic velocity of the star. It will be possible with ALMA to extend this type of observations to stars a few kpc away. From [Guélin et al. 1996].

Because of sensitivity and angular resolution limitations, the shapes and sizes of the CSE remain poorly known. To date, only 40 or so of the few hundreds of CSE detected in

the CO-mm lines and/or in the millimeter/submillimeter continuum [Loup et al. 1993], have been mapped, in most cases too crudely to observe asymmetries and outflows [Neri et al. 1998]. The present studies are hampered by insufficient sensitivity and low angular resolution. In order to study the 1000 brightest CSE, one needs to map ^{12}CO(2-1) lines of 0.1 Jy in sources with diameters of 1″. This will be possible with ALMA. Detailed maps of ^{12}CO, ^{13}CO, and of the thermal dust emission of these stars will teach us about the timescale of the mass loss episodes and the strength of the interstellar radiation field.

The most important challenge for ALMA in this field will be to study CSE at different galactocentric radii. Both the initial chemical composition of the stars and their formation rates depend on the location in the Galaxy. One would like to measure in remote envelopes, barely resolvable even with ALMA, the size of the CO source, the shape and width of the global CO line profiles, the envelope molecular content and their isotopic content. The isotopic abundance ratios in an envelope tell us about the mass of the central star and about its degree of evolution. Measuring these ratios will be particularly interesting for the CSEs located in the central region of the Galaxy.

4.4   Post-AGB Sources

The circumstellar envelopes of asymtoptic giant branch (AGB) stars undergo major modifications during the rapid transition to planetary nebulae (PNe). During this proto-PN (PPN) phase fast winds emitted by the central star generate shocks which compress and accelerate the neutral envelopes. An important effect of this interaction is the shaping of the envelope, since it will largely determine the morphology which later on characterizes the PN phase (e.g., [Huggins et al. 1996, Sahai & Trauger 1998]. The complex morphologies and kinematics found in PPN point to a radical change of the stellar wind behaviour at the end of the AGB phase (increase in velocity and mass-loss rate, evidence of precession) but the causes are still unknown [Kwok 1993, Cox et al. 2000] - see Fig. 36. Since these changes occur deep inside the precursor AGB envelope, high angular resolution observations coupled with kinematic information are crucial for our understanding of the mechanisms occurring at the end of the evolution of stars of a few M$_\odot$. It is clear that ALMA will make it possible to study these key sources in much greater depth than has been possible with the best instruments to date.

In spite of the wind interaction and the onset of photo-ionization through the post-AGB phase, a significant component of molecular gas is found in many bone fide PNe [Huggins 2000], even in highly evolved ones such as the Helix nebula [Young et al. 1999]. CO and H$_2$ have been detected in more than 40 PNe and other molecular species have been detected in the neutral gas indicating an on-going chemistry. In most cases, the molecular gas is found around the waist of the ionized gas in toroid-like shapes and represent a main structural feature of the nebula and an important key to its morphology (Fig. 37). In addition to molecular gas, there is evidence for neutral atomic gas in PNe, e.g., from observations of the fine-structure lines of carbon. This gas is at the interface between the molecular and ionized gas, and in envelopes that are essentially completely atomic. The masses in these components are substantial but they have not been studied in large numbers of PNe or at high angular resolution.

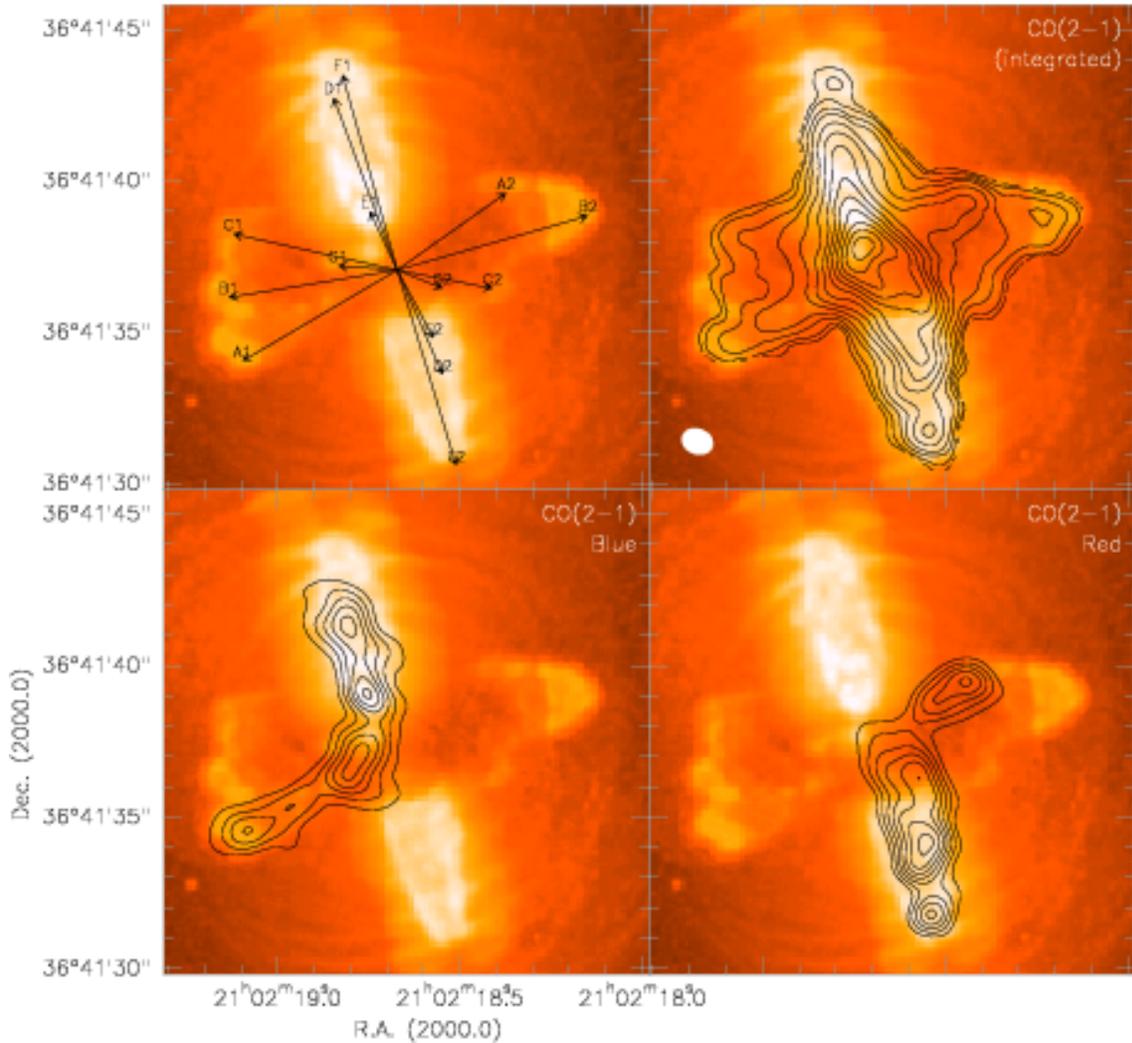The detailed structure of the molecular gas in PNe is of great interest since it contains

Figure 36: CO and HST images of the proto-planetary nebula CRL 2688. The HST image (background) shows reflected light from the remnant AGB envelope (suggesting spherical, episodic mass loss) and shocked molecular gas (probed by H_2 emission) - from [Sahai & Trauger 1998]. The upper right image shows in superimposed contours the inner regions of the AGB envelope (traced by the velocity integrated CO(2–1) line emission). The lower panels show the blue-shifted (-80 to -60 km.s^{-1}) and red-shifted (-22 to -2 km.s^{-1}) CO emission. The cold neutral gas outlines a series of collimated high-velocity outflows (identified in the left upper panel) that end in the shocked regions - from [Cox et al. 2000]. The beam of the CO image (white ellipse) corresponds to a physical size of $\sim 1.5 \times 10^{16}$ cm. It will be possible with ALMA to study in greater detail the physics and chemistry occurring in this crucial but still poorly understood phase of stellar evolution.
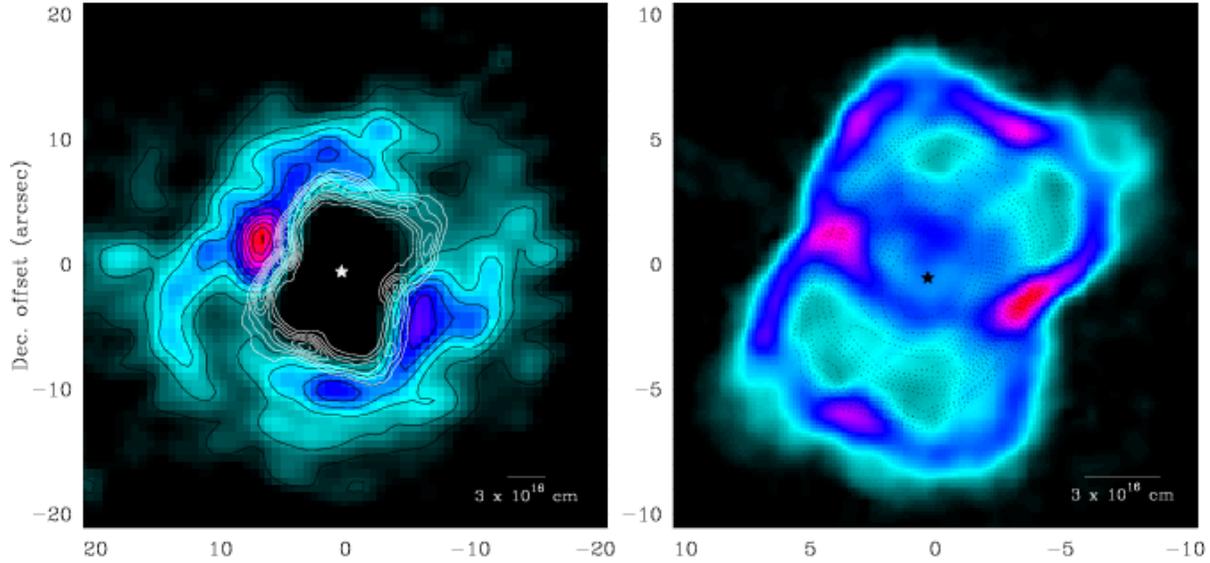
Figure 37: An overview of the relation between the cold and warm molecular gas and the ionized gas in the young planetary nebula NGC 7027. *Left panel*: Distributions of the millimeter CO(1–0) emission (color map) tracing the cold molecular AGB envelope and near-infrared H_2 emission (contours) tracing the warm and dense gas in the photodissociation region between the ionization front and the inner border of the expanding molecular envelope. Both emissions are integrated in a narrow velocity interval centered on the systemic velocity of the nebula. *Right panel*: Zoom on the H_2 distribution and the ionized cavity (contours). The offsets are given in arcsec with respect to the central exciting star (shown as a filled star symbol). ALMA will be able to study the different components associated with planetary nebulae, in particular the warm dense gas via high level molecular transitions in the submillimeter.

information on the physical processes that produce the nebulae. The molecular gas in PNe is characterized be a high degree of fragmentation. For instance, the envelope of the Helix is found to be made of thousands of small (a few ″) dense ($10^5\,\mathrm{cm}^{-3}$) clumps slowly evaporating in the radiation of the central white dwarf [Young et al. 1999, Cox et al. 1999]. The origin of these tiny structures, which could result from inhomogeneities already present in the AGB envelope, remains completely open. Another aspect of the distribution of molecular gas is its global structure which preserves imprints of the early interaction of the envelope with collimated, bipolar outflows or jets just after the AGB phase.

The increase in sensitivity and angular resolution provided by ALMA will allow us to study the molecular and atomic gas in many more PNe. In addition, due to its possibility to measure at high frequencies and to its flexibility in frequency set-up, ALMA will open up the exciting possibility to observe for the first time at high spatial resolution the warm dense gas as well as the dust continuum in planetary nebulae. These observations will provide key information to further explore the physical and chemical conditions pertaining in the fragmented, neutral equatorial structures which have been only recently realized to be common and important features of planetary nebulae.

4.5 Supernovae

Millimeter observations of supernovae (SN) offer exciting possibilities, complementing observations at other wavelengths in important ways. On first look one would guess that microwave emission from a SN with an intrinsic spectrum dominated by "normal" synchrotron emission, say, $\propto \nu^{-0.7}$, is best observed at radio wavelengths. However, the radio flux can be strongly reduced by absorption, both free-free absorption by the circumstellar gas and, especially at early times, synchrotron self-absorption.

Considering that the intrinsic emission decays on average like $t^{-0.7}$ and that the circumstellar free-free absorption decays like $t^{-3}\nu^{-2.1}$ (the circumstellar gas is the pre-SN stellar wind, so that the density decreases like r^{-2}, which for a constant wind expansion velocity, is also $\propto t^{-2}$), the resulting light curve at any one frequency will have a peak at a time when the optical depth at *that* frequency is 0.7/3=0.23. With simple algebra one finds that for a given amount of circumstellar gas the time of the maximum varies as $\nu^{-0.7}$ and the measured flux density at the peak varies as $\nu^{-0.49}$.

Therefore, the higher the frequency, the earlier the light curve peak occurs and the higher the peak flux density. Thus, observing SNe with ALMA will allow one to reach greater distances and to notice explosive events much more promptly than at centimeter wavelengths. For example the "median" SN among the ones detected by [Weiler et al. 1998] reached an absolute radio luminosity of 1×10^{27} erg s^{-1} Hz^{-1} at 5 GHz about 300 days after explosion. Such a flux can be measured at the 1 mJy level up to a distance of 30 Mpc if observing at 5 GHz, but at 1 mm one would expect the peak about 40 days after the explosion and the 1 mJy level would correspond to about 80 Mpc: the increase of accessible volume is more than a factor of 20!

The brightest SNe in a sample of 12 well observed Type II supernovae (SNII) have peak luminosities about 20 times brighter than the median value, and the weakest have about 10 times fainter luminosities. These very bright SNII could easily be detected *and* monitored with ALMA up to a distance of 350 Mpc, i.e. $z \sim 0.1$.

4.6 Gamma ray bursts

Gamma ray bursts (GRBs) lie at cosmological distances, with estimated electromagnetic energy releases of $10^{51} - 10^{53}$ erg, making them the brightest transient phenomena in the Universe, out-shining quasars and supernovae by factors of 10^4 to 10^7. Currently popular GRB models fall into two categories: (i) the coalescence of compact objects (neutron stars, black holes and white dwarfs [Narayan et al. 1992]) and (ii) the collapse of the central iron core of a massive star to a spinning black hole, a "collapsar" [MacFadyen & Woosley 1999]. Sensitive sub-millimeter and millimeter wavelength observations of GRB afterglow emission provide vital constraints on the parameters of the explosion that are difficult or impossible to obtain at other wavelengths.

Sub-millimeter and millimeter observations allow give the peak frequency and the peak flux density of the afterglow emission, which at a given time sets its entire energy scale. Owing to the rapid spectral evolution of the fireball, X-ray and optical observations do not measure this peak. Likewise, centimeter measurements at the VLA are plagued by
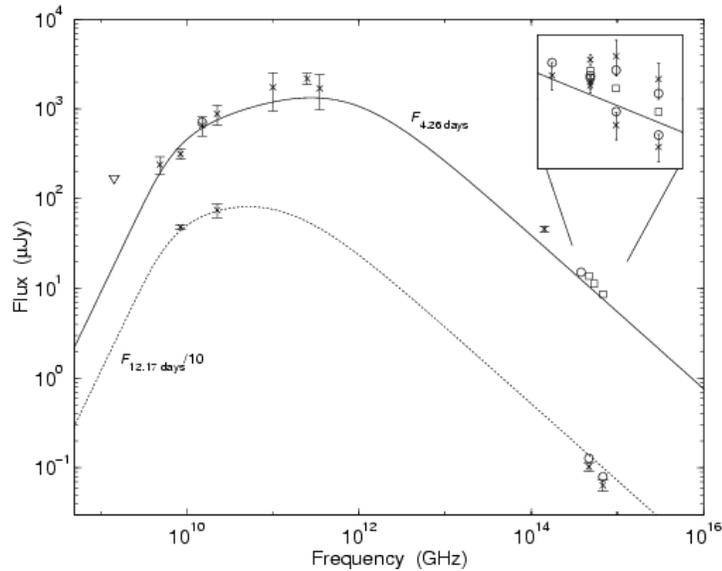
The radio to optical spectral flux distribution of GRB 000301C at $\Delta t \approx 4.3$ and 12.2 days after the burst ([Berger et al. 2000]). The solid and dashed lines are the global fits based on the smoothed synchrotron emission spectrum [Granot et al. 1999]. Note that the overall normalization of the earlier spectrum is determined solely by millimeter observations.

Figure 38: Spectrum of a Gamma-ray burst

interstellar scattering at early times and therefore provide inaccurate measurements. Sub-millimeter and millimeter observations, when incorporated into broad-band global model fitting, can be used to derive the physical parameters (total energy, density, magnetic field, geometry, etc) of the fireball and the medium into which it is expanding, and thus hold the key to unraveling the identity of the central engine(s) responsible for these energetic explosions. Without (sub)millimeter observations, it is not possible, e.g., to distinguish whether the ejecta are collimated into a jet-like outflow or whether the shock is expanding isotropically, nor would it be possible to tell whether the burst expands in a constant density ISM or into the wind of a massive stellar progenitor.

Only two GRB afterglows have yet been detected at millimeter wavelengths, with flux densities at 250 GHz of ≈ 2 mJy [Berger et al. 2000, Galama et al. 2000] (see Fig.38). The vast majority of all GRB afterglows are too faint for current instruments, and even the brightest are only detectable with bolometers at the IRAM 30 m for some days near their peak emission. ALMA will bring a dramatic improvement, enabling the detection and flux monitoring of essentially *all* GRB afterglows currently detectable in the optical, which is about one each month.

There is marginal evidence for short-term ($\sim$1 hr) achromatic flux variability in the millimeter afterglow emission [Galama et al. 2000], which might be the result of microlensing of the afterglow [Garnavich et al. 2000]. Current instruments are unable to quantify millimeter variability. ALMA however will allow detailed studies of any short time flux variablity. Since GRBs are associated with massive stars, ALMA may also be able to detect the emission from the star-forming regions that GRBs may be associated with. Thus, ALMA observations of GRBs may one day offer a complementary view of the star formation history of the early Universe.

5 The Solar System

5.1 Planetary atmospheres

Heterodyne spectroscopy at millimeter/submillimeter wavelengths has proven over the last 20 years to be a powerful tool to study planetary atmospheres. Detection of minor species is often more sensitive than in any other spectral range. The high spectral resolving power allows the detailed investigation of line shapes, providing information on the atmospheric temperature structure and the vertical profiles of molecular abundances, and, when the source is resolved, allowing direct wind measurements from the determination of Doppler shift of line cores. As of today, molecular rotational lines from Mars, Venus, the Giant Planets, Io and Titan have been observed. While large single-dish telescopes and current interferometers already permit a modest resolution of the largest of these bodies (Mars, Venus, Jupiter), ALMA will resolve the planetary disks down to scales of 100 kilometers. Because the distribution of minor species in planetary atmospheres generally reflects the interplay between chemical and dynamical phenomena, ALMA will be a unique tool to provide a three-dimensional dynamical picture (composition, temperature and wind fields) of these atmospheres, one of the major goals in planetary research. Its versatility in terms of spatial resolution, spectral resolution and bandwidth make it particularly suited to study the variety of source size, line strengths, linewidths and temperature conditions in planetary atmospheres. In particular, the broad spectral bandwidth will be useful for studying broad (several GHz) lines at Venus and in the tropospheres of the Giant Planets. The increased sensitivity, including the ability to isolate planetary limbs (thereby increasing the line-of-sight), will allow a search for many new compounds, and the first detection of line emission from fainter bodies such as Triton and Pluto can be envisaged. Some major specific objectives are illustrated below.

5.1.1 Mars and Venus

Atmospheric temperature maps will be obtained from inversion of the CO lines, providing the temperature profile from 0 to 70 km at Mars and 70 to 120 km at Venus. Given S/N constraints, the attainable spatial resolution will be about $0.2'' = 100$ km. In the case of Mars, this is enough to resolve regional (e.g topographic) scales. The probed vertical range extends somewhat higher than in infrared sounding from martian orbiters. Middle-atmosphere winds (near 50 km for Mars, 100 km for Venus, see Fig.39), inaccessible by any other technique, will be simultaneously measured, at a spatial resolution and accuracy sufficient to study the fine structure of the global circulation (zonal jets restricted to some latitudinal bands, meridional winds, possibly orographic winds and planetary waves...). The water cycle of Mars, a key topic in current research, will be studied from mapping of the HDO lines over several Martian years. This will allow, in particular, to monitor condensation and sublimation exchanges between the atmosphere, the polar caps and the regolith. Martian photochemistry will also be studied by mapping, monitoring, and correlating the abundances of H_2O (HDO), O_2 (through $^{16}O^{18}O$), O_3, CO and possibly H_2O_2. Searches with unprecedented sensitivity of new minor species (e.g. H_2CO and NO on Mars; HCl, sulfur-bearing species, $^{16}O^{18}O$ and O_3 on Venus) will also be performed.

5.1.2 Giant Planets

Stratospheric emissions from the Giant Planets include millimeter/submillimeter lines of external H_2O (detected by ISO on all four Giant Planets and Titan), CO and HCN in Neptune, and CO, HCN and CS observed in Jupiter since the Shoemaker-Levy 9 impacts in 1994. Mapping and monitoring of the strong HCN and CO lines in Neptune by ALMA will provide keys to their origin. For example, if the Nitrogen contained in Neptune's HCN originates from Triton's atmosphere, HCN should exhibit local increases at specific latitudes; variations in CO could be associated with variations of cloud activity through variations in vertical transport. Sensitive searches for these species should be conducted in Saturn and Uranus, as well as other nitriles (HC_3N, CH_3CN, ...), hydrocarbons (e.g. CH_3CCH) and oxygen species in all four Giant Planets. In Jupiter, monitoring the horizontal and vertical distribution of the SL9-injected species, which are not expected to disappear before tens of years, will allow a measurement of horizontal and vertical mixing timescales, with dynamical implications. Another major, though difficult, objective would be to measure (and map) HDO in the Giant Planet stratospheres. Combined with current or FIRST measurements of H_2O, this would provide the D/H ratio in this external water, a key as to its origin (interplanetary vs. local). Finally, the strongest emission lines could be used for direct wind measurements in the Giant Planet stratospheres, not possible with any other technique. The study of Giant Planet troposphere will benefit from the broad bandwidth of ALMA spectrometers. Particularly appealing are observations of PH_3 and CO. Their mapping could reveal latitudinal variations (as has been suggested for Jupiter) linked to variations in the vertical transport strength. The first detection of PH_3 on Uranus and Neptune could be achieved. Similar studies could also probably be performed from NGST at 4.7 micron, provided sufficient spectral resolution is available. New disequilibrium species like HCl or HCP could also be detected.

5.1.3 Titan

Titan's atmosphere contains a wealth of hydrocarbon and organic (nitriles) molecules, most of which exhibit latitudinal variations. This primarily reflects a seasonal modulation of these photochemically-produced species, but their spatial distribution is certainly affected by dynamical phenomena (e.g. meridional winds) as well. Thus a simultaneous mapping (at $\sim 0.2''$) of the species reachable in the millimeter/submillimeter (CO, CH_3CCH, HCN, HC_3N, CH_3CN, perhaps heavier nitriles or more complex species like CH_2NH...) combined with direct wind measurements from the strong lines of HCN or CO will be of great interest for understanding the dynamical-chemical couplings in Titan's atmosphere, and its variations with season. Part of this study (mapping of some of the above and other species) will be achieved by Cassini in 2004-2007, but the simultaneous access to the global circulation will be a unique feature of ALMA.

5.1.4 Tenous atmospheres (Io, Pluto, Triton,...)

Io's atmosphere, observed at millimeter and UV wavelengths, appears to be patchy (i.e. shows large variations in surface pressure), but its exact distribution and the relative importance of frost sublimation and direct volcanic output in its maintenance are uncertain.
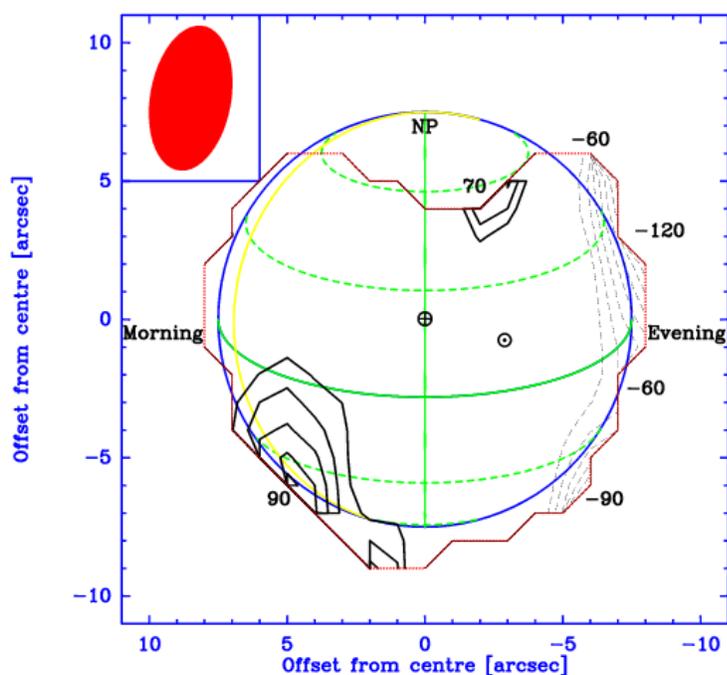
Winds near 50 km altitude in the atmosphere of Mars determined from IRAM Plateau de Bure observations of CO 1-0 lines in May 1999. Positive values indicate receding winds. Contours are separated by 15 m/s [Moreno et al. 1999]

Figure 39: The wind pattern of Mars

Mapping of the SO_2 and SO lines detected at IRAM and detailed study of the associated Doppler shifts will be key in localizing and revealing the nature of Io's atmosphere. For example, a volcanic dynamic atmosphere, as opposed to a stratified atmosphere, would result in redshifts; interaction of the gas with the Io plasma torus would also shift line cores. The high sensitivity of ALMA will also permit studies of short term variability expected to occur in this atmosphere. Many minor compounds predicted to be present will be searched for (H_2S, OCS, NaOH, S_2O, ClO, NaCl...). Isotope ratio studies could be conducted (notably the $^{32}S/^{34}S$ ratio, recently discovered to be anomalous in Jupiter).

Pluto's and Triton's atmospheres have so far escaped detection in the millimeter/submillimeter, but should be relatively easy targets for ALMA. The detection of CO and perhaps HCN is anticipated, and the angular resolution would be sufficient to get images and first ideas on the general circulation pattern. In a more general way, CO could be searched for in other small bodies of the Solar System (Transneptunian objects, small satellites).

5.2   Asteroids and Comets

Observations of comets with ALMA will directly aid our understanding of the nature, origin and diversity of comets. Millimeter and submillimeter spectroscopy recently proved to be a major tool for the study of comets and specifically the identification of the volatile molecules outgassed from their nuclear ices. However, the detailed knowledge of the chemical composition of comets is now limited to a very small number of objects, which were very bright (such as comet Hale-Bopp) or studied by space probes (such as P/Halley and P/Wirtanen). ALMA will expand by one order of magnitude the sample for such investigations. It will allow us to probe both comets coming from the Oort Cloud (which provides

most of the bright, unexpected comets) and comets born in the Kuiper Belt (which evolved into short-period comets of the Jupiter family, usually weaker).

Observations of asteroids, comet nuclei and other Solar System small bodies with ALMA, complemented by observations at other wavelengths, will give us insights into their sizes and surface properties.

5.2.1 The composition of cometary ices and the origin of comets

Millimeter and submillimeter spectroscopy has by now discovered more than 20 molecules in comets [Bockelée-Morvan et al. 2000]. Most of these molecules are not accessible to optical observations. The composition of cometary ices is found to be highly analogous to interstellar material and indicates that comets are relics of protosolar chemistry. Complex organics such as $HCOOH$ or $HCOOCH_3$ have been observed, and some species with abundances as low as 0.0002 relative to water have been detected, but the chemical inventory is far from complete. The large collecting area of ALMA used in single-dish, autocorrelation mode, will permit us to complete this inventory and to search for less abundant molecules, radicals, and new ions.

ALMA will also be a key instrument for investigating isotopic ratios in several molecular species and many comets. Up to now, the D/H ratio in water is only known in three comets, all coming from the Oort Cloud. One expects that the D/H ratio depends upon the comet formation site. It is therefore important to measure this ratio in a sample of comets with different origins and evolution, in order to constrain models of Solar System formation. The measurement of D/H in Jupiter-family comets is especially required.

5.2.2 Physics and chemistry of cometary atmospheres

ALMA will be able to map molecules and dust continuum emission in the coma of comets, as was done in the maps of comet Hale-Bopp shown in Fig.40, but with much greater sensitivity and resolution. Some molecular species such as CO and H_2CO are known to come not only from the nucleus, but also from a distributed source within the coma whose nature is ill known. ALMA will have a spatial resolution of 15 km at 1 mm wavelength for a comet at 1 AU. This will easily allow us to assess which molecules are truly coming from the nucleus and what are the properties of distributed sources.

Because cometary activity varies on short time scales, ALMA will be ideal for providing fast images (snapshots). Such images will allow us to study structures in the inner coma, such as fans and rotating jets, and to investigate to what extent dust and chemistry in the coma are involved in the production of molecules. In this respect, ALMA will be superior to optical telescopes, since it should also provide the velocity information, allowing to reconstruct a full 3 dimensional picture of the ejection process. Maps of the distribution of rotational temperatures of different molecular species will help studies of the thermodynamics, excitation processes, and physical conditions in the coma of comets.

Continuum maps with ALMA will allow us to separate the contribution of dust from that of the nucleus itself, even if the nucleus is not resolved [Altenhoff et al. 1999]. Dust thermal emission at radio wavelengths probes large-sized dust particles, which are related
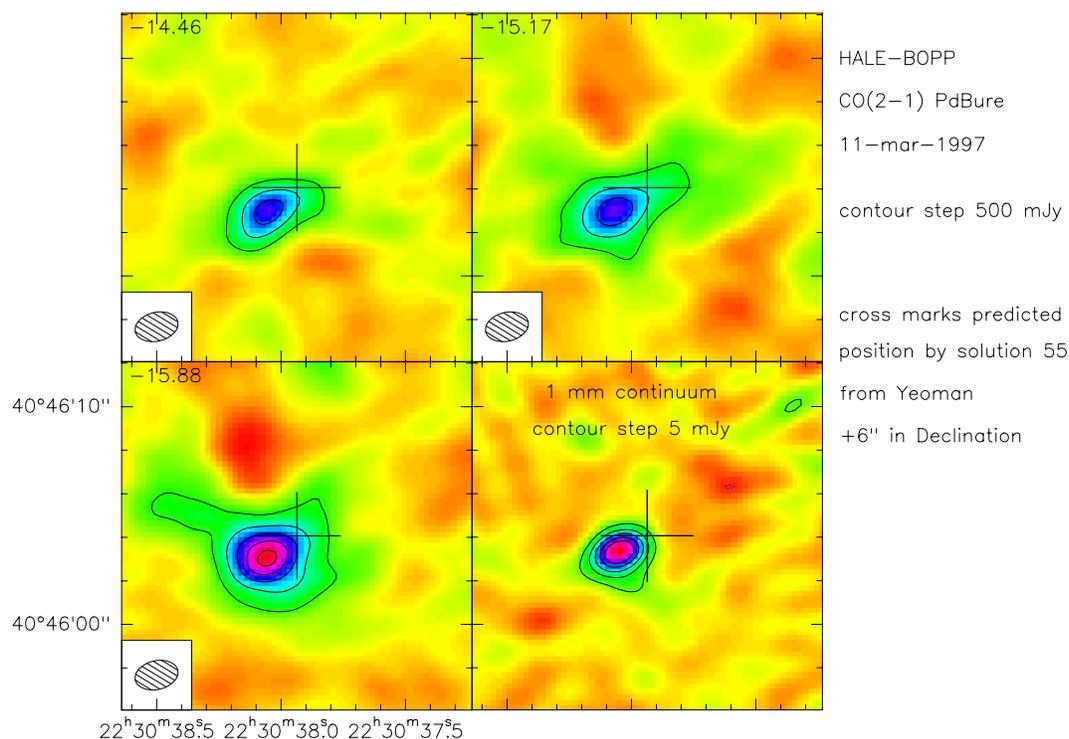
Figure 40: Maps of carbon monoxide and dust in comet Hale-Bopp obtained with the IRAM interferometer. The four panels show the CO(2-1) line in various velocity channels and (lower right) dust continuum emission. The spatial resolution is $1''$, or 1000 km at the comet.

to cometary trails and to meteors. Such particles are only observable in the far-infared, in the millimeter and by radar. The nucleus thermal radio emission, compared with the reflected sunlight observed at optical wavelengths, allows a determination of the nucleus albedo and size.

### 5.2.3   Activity of distant comets and asteroids

The activity of comet Hale-Bopp was traced up to more than 10 AU from the Sun, by observing its CO(2-1) line with SEST. The high sensitivity of ALMA will make it possible to detect CO and other species in many distant comets and to study the evolution of their outgassing as they approach the Sun. Such studies will provide clues to the sublimation processes and physical properties of cometary ices. It will also be possible to look for weak levels of outgassing in asteroids and in giant comet-like objects such as Centaurs.

5.2.4   The surface of small bodies

Continuum observations with ALMA will permit an in-depth study of the thermal emission of Solar System small (quasi)airless bodies: asteroids, comet nuclei, Centaurs, trans-Neptunian objects, as well as outer planet satellites (such as Triton) and Pluto and Charon separately. A typical trans-Neptunian object of 200 km diameter at 45 AU has a flux density of 60 μJy at 1 mm wavelength and will be easily detected in a one-hour observation.

In particular, thermal light curves at millimeter wavelengths will be measured. Combined with measurements in other spectral ranges (thermal infrared by SIRTF, visible and near IR by large ground-based telescopes and NGST), this will provide a determination of their surface properties (albedo, emissivity, thermal inertia, subsurface conduction). Thermal maps of asteroids (and Mercury) will provide insight into the emission "beaming effect" and roughness properties of their surfaces.

Fig.41 illustrates these possibilities for the Pluto-Charon system. Current data suggest a bimodal temperature distribution with Nitrogen ice at 35 K and higher temperature regions at 55 to 70 K [Jewitt 1994]. ALMA could provide a thermal map of the Pluto surface at 0.02″ resolution with 0.5 K rms noise in just an hour.
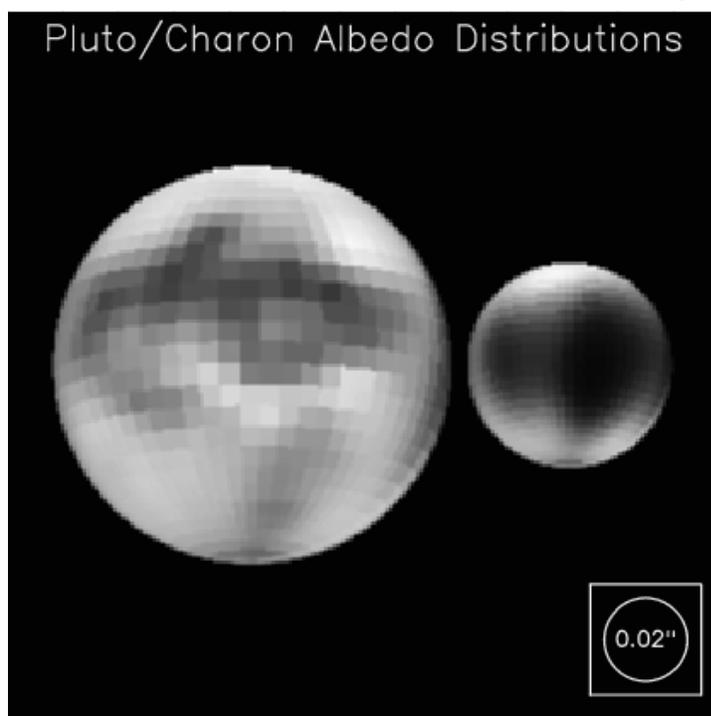
B band albedo distributions of Pluto and Charon reconstructed from multiple mutual occultation events using a maximum entropy method (courtesy Marc W.Buie, Lowell Observatory). ALMA could provide a thermal map of the surfaces of both objects at the same 0.02″ resolution with 0.5 K rms noise in just an hour.

Figure 41: The Pluto-Charon system

5.3   Extrasolar planets

Five years after the discovery of the first extrasolar planet, orbiting 51 Peg [Mayor & Queloz 1995], the number of extrasolar planets identified around solar type stars now approaches 50. All of these were detected indirectly from measurements of the reflex motion of the star that they orbit, with one confirmation through occultations of the same parent star. Detection and analysis of the planetary light would provide access to a wealth of additional information, including for instance the chemical composition of their atmosphere. This is the main scientific driver behind a number of planned space and ground based IR interferometers.

Three main hurdles have to be passed in order to detect an extrasolar planet next to

its parent star: contrast, resolution, and sensitivity. In terms of contrast, the Rayleigh-Jeans regime in which ALMA will operate is most favorable, since the flux of a blackbody depends only linearly on its temperature. The contrast in the ALMA frequency range between the Sun (1 $R_\odot$, T=6000 K) and Jupiter (0.1 $R_\odot$, T=170 K) is below 10^{-4}, within the expected dynamic range of ALMA. ALMA also has adequate angular resolution to separate most nearby extrasolar planets from their stars: "hot-Jupiters" ($\sim$0.05 AU semi-major axis) would only be separated (by the 10 km array in the 1.3 mm band) out to $\sim$2pc, but the more numerous planets in wider orbits could be separated out to beyond 20 pc. Sensitivity turns out to be more problematic. Because the giant planet radius is 0.1 $R_\odot$, independent of mass from a Jupiter-mass up to the brown dwarf limit, the 350 GHz flux at a distance of 1 pc is only 0.02μJy per K of brightness temperature. Hot (1000 K) Jupiters could be detectable around the nearest stars in a few tens of hours, but any more "normal" (or more distant) planet would require far longer integration times.

Much more promising is the indirect detection of planets with ALMA through astrometric wobble. This wobble (in arcsecond) is $\theta_w = (m_p/M_*)(a/d)$ where m_p is the planet mass, M_* the stellar mass, a the semi-major axis of the planet orbit in AU, and d the distance in parsec. For $3 < a < 10$ AU, which gives periods between 5 and 30 years, θ_w is in the milliarcsec range for stars at less than 10 pc. Such measurements would be quite complementary to the optical radial velocity measurements which are sensitive to shorter orbital periods. The astrometric accuracy of a measurement is limited by signal to noise to $\sigma_w = \lambda/(2\pi B\,\mathrm{SNR})$ where SNR is the signal to noise ratio of the observation, and B the baseline length. A precision of 0.1 mas could be reached in 2 hours for a solar type star at 10 pc. Baseline and atmospheric pathlength errors can also be kept within 0.2 mas provided a calibrator closer than about 6° angular offset is used, which should be easy with ALMA. There are 300 hundred stars earlier than M5 within 10 pc from the sun. Within a couple of weeks of observing time, ALMA could survey ~ 30 stars for astrometric motions twice per year with the required accuracy, if the configuration allows. Space and ground-based optical or near/mid-IR interferometers will also attempt similar experiments. Space missions may lack the long time span required to sample 10 AU orbits, while ground-based experiments still have to demonstrate the relative phase referencing technique. ALMA will have an important role to play in this field.

6 Synergy with other Major Astronomical Facilities

ALMA will be an essential millimeter/submillimeter counterpart of the other major astronomical facilities of the world. It will be the first telescope operating at these wavelengths to provide both the angular resolution and sensitivity corresponding to the state-of-the-art in other regions of the electromagnetic spectrum.

However, the synergies go far beyond the similarities in sensitivity and resolution. As elaborated in previous sections, the same dust that obscures objects in the ultraviolet and optical wavebands radiates brightly in the millimeter/submillimeter wavebands. Thus, ALMA can study the dust-obscured star-forming galaxies and star and planet formation regions that the VLT and HST simply cannot see. A large millimeter/submillimeter telescope is essential for a complete understanding of the Universe. It is now known that the extragalactic background radiation in the far-IR and submillimeter bands is comparable to that in the optical/near-IR, and probably greater at high redshifts. ALMA will be sensitive not only to star-forming galaxies whose light is dimmed by dust in the UV and optical, but also to objects at very high redshifts whose light has been redshifted out of the UV and optical wavebands. ALMA and the Next Generation Space Telescope (NGST) are often mentioned as the two instruments that will detect and study the first luminous objects in the Universe - those that reionized the Universe and brought an end to the "Dark Ages".

From these high redshifts to detailed studies of objects in our own solar system, the synergies between ALMA and other facilities are many and varied. Several have been mentioned in the previous sections, and an overview was given in the 1995 workshop on Science with Large Millimeter Arrays (Lequeux, 1995). ALMA and the VLT will together give an accounting of the bolometric luminosities of distant galaxies. They will both be used to study complementary absorption lines in the spectra of distant quasars – molecular and atomic. ALMA will be able to study the gas and dust in the host galaxies of many quasars, without the blinding effect of the bright central source that dominates in the UV and optical. ALMA and X-ray telescopes such as Chandra and XMM will determine the incidence of active galactic nuclei in dust-obscured star-forming galaxies. ALMA will study the kinematics of the nuclear regions of other galaxies, in many cases obscured in the optical by dust. Spectroscopic and proper motion studies of the center of our own galaxy will greatly add to what has already been learned from the pioneering studies in the near-infrared with the NTT. ALMA will be able to measure the abundances of more than a hundred gas-phase molecules in star and planet forming regions, whereas mid-infrared instruments on the VLT, SOFIA, SIRTF and NGST will probe the solid-state component. Observations of thermal emission from H_2O will be possible with FIRST. Together, these facilities provide a nearly complete inventory of the gas and dust. In our own solar system, combined observations using ALMA in conjunction with spacecraft will greatly enhance studies of the planets and their satellites. Ground-based work has the advantage of regularly updated instrumentation and the possibility of monitoring and follow-up observations.

ALMA will also be essential in follow-up observations of sources detected with other instruments. For example, the optically-selected Lyman-break galaxies are expected to have (sub)millimeter flux densities that will be detectable in minutes using ALMA. It is important to know what fraction of the bolometric luminosity is being missed in the

optical/UV surveys and re-radiated in the far-infrared/submillimeter bands. Infrared-selected galaxies found with 175 μm flux densities of > 100 mJy using ISO are expected to have 850 μm flux densities of several mJy if they are at $z \sim 1$. Much larger samples of similar objects will come in the next few years from facilities such as SIRTF. ALMA will be sufficiently sensitive to rapidly search the error circles and identify the sources. Large samples of submillimeter-selected sources will come from BOLOCAM on the Large Millimeter Telescope and from the FIRST and Planck space missions. While the Planck survey is primarily intended to study the microwave background, it will also detect tens of thousands of galaxies at 350 GHz with a flux density of greater than 100 mJy. ALMA will be able to identify such sources with integration times of seconds, and measure their spectral energy distributions. This will produce a catalogue of all the most luminous submillimeter galaxies and AGN over the southern sky.

This is a period of rapid development in astronomy. On the ground, several new 8-10 m class optical/infrared telescopes now exist or are under construction - the VLT/VLTI, Keck, GEMINI, SUBARU, and others. At radio wavelengths a major enhancement of the VLA is proposed, very large meter-wave arrays (LOFAR, Square Kilometer Array) are under study, and a 50m diameter Large Millimeter Telescope (LMT) is under construction in Mexico. In space, HST has now been joined by the new Chandra and XMM X-ray telescopes, the infrared spacecraft SIRTF will be launched within a couple of years, and the Far Infrared and Sumillimeter Telescope (FIRST) and Planck cosmic background experiment will come a few years later. NGST will provide vastly increased capabilities in the optical, near and mid-infrared by the end of the decade. A corresponding capability is essential at millimeter/submillimeter wavelengths, and that will be provided by the Atacama Large Millimeter Array.

References

[Aghanim et al. 2000]   Aghanim, N., Balland, C., and Silk, J. 2000, A&A 357, 1

[Altenhoff et al. 1994]   Altenhoff, W.J., Thum, C., and Wendker, H.J. 1994, A&A 281, 161

[Altenhoff et al. 1999]   Altenhoff, W.J. et al. 1999, A&A 348, 1020

[André 2000]   André, P. 2000, in "Protostars and Planets IV" (Tucson: University of Arizona Press; eds Mannings, V., Boss, A.P., Russell, S.S.)

[Ayres 1995]   Ayres, T.R. 1995, in "Infrared Tools for Solar Astrophysics: What's Next?", J.R. Kuhn & M.J. Penn (eds.), p. 289

[Bachiller 1996]   Bachiller, R. 1996, Ann. Rev. Astron. Astrophys. 34, 111

[Bachiller et al. 2000]   Bachiller, R., Pérez Gutiérrez, M., Nandakumar, M.S., Tafalla, M. 2000, to be submitted to A&A

[Backman et al. 1993]   Backman, D., Paresce, F. 1993, in Protostars & Planets III, ed. J. Lunine & E. Levy (Tucson: Univ. Arizona)

[Bastian et al. 1998]   Bastian T. S., Benz A. O., Gary D. E. 1998, Ann. Rev. Astron. Astrophys. 36, 131

[Beckwith et al. 1990]   Beckwith, S.V.W., Sargent, A.I., Chini, R.S., and Güsten, R. 1990, AJ 99, 924

[Benson et al. 2000]   Benson, A.J., Nusser, Adi, Sugiyama, Naoshi, Lacey, G.G. 2000, MNRAS in press (astro-ph/0002457)

[Berger et al. 2000]   Berger, E. et al. 2000 ApJ, in press (astro-ph/0005465)

[Bertoldi et al. 2000]   Bertoldi, F. et al. 2000, in Cold Gas and Dust at High Redshift, ed. D. Wilner (Kluwer, Dordrecht), in preparation

[Blain 1998]   Blain A.W. 1998, MNRAS 297, 511.

[Blain 1999]   Blain A.W. 1999, MNRAS 309, 955

[Blain 2000]   Blain, A.W. 2000, in Wootten A. ed. "Science with ALMA", ASP Conf. Series in press (astro-ph/9911449).

[Blain et al. 2000]   Blain A.W., Frayer D.T., Bock J.J., Scoville N.Z. 2000, MNRAS 313, 559.

[Blake et al. 1987]   Blake, G.A., Sutton, E.C., Masson, C.R., Phillips, T.G. 1987, ApJ 315, 621

[Bockelée-Morvan et al. 2000] Bockelée-Morvan, D. et al. 2000, A&A 353, 1101.

[Bodenheimer et al. 2000] Bodenheimer, P., Burkert, A., Klein, R. I. & Boss, A. P. 2000, in "Protostars and Planets IV" (Tucson: University of Arizona Press; eds Mannings, V., Boss, A.P., Russell, S.S.), p. 675

[Bonnell et al. 1998]   Bonnell, I.A., Bate, M.R., Zinnecker, H. 1998, MNRAS 298, 93

[Bontemps et al. 1996]   Bontemps, S., André, P., Terebey, Cabrit, S, 1996, A&A 311, 858

[Bontemps et al. 2000]   Bontemps, S., André, P., Kaas, A. et al. 2000, A&A, in press

[Brandner et al. 2000]   Brandner, W., Grebel, E.K., Chu, You-Hua, Dottori, H., Brandl, B., Richling, S., Yorke, H.W., Points, S.D., Zinnecker, H. 2000, AJ 119, 292

[Brown & vanden Bout 1991] Brown, R.L., and vanden Bout, P. 1991, AJ 102, 1956

[Browne 2000]   Browne, I.W.A., Mao, S., Wilkinson, P.N., Kus, A.J., Birkinshaw, M. 2000, in "Radio telescopes" Proc of SPIE, Vol 4015, Ed H.R.Butcher.

[Carilli & Yun 1999]   Carilli, C. L. & Yun, M. S. 1999, ApJ 513, L13

[Carilli & Yun 2000]   Carilli, C. L. & Yun, M. S. 2000, ApJ 530, 618 (erratum: 539, 1024)

[Cernicharo et al. 2000]   Cernicharo, J., Guélin, M, Kahane, C. 2000, A&A Suppl. 142, 181

[Charnley et al. 1992]   Charnley, S.B., Tielens, A.G.G.M., Millar, T.J. 1992, ApJ 399, L71

[Charmandaris et al. 2000]   Charmandaris, V., Combes, F., van der Hulst, J. M. 2000, A&A 356, L1

[Chiang & Goldreich 1997]   Chiang, E., Goldreich, P. 1997, ApJ 490, 368

[Chini et al. 1990]   Chini, R., Krügel, E., and Kreysa, E. 1990 A&A 227, L5

[Clark et al. 1995]   Clark T.A., Lindsey C., Rabin D.M., Livingston, W.C. 1995, in "Infrared Tools for Solar Astrophysics: What's Next?", J.R. Kuhn & M.J. Penn (eds.), p. 133

[Clarke et al. 2000]   Clarke C.J., Bonnell I.A., Hillenbrand L.A. 2000, in "Protostars and Planets IV" (Tucson: University of Arizona Press; eds Mannings, V., Boss, A.P., Russell, S.S.), p.151

[Combes et al. 1996]   Combes, F., Q-Rieu, N., Wlodarczak, G. 1996, A&A 308, 618

[Combes & Wiklind 1997]   Combes F., Wiklind T. 1997, in The Green Bank Workshop on *Highly Redshifted Radio Lines*, eds. C.L. Carilli, K.M. Menten, G. Langston, Green Bank, USA, October 9-12 1997

[Combes et al. 1999]   Combes F., Maoli R., Omont A. 1999, A&A 345, 369

[Cooray 1998]   Cooray, A.R., Grego, L., Holzapfel, W.L., et al. 1998, AJ 115, 1388.

[Cox et al. 1999]   Cox, P., Boulanger, F., Huggins, P.J. et al. 1999, ApJ 495, L23

[Cox et al. 2000]   Cox, P., Lucas, R., Huggins, P.J., Forveille, T., Bachiller, R., Guilloteau, S., Maillard, J.-P., & Omont, A. 2000, A&A 353, L25

[Dallacasa et al. 2001]   Dallacasa, D., Stanghellini, C., Centonza, M., & Fanti, R. 2001, A&A Supp. in press

[Delfosse et al. 1998]   Delfosse X., Forveille T., Mayor M., Perrier C., Naef D., Queloz D. 1998, A&A 338, L67–70.

[Downes et al. 1999]   Downes D. et al. 1999, A&A 347, 809

[Downes & Solomon 1998]   Downes D., Solomon P.M. 1998, ApJ 507, 615

[Downes et al. 1999]   Downes, D., Neri, R., Wiklind, T., Wilner, D.J., Shaver, P.A. 1999, ApJ 513, L1

[Dulk et al. 1989]   Dulk, G.A., Gary, D.E., Hjellming, R.M., Kundu, M.R., and Bastian, T.S. (1989) *Report of the Working Group on "The Sun and Stars"*, First MMA Science Workshop

[Dunne et al. 2000]   Dunne, L. et al. 2000, MNRAS, in press

[Dutrey et al. 1996]   Dutrey, A., Guilloteau, S., Duvert, G., et al. 1996, A&A 309, 493

[Dutrey et al. 1997]   Dutrey A., Guilloteau S., Guélin M. 1997, A&A 317, L55

[Dutrey 2000]   Dutrey A. 2000, in Wootten A. ed. "Science with ALMA", ASP Conf. Series in press.

[Ehrenfreund 1999]   Ehrenfreund, P. 1999, AAS 194.4101

[Falcke et al. 2000]   Falcke, H., Melia, F., & Algol, E. 2000, ApJ 528, L13

[Falgarone et al. 1991]   Falgarone, E., Phillips, T. G., Walker, C. K. 1991, ApJ 378, 186

[Falgarone et al. 1998]   Falgarone, E., Panis, J.-F., Heithausen, A., Perault, M., Stutzki, J., Puget, J.-L., Bensch, F. 1998, A&A 331, 669

[Fontenla et al. 1993]   Fontenla, J. M., Avrett, E. H., Loeser, R. 1993, ApJ 406, 319

[Flower et al. 1998]   Flower D., Pineau des Forêts G. 1998, MNRAS 297, 1182

[Frayer et al. 1999]   Frayer D. T. et al., 1999, ApJ 514, L13

[Fuente et al. 2000]   Fuente, A., Neri, R., Martin-Pintado, J., Bachiller, R., Rodriguez-Franco, A., Palla, F. 2000, submitted to A&A

[Galama et al. 2000]   Galama, T. J. et al. 2000, ApJ 541, L45

[Gallimore et al. 1997]   Gallimore, J.F., Baum, S.A, and O'Dea, C.P. 1997, Nature 388, 852

[Garcia-Burillo et al. 1998]   Garcia-Burillo, S., Sempere, M. J., Combes, F., Neri, R. 1998, A&A 333, 864

[Garnavich et al. 2000]   Garnavich, P. M., Loeb, A., Stanek, K. Z. 2000, ApJ, in press

[Gear et al. 2001]   Gear W. K., et al., 2001, MNRAS, in press (astro-ph/0007054)

[Glassgold 1996]   Glassgold, A.E. 1996, Ann. Rev. Astron. Astrophys. 34, 241

[Gibb et al. 2000]   Gibb, E., Whittet, D.C.B., Schutte, W.A., et al. 2000, ApJ 536, 347

[Granot et al. 1999]   Granot, J., Piran, T., Sari, R. 1999, ApJ 513, 679

[Greaves et al. 1998]   Greaves, J., Holland, W., Moriarty-Schieven, G., et al. 1998, ApJ 506, L133

[Greenhill & Gwinn 1997]   Greenhill, L.J., and Gwinn, C.R. 1997, Ap&SS 248, 261

[Guélin et al. 1996]   Guélin, M., Lucas, R., Neri, R. 1996, in *Science with Large mm Arrays*, p. 276, P.A. Shaver, Ed. Springer

[Guesten et al. 1987]   Guesten, R., Genzel, R., Wright, M.C.H., Jaffe, D.T., Stutzki, J., and Harris, A.I. 1987, ApJ 318, 124

[Gueth et al. 2001]   Gueth, F., Dutrey, A., & Guilloteau S. 2001, A&A, in preparation

[Gueth & Guilloteau 1999] Gueth, F., Guilloteau S. 1999, A&A 343, 571

[Gueth et al. 1997]   Gueth, F., Guilloteau, S., Dutrey A., Bachiller, R. 1997, A&A 323, 943

[Guiderdoni et al. 1999]   Guiderdoni, B., Bouchet, F., Devriendt, J. Hivon, E., Puget, J.L. 1999, in "The Birth of Galaxies", B. Guiderdoni, F.R. Bouchet, T.X. Thuan & J. Tran Thanh Van (eds), Editions Frontieres (astro-ph/9902141)

[Guilloteau et al. 1999]   Guilloteau S., Dutrey A., Simon M. 1999, A&A 348, 57

[Guilloteau 2000]   Guilloteau S., 2000, in Wootten A. ed. "Science with ALMA", ASP. Conf. Ser. in press.

[Guilloteau et al. 2001]   Guilloteau S., Dutrey A., Simon M. 2001, A&A, in preparation

[Habing et al. 1999]   Habing, H.J., et al. 1999, Nature 401, 456

[Heiles 1997]   Heiles C. 1997, ApJ 481, 193

[Heithausen et al. 1998]   Heithausen, A., Bensch, F., Stutzki, J., Falgarone, E., Panis, J. F. 1998, A&A 331, L65

[Helfer & Blitz 1996]   Helfer T.T., and Blitz, L. 1995, ApJ 450, 90

[Hodapp 1994]   Hodapp, K. 1994, ApJS 94, 615

[Hogerheijde et al. 1995] Hogerheijde, M.R., de Geus, E.J., Spaans, M., van Langevelde, H.J., van Dishoeck, E.F. 1995, ApJ 441, L93

[Hogerheijde et al. 1999] Hogerheijde, M.R., van Dishoeck, E.F., Salverda, J.M., Blake, G.A. 1999, ApJ 513, 350

[Holland et al. 1997]   Holland, W.S. et al. 1997, Nature 392, 788

[Holland et al. 1999]   Holland, W.S. et al. 1999, MNRAS 303, 659.

[Hollenbach et al. 1997]   Hollenbach, D.J., Tielens, A.G.G.M. 1997, Ann. Rev. Astron. Astrophys. 35, 179

[Hollis et al. 2000]   Hollis, J.M., Lovas, F.J., Jewell, P.R. 2000, ApJ 540, L107

[Holzapfel et al. 2000]   Holzapfel, Wl.L, Carlstrom, J.E., Grego, L., Holder, G., Joy, M., Reese E.D. 2000, ApJ 539, 57

[Huggins et al. 1996]   Huggins, P.J., Bachiller, R., Cox, P. & Foveille, T. 1996, A&A 315, 284

[Huggins 2000]   Huggins, P.J. 2000, in *Asymmetrical Planetary Nebulae II: From Origins to Microstructures* ASP Conference Series XXX, J.H. Kastner, N. Soker & S. Rappaport (eds.)

[Hughes et al. 1998]   Hughes, D. et al. 1998, Nature 394, 341

[Hutter and Mufson 1986]   Hutter, D.J., & Mufson, S.L. 1986, ApJ 301, 50

[Ivison et al. 2000]   Ivison R. J., Smail I., Barger A. J., Kneib J.-P., Blain A. W., Owen F. N., Kerr T. H., Cowie L. L. 2000, MNRAS 315, 209

[Jewitt 1994]   Jewitt, P. 1994, AJ 107, 372-378

[Johansson et al. 1998]   Johansson L.E.B., Greve A., Booth R.S. et al. 1998, A&A 331, 857

[Joulain et al. 1998]   Joulain, K., Falgarone, E., Pineau des Forêts, G. , Flower, D. 1998, A&A 340, 241

[Junor et al. 1999]   Junor, W., Birretta, J.A.,& Livio, M. 1999, Nature 401, 891

[Kastner et al. 1997]   Kastner, J., Zuckerman, B., Weintraub, D., Forveille, T. 1997, Science 277, 67

[Kedziora-Chudzer et al. 1997] Kedziora-Chudzer, L., Jauncey, D.L., Wieringa, M.H., Walker, M.A., Nicolson, G.D., Reynolds, J.E., and Tzioumis, A.K. 1997, ApJ 490, L9

[Knapp et al. 1989]   Knapp G.R., Guhathakurta P., Kim D.W., Jura M. 1989, ApJS 70, 321

[Kneib et al. 1998]   Kneib J.-P., Alloin D., Mellier Y., Guilloteau S., Barvainis R., Antonucci R. 1998, A&A 329, 827

[Koerner & Sargent 1995]   Koerner, D.W., Sargent, A.I. 1995, AJ 109, 2138

[Kopp et al. 1992]   Kopp G. et al. 1992, ApJ 308, 203

[Königl 1981]   Königl, A. 1981, ApJ 243, 700.

[Krichbaum et al. 1998]   Krichbaum. T.P., et al. 1998, A&A 335, L106.

[Krichbaum et al. 2000]   Krichbaum. T.P., 2000, Proc 5th EVN Symposium, Publ Chalmers University of Technology, Eds J.E.Conway, A.Polatidis, R.Booth and Y, Pihlström

[Kroupa et al. 1993]   Kroupa, P., Tout, C. A., & Gilmore, G. 1993, MNRAS 262, 545

[Kundu et al. 1994]   Kundu, M. R., White, S. M., Gopalswamy, N., Lim, J. 1994, ApJS 90, 599

[Kwok 1993]   Kwok, S. 1993, Ann. Rev. Astron. Astrophys. 31, 63

[Lagrange 1999]   Lagrange A.-M., 1999 in "Proto-Stars & Planets IV" eds. V. Mannings et al. (Tucson: Univ. of Arizona)

[Langer et al. 1997]   Langer, W.D., Velusamy, T., Kuiper, T.B.H., et al. 1997, ApJ 480, L63

[Langer et al. 2000]   Langer, W.D., van Dishoeck, E.F., Blake, G.A., et al. 2000, in "Protostars and Planets IV" (Tucson: University of Arizona Press; eds Mannings, V., Boss, A.P., Russell, S.S.)

[Lis et al. 1996]   Lis, D. C., Pety, J., Phillips, T. G., Falgarone, E. 1996, ApJ 463, 623

[Liszt & Lucas 2000]   Liszt, H.S., Lucas, R. 2000, A&A 355, 333

[Looney et al. 2000]   Looney, L., Mundy, L., and Welch, W.J. 2000, ApJ 529, 477.

[Loup et al. 1993]   Loup, C., Forveille, T., Omont, A., Paul, J.F. 1993, A&AS 99, 291

[Lucas & Liszt 1993]   Lucas, R., Liszt, H.S. 1993, A&A 276, L33

[Lucas & Liszt 1996]   Lucas, R., Liszt, H.S. 1996, A&A 307, 237

[Lucas & Liszt 1997]   Lucas, R., Liszt, H.S. 1997, in *Molecules in Astrophysics, Probes and Processes*– IAU Symposium 178, ed. E.F. vanDishoek, Dordrecht, Kluwer Ac. Publishers.

[Luhman et al. 1998]   Luhman et al. 1998, ApJ 504, L11

[Mc Caughrean et al. 1994] Mc Caughrean, M.J., Rayner, J.T., Zinnecker, H. 1994, ApJ 436, L189

[Mac Low & Smith 1997]   Mac Low M.-M., Smith M.D. 1997, ApJ 491, 596

[MacFadyen & Woosley 1999] MacFadyen, A.I., Woosley, S.E. 1999, ApJ 524, 262

[Maloney et al. 1996]   Maloney, P.R., Hollenbach, D.J., and Tielens, A.G.G.M. 1996, ApJ 466, 561

[Mannings & Sargent 1997] Mannings, V.G., Sargent, A.I. 1997, ApJ 490, 792

[Maquart et al. 2000]   Macquart, J-P., Kedziora-Chudczer, L., Rayner, D.P., Jauncey, D.L. 2000, ApJ 538, 623

[Mardones et al. 1997]   Mardones, D., Myers, P.C., Tafalla, M., Wilner, D.J., Bachiller, R., Garay, G. 1997, ApJ 489, 719

[Marsher et al. 1991]   Marsher, A.P., Bania, T.M., Wang, Z. 1991, ApJ 371, L77

[Mayor & Queloz 1995]   Mayor & Queloz, 1995, Nature 378, 355.

[Menten 2000]   Menten K., 2000, in "From Extrasolar Planets to Cosmology: the VLT Opening Symposium", J.Bergeron & A.Renzini eds.

[Mirabel et al. 1998]   Mirabel, F. et al. 1998, A&A 333, L1

[Moreno et al. 1999]   Moreno et al. 1999, Bull.Amer.Astron.Soc. 31, 1149

[Motte et al. 1998]   Motte, F., André, P., & Neri, R. 1998, A&A 336, 150

[Myers & Lazarian 1998]   Myers P., Lazarian A. 1998, ApJ 507, L157

[Narayan et al. 1992]   Narayan, R., Paczyński, B., Piran, T. 1992, ApJ 395, L83

[Natta & Hollenbach 1998]   Natta, A. & Hollenbach, D. 1998, A&A, 337, 517

[Natta et al. 2000]   Natta, A., Grinin, V.P., Mannings, V. 2000, in "Protostars and Planets IV" (Tucson: University of Arizona Press; eds Mannings, V., Boss, A.P., Russell, S.S.)

[Neri et al. 1998]   Neri, R., Kahane, C., Lucas, R., Bujarrabal, V., Loup, C. 1998, A&AS 130, 1

[Omont et al. 1996]   Omont, A., Petitjean, P., Guilloteau, S., McMahon, R. G., Solomon, P. M., Pecontal, E. 1996, Nature 382, 428

[Osterloh & Beckwith 1995]   Osterloh, M., and Beckwith, S.V.W. 1995, ApJ 439, 288

[Owisanik & Conway 1998]   Owisanik, I., & Conway, J.E. 1998, A&A 337, 69

[Pallavicini & White 1996]   Pallavicini, R., and White, S.M. 1996 in "Science with the Large Millimeter Array" (P.A. Shaver ed.), p. 268

[Papadopoulos et al. 2000]   Papadopoulos, P.P., Rttgering, H.J.A., van der Werf, P.P., Guilloteau, S., Omont, A., van Breugel, W.J.M., Tilanus, R.P.J. 2000, ApJ 528, 626P

[Palla et al. 2000]   Palla et al. 2000, in "Protostars and Planets IV" (Tucson: University of Arizona Press; eds Mannings, V., Boss, A.P., Russell, S.S.)

[Pierce-Price et al. 2000]   Pierce-Price et al. 2000, ApJ Letters in press (astro-ph/0010236)

[Pety & Falgarone 2000]   Pety, J., Falgarone, E. 2000, A&A 356, 279

[Pfenniger & Combes 1994]   Pfenniger, D., Combes, F. 1994, A&A 285, 94

[Reid & Menten 1997]   Reid, M. J., Menten, K. M. 1997, ApJ 476, 327

[Richer et al. 2000]   Richer, J., Sepherd, D., Cabrit, S., Bachiller, R., Churchwell, E. 2000, in "Protostars and Planets IV" (Tucson: University of Arizona Press; eds Mannings, V., Boss, A.P., Russell, S.S.)

[Sahai & Trauger 1998]   Sahai, R. & Trauger, J.T. 1998, AJ 116, 1357

[Sakamoto et al. 1999]   Sakamoto, K., Scoville, N.Z., Yun, M.S., Crosas, M., Genzel, R., and Tacconi, L.J. 1999, ApJ 514, 68

[Sanders & Mirabel 1996]   Sanders D. B., Mirabel I. F. 1996, Ann. Rev. Astron. Astrophys. 34, 759

[Schilke et al. 1997]   Schilke, P., Walmsley, C.M., Pineau des Forêts, G., Flower, D.R. 1997, A&A 321, 293

[Schilke et al. 2000]   Schilke, P., Phillips, T. G., Mehringer, D. M. 2000, Proceedings of the 3rd Cologne-Zermatt Symposium, Eds.: V. Ossenkopf, J. Stutzki, and G. Winnewisser, GCA-Verlag Herdecke, ISBN 3-928973-95-9

[Schiminovich et al. 1994]   Schiminovich D., van Gorkom, J.H., van der Hulst, J.M, Kasow S. 1994, ApJ 432, L101

[Schinnerer et al. 2000]   Schinnerer, E., Eckart, A., Tacconi, L.J., Genzel, R., and Downes, D. 2000, ApJ 533, 850

[Simcell & Coppi 1996]   Simcell, M.W., & Coppi P.S. 1996, ApJ 460, 163

[Simpson & Eisenhardt 1999] Simpson, C., and Eisenhardt, P. 1999, PASP 111, 691

[Simon et al. 2001]   Simon M., Dutrey A., Guilloteau S. 2000, ApJ in press (astro-ph/0008370)

[Smail et al. 2000]   Smail, I., Ivison, R., Blain, A., Owen, F., and Kneib, J.-P. 2000, ApJ 528, 612

[Steidel et al. 1998]   Steidel, C., Adelberger, K., Giavalisco, M., Dickinson, M., and Pettinin, M. 1999, ApJ 519, 1

[Steiner et al. 1996]   Steiner O., Grossmann-Doerth U., Schüssler M., Knölker M. 1996, Solar Physics 164, 223

[Strom 1995]   Strom, S. 1995, Rev.Mex.Astr.Astrof.Conf.Ser. 1, 317

[Stutzki et al. 1998]   Stutzki, J., Bensch, F., Heithausen, A., Ossenkopf, V., Zielinsky, M. 1998, A&A 336, 697

[Tacconi et al. 1997]   Tacconi, L., Downes, D., Eckart, A., et al. 1997, IAU Symp. 184, 112

[Tacconi et al. 1999]   Tacconi, L.J., Genzel, R., Tecza, M., Gallimore, J.F., Downes, D., and Scoville, N.Z. 1999, ApJ 524, 732

[Tafalla et al. 1998]   Tafalla et al. 1998, ApJ 504, 900

[Testi & Sargent 1998]   Testi, L., & Sargent, A.I. 1998, ApJ 508, L91

[Testi et al. 1999]   Testi, L., Palla, F., Natta, A. 1999, A&A 342, 515

[Tielens 1989]   Tielens A., 1989 IAU Symposium 135, p239

[Türler et al. 1999] Türler, M., Courvoisier, T.J.-L. & Platini, S. 1999, A&A 349, 45

[van Dishoeck & Blake 1998] van Dishoeck, E.F., Blake, G.A. 1998, Ann. Rev. Astron. Astrophys. 36, 317

[Vidal-Madjar et al. 1994] Vidal-Madjar, A., et al. 1994, A&A, 290, 245

[Walmsley et al. 1991] Walmsley, C. M., Chini, R., Kreysa, E., Steppe, H., Forveille, T., Omont, A. 1991, A&A 248, 555

[Walmsley 1992] Walmsley, C.M. 1992, in Chemistry and Spectroscopy of Interstellar Molecules, ed. D.K. Bohme et al. (Tokyo: Univ. Tokyo)

[Wang et al. 1992] Wang, Z., Schweizer, F., Scoville, N.Z. 1992, ApJ 396, 510

[Ward-Thompson et al. 2000] Ward-Thompson, D., et al. 2000, ApJ 537, L135

[Weiler et al. 1998] Weiler, K. W., van Dyk, S. D., Montes, M. J., Panagia, N., Sramek, R. A. 1998, ApJ 500, 51

[Williams et al. 2000] Williams, J. P., Blitz, L., McKee, C. F. 2000, in "Protostars and Planets IV" (Tucson: University of Arizona Press; eds Mannings, V., Boss, A.P., Russell, S.S.), p.97

[Wilner et al. 2000] Wilner, D., Depree, C.G., Goss, W.M., Welch, W.J., mcGrath, E. 2000, in *Science with ALMA* ASP Conf. Series in press

[Wilson et al. 2000] Wilson, C.D., Scoville, N., Madden, S.C., Charmandaris, V. 2000, 5th IAP meeting, ASP Conf. Series, Vol. 197, 359.

[White & Kundu 1992] White, S.M., Kundu, M.R. 1992, Solar Phys. 141, 347.

[Whitmore et al. 1999] Whitmore, B.C., Zhang, Q., Leitherer, C., Fall, S.M., Schweizer, F., Miller, B.W. 1999, AJ 118, 1551

[Wiklind et al. 1995] Wiklind, T., Combes, F., Henkel, C. 1995, A&A 297, 643

[Wiklind & Combes 1998] Wiklind, T., Combes, F. 1998, ApJ 500, 129

[Wiklind & Combes 1997] Wiklind, T., Combes, F. 1997, in The Green Bank Workshop on *Highly Redshifted Radio Lines*, eds. C. L. Carilli, K. M. Menten, G. Langston, Green Bank, USA, October 9-12 1997

[Wootten 2000] Wootten, A., ed., 2000, "Science with ALMA", ASP Conf. Series in press.

[Young et al. 1999] Young, K., Cox, P., Huggins, P.J., Forveille, T., & Bachiller, R. 1999, ApJ 522, 387

[Zadelhoff et al. 2000] van Zadelhoff, G-J., van Dishoeck, E.F., Thi, Wing-Fai, Blake, G.A. 2000, IAU Symposium 202

[Zuckerman et al. 1995] Zuckerman, B., Forveille, T., Kastner, J. 1995, Nature 373, 494